

**Polymerbasierte chromatographische Trennmaterialien:
Synthese, Charakterisierung und Anwendung**

**Polymer-based chromatographic sorbents:
Synthesis, characterization, and application**

DISSERTATION

der Fakultät für Chemie und Pharmazie
der Eberhard-Karls-Universität Tübingen
zur Erlangung des Grades eines Doktors
der Naturwissenschaften

2005

vorgelegt von
Christoph Meyer

Tag der mündlichen Prüfung:

29. Juli 2005

Dekan:

Professor Dr. S. Laufer

1. Berichterstatter:

Professor Dr. K. Albert

2. Berichterstatter:

Professor Dr. V. Schurig

Die vorliegende Arbeit wurde am Institut für Organische Chemie der Eberhard-Karls-Universität Tübingen unter der Anleitung von Herrn Professor Dr. Klaus Albert im Zeitraum von Dezember 2002 bis Juli 2005 durchgeführt.

Bei Herrn Professor Dr. Klaus Albert möchte ich mich sehr herzlich für die interessante und fruchtbare Themenstellung, für sein stetiges Interesse an meiner wissenschaftlichen Arbeit und für die Bereitstellung der optimalen Ausstattung, ohne welche die Durchführung dieser Arbeit unmöglich gewesen wäre, bedanken. Zudem förderte er die Vertiefung meines fachlichen Wissens durch internationale Forschungsaufenthalte und durch die Teilnahme an zahlreichen Tagungen.

Mein Dank gilt allen meinen Kollegen und Kooperationspartnern, ohne deren Unterstützung die erfolgreiche Fertigstellung der vorliegenden Arbeit undenkbar gewesen wäre. Besonders möchte ich mich bedanken bei:

Dr. Urban Skogsberg für die Anleitung, Unterstützung, und die wertvollen wissenschaftlichen Diskussionen.

Brigitte Schindler, Paul Schuler und allen anderen Mitarbeitern der NMR-Abteilung.

Dr. Manfred Krucker als „großer Bruder“ im Arbeitskreis.

Norbert Welsch für die unzähligen Diskussionen und die hervorragende Zusammenarbeit.

Dr. Daniel Zeeb für das Einarbeiten in die Synthese stationärer Trennphasen.

Dr. Gerd Fischer für die „Einführung“ in den Arbeitskreis.

Marc-David Grynbaum und Dr. Karsten Putzbach für die Kapillar-LC-NMR Experimente.

Meinen Kollegen Benjamin Dietrich, Dr. Heidrun Händel, Petra Hentschel, Volker Friebolin, Dr. Elke Gesele, Christof Krieg, Hans Kühnle, Jens Rehbein, Dr. Telma Schanz, Siri Schauff, Dr. Ismail Warad und Prof. Dr. Hong-Bin Xiao für die Hilfsbereitschaft bei allen Fragen und Problemen, sowohl fachlicher als auch organisatorischer Natur, sowie das freundschaftliche Arbeitsklima.

Dr. Lane Sander und Dr. Stephen Wise für die freundliche Aufnahme und fachliche Anleitung während meines Aufenthaltes am National Institute of Standards and Technology (NIST), U.S. Department of Commerce.

Priv.-Doz. Dr. Detlef Reichert und Dr. Ovidiu Pascui, Univesität Halle, für die tolle Zusammenarbeit bei der Charakterisierung neuer Trennphasen.

Prof. Dr. Günther Gauglitz für die Möglichkeit, ellipsometrische Messungen an neuen Materialien zusammen mit Stefan Busche durchzuführen.

Priv.-Doz. Dr. Börje Sellergren für die Möglichkeit zur aktiven Teilnahme am AquaMIP EU-Projekt.

Venkata Krishnan und Gokulakrishnan Srinivisan für die Zusammenarbeit im Graduiertenkolleg.

Prof. Dr. Peter Molnar für freundliche Bereitstellung verschiedener Carotinoidproben.

Der Firma Bischoff Chromatography, insbesondere Dr. Rainer Brindle und Dr. Stefan Lamotte, für die fachlichen Diskussionen über neue stationäre Trennphasen.

Der Firma EKA Chemicals, insbesondere Dr. Johan Ekeroth, für die zahlreichen Anregungen zur Synthese- und Charakterisierung neuer chromatographischer Trennphasen.

Der BASF AG, insbesondere Dr. Jesper Feldthusen und Dr. Christian Köpsel, für die zahlreichen Diskussion über Carotinoide.

Insbesondere bedanke ich mich bei meinen Eltern, meiner Familie und meinen Freunden für ihre uneingeschränkte Unterstützung während des gesamten Studiums.

Und schließlich vor allem bei Chrissy...

TABLE OF CONTENT

1 INTRODUCTION.....	1
2 SCOPE.....	3
3 CHEMISTRY IN INTERPHASES.....	5
3.1 The interphase concept.....	5
3.2 Interphases in HPLC.....	5
4 SYNTHESIS AND CHARACTERIZATION OF POLY(ETHYLENE-CO- ACRYLIC ACID) CHROMATOGRAPHIC SORBENTS.....	8
4.1 Synthesis.....	8
<i>4.1.1 Immobilization of RP stationary phases on silica gel.....</i>	<i>8</i>
<i>4.1.2 Immobilization of poly(ethylene-co-acrylic acid) on silica gel.....</i>	<i>11</i>
4.2 Characterization.....	14
<i>4.2.1 Solid-state NMR spectroscopy.....</i>	<i>15</i>
4.2.1.1 ²⁹ Si solid-state NMR spectroscopy.....	16
4.2.1.2 ¹³ C solid-state NMR spectroscopy.....	20
<i>4.2.2 Ellipsometry.....</i>	<i>26</i>
<i>4.2.3 Contact angle measurements.....</i>	<i>30</i>
5 APPLICATION IN HPLC AND DEPENDENCE OF THE SEPARATION MECHANISM.....	33
5.1 Influence of different acrylic acid mass fractions in the copolymer.....	34
5.2 Influence of the spacer molecule.....	38

5.2.1 Separation of carotenoid isomers.....	38
5.2.2 Separation of SRM 869.....	39
5.3 Influence of the mobile phase composition.....	41
5.3.1 Separation of xanthophylls and geometric β -carotene isomers.....	41
5.3.2 ^{13}C suspended-state HPDEC NMR spectroscopy.....	46
5.4 Influence of the surface coverage.....	49
5.4.1 Separation of shape constrained solutes.....	50
5.4.2 ^{13}C solid-state NMR spectroscopy.....	53
5.5 Influence of the temperature.....	55
5.5.1 Temperature dependent ^{13}C NMR investigations.....	56
5.5.1.1 ^{13}C solid- and suspended-state CP/MAS NMR spectroscopy.....	56
5.5.1.2 ^{13}C solid- and suspended-state DIPSHIFT NMR spectroscopy.....	58
5.5.2 Temperature dependent separation of shape constrained solutes.....	63
6 APPLICATION IN CAPILLARY HPLC-NMR HYPHENATION.....	70
6.1 Capillary HPLC separation of tocopherol homologues.....	76
6.2 Identification of tocopherol homologues using on-line capillary HPLC- NMR hyphenation.....	78
7 CHIRAL POLY(ETHYLENE-CO-ACRYLIC ACID) CHROMATOGRAPHIC SORBENTS.....	83
7.1 Synthesis strategy.....	86

7.2 Characterization.....	88
7.3 Application in the RP and NP mode.....	93
7.4 Discussion.....	95
8 SUMMARY AND OUTLOOK.....	101
9 EXPERIMENTAL.....	104
9.1 Chemicals.....	104
9.2 Synthesis of the poly(ethylene- <i>co</i> -acrylic acid) chromatographic sorbents.....	105
9.3 Synthesis of the poly(ethylene- <i>co</i> -acrylic acid) silica wafers.....	107
9.4 NMR spectroscopy.....	108
9.5 Ellipsometry.....	111
9.6 Contact angle measurements.....	112
9.7 HPLC.....	112
9.8 Capillary HPLC-NMR hyphenation.....	113
10 REFERENCES.....	116

ABBREVIATIONS

1D	One dimensional
2D	Two dimensional
Å	Ångström
α	Selectivity
ACN	Acetonitrile
APS	Aminopropyltriethoxysilane
B_0	Static magnetic field
CapLC	Capillary HPLC
COSY	Correlated spectroscopy
CP	Cross polarization
CSA	Chemical shift anisotropy
δ	Chemical shift
d	Day
<i>d</i> ₉	Delay time
DAD	Diode array UV detector
DICI	Diisopropylcarbodiimide
DIPSHIFT	Dipolar and chemical shift correlation
D ₂ O	Deuterium oxide
EPA	Environmental protection agency
FID	Free induction decay
FSLG	Frequency switched Lee-Goldburg
γ	Gyromagnetic ratio
GOPS	Glycidoxypropyltrimethoxysilane
h	Hour
H ₂ O	Water
HETP	Height equivalent of a theoretical plate
HOBT	Hydroxybenzotriazole

HPDEC	High power decoupling
HPLC	High performance liquid chromatography
I	Spin of nucleus
I.D.	Inner diameter
k'	Retention factor
K	Binary kilo (= $2^{10} = 1024$)
K	Kelvin
<i>l</i> ₀	Repetition cycle
LC	Liquid chromatography
M	Molar (mol/l)
MAS	Magic angle spinning
MeOH	Methanol
min	Minute
MS	Mass spectrometry
M/MW	Molecular weight
N	Number of theoretical plates
NIST	National Institute of Standards and Technology
NMR	Nuclear magnetic resonance
PAH	Polycondensed aromatic hydrocarbon
PEA	Poly(ethylene- <i>co</i> -acrylic acid) copolymer
ppm	Parts per million
Q ⁿ	Silandiol (Q ²), silanol (Q ³), and siloxan (Q ⁴) units of silica gel
RF	Rotation frequency
RP	Reversed phase
S	Standard deviation
S/N	Signal-to-noise ratio
SRM	Standard reference material
T	Temperature
T ⁿ	Trifunctional silicium units

T_1	Longitudinal relaxation time
$T_{1\rho H}$	Longitudinal relaxation time in the rotating frame
T_2	Transversal relaxation time
t_m	Mixing time
T_{CH}	Cross polarization constant
TFA	Trifluoro acetic acid
TMOS	Tetramethoxysilane
TMS	Tetramethylsilane
UV	Ultraviolet
v/v	Volume-to-volume ratio
θ	Angle between B_0 and nuclei axis

1 INTRODUCTION

Fast and efficient analytical tools in order to separate, quantify, and identify unknown compounds are essential for biomedical and biotechnical research. Analytical and bioanalytical chemical methods have to meet highest demands in industry and sciences. Methodical developments for advanced rapid and quantitative evaluation of analytical tasks encountered with genomics, proteomics, and metabolomics are indispensable.

Depending on the analyte mixtures, one of the most common and powerful separation techniques is reversed-phase high performance liquid chromatography (RP-HPLC). Detection systems to identify the separated compounds vary from ultraviolet (UV) detection, mass spectrometry, and nuclear magnetic resonance (NMR) spectroscopy. Hyphenated techniques such as liquid chromatography-mass spectrometry (LC-MS) and high performance liquid chromatography-nuclear magnetic resonance (HPLC-NMR) provide the greatest potential for the generation of informative data to elucidate the structure of unknown compounds.

Even though column technology in RP-HPLC advanced all along, it still mostly relies on long alkyl chain stationary phases covalently immobilized on a pressure stable silica gel core. In order to separate alike as well as highly complex analyte mixtures, however, commercially available chromatographic sorbents (approximately 80 % of the market share are C₁₈ columns) not always yield the desired separation success. Also, hyphenated instruments require highly efficient column materials to obtain pure and

concentrated analytes in the respective detection systems. For this reason, the development and characterization of novel stationary phases tailored for certain separation tasks is of substantial importance for modern pharmaceutical and biomedical research. Thereby, analytical tools to monitor the synthesis process and to characterize the final chromatographic sorbents are indispensable. Here, solid-state NMR spectroscopy is the method of choice as a non-destructive method to elucidate the stationary phase surface morphology and dynamics in chromatographic sorbent materials. Furthermore, suspended-state NMR spectroscopy allows to achieve a unique insight into the dynamics of stationary phases in presence of the mobile phase. Direct comparison with the chromatographic capability leads to a more complete picture of the separation mechanism. Thus, NMR helps to understand the performance of recognition centers in stationary phases and is therefore an outstanding characterization tool for further developments.

2 SCOPE

The objective of the on-hand work is the further development and application of novel polymer based highly efficient and shape selective RP-HPLC sorbent materials. Thereby, different poly(ethylene-*co*-acrylic acid) copolymers are covalently immobilized on silica gel via different linker molecules.

The influence of parameters such as the composition of the polymer, the immobilization technique (thus, the usage of different linker molecules), the surface coverage but also experimental variables such as the mobile phase composition and the temperature are of interest. Both, NMR as the most powerful spectroscopic tool to investigate the morphology and structure of sorbent materials and also extensive chromatographic studies are undertaken and compared with each other. Hereby, the shape selectivity effects of stationary phases are examined. They crucially influence the separation mechanism in RP-HPLC, that is mainly governed by hydrophobic interactions. The separation of geometric carotenoid isomers and shape constrained polycyclic aromatic hydrocarbons (PAHs) is a challenge. It depends on the conformation of the stationary phase investigated by a direct comparison of solid- and suspended-state NMR spectroscopic evidences with chromatographic experiments.

The polymer based sorbent materials are also investigated with respect to overloading effects, and checked upon their loading capacity. Especially, when capillary HPLC is hyphenated to NMR, a high analyte concentration in the detection probe is desired resulting in a better signal-to-noise ratio (S/N). Therefore, the polymer based

chromatographic sorbent was tested in the miniaturized capillary HPLC separation system.

Many compounds can be separated and purified using RP-HPLC methods due to their differences in polarity and shape. Other substances, however, exist as enantiomers and differ drastically in bioactivity. For example, the (*S*)-enantiomer of (\pm)-*N*-(2,6-dioxo-3-piperidyl)phthalimid is believed to be the cause of the teratogenic effect of thalidomide. Therefore, the development of active ingredients for novel drugs requires chiral separation materials which are unconditionally reliable. Most chiral separation methods in HPLC rely either on covalently bound normal-phase (NP) selector molecules or on polymers coated around a pressure stable inorganic core. In order to combine the shape selectivity and loading capacity of the poly(ethylene-*co*-acrylic acid) copolymer with chiral recognition, a chiral selector molecule is incorporated in the polymer based chromatographic sorbent. This can be achieved by covalently attaching the copolymer and also the chiral selector on the silica surface using different immobilization strategies. The obtained novel chiral sorbent material is characterized by solid-state NMR spectroscopy and chromatographically tested by separating enantiomers.

3 CHEMISTRY IN INTERPHASES

3.1 The interphase concept

The interphase concept describes the sphere in which a mobile component interpenetrates a stationary phase on a molecular level. Thereby, the stationary phase is usually immobilized by a linker on a supporting substrate, usually an inorganic, an organic or an organic/inorganic polymer. The stationary phase bears the interaction/reaction centers that can either consist of organic molecules, organometallic complexes but also enzymes functioning as bioactive catalysts to which the target reactands/analytes are centripetal by the mobile phase. Even though no homogenous phase is formed, however, due to existent swelling properties of the stationary phase effective interplay between the immobilized and dissolved molecules is possible. The concept can be applied to catalytic reactions, solid phase syntheses in organic chemistry and also to gas and liquid chromatography. In the case of chemical reactions the concept offers the advantage of easy and complete separation of the products from the stationary phase.

3.2 Interphases in HPLC

With respect to HPLC the interphase concept is used to obtain a further understanding of recognition effects on a molecular level, thus is used to advance the

development of novel highly selective and effective stationary phases tailored for specific separation problems. Figure 1 shows a visualization of the interphase concept in RP-HPLC. The analyte, in this case a bend β -carotene molecule, is interacting via hydrophobic hydrogen bonds with the immobilized stationary phase.

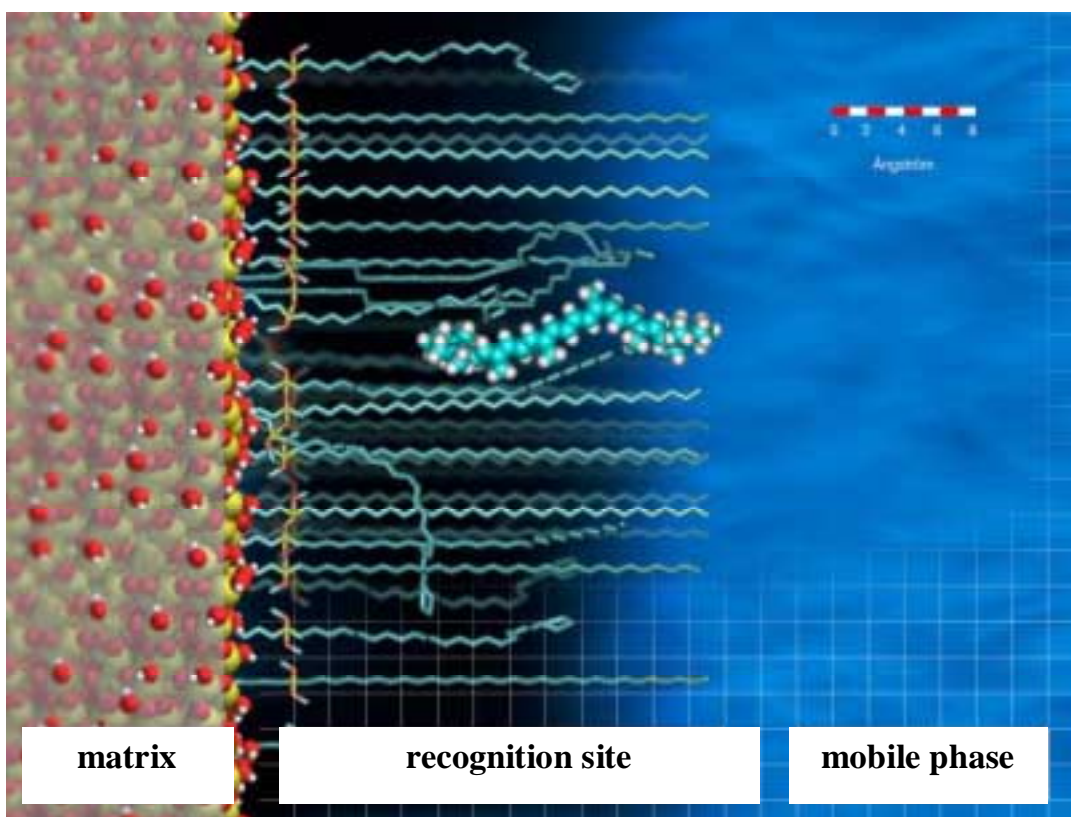


Figure 1 Visualization of the interphase concept in reversed-phase high performance liquid chromatography. The analyte molecule dissolved in the polar mobile phase interacts with the hydrophobic stationary phase (recognition site), which is immobilized on a pressure stable silica gel support (matrix)

Most separation problems in RP-HPLC are generally addressed employing silica based C_{18} sorbent materials [1, 2]. Within the complex interplay between the analyte, the

mobile phase, and the stationary phase the separation process in RP-HPLC, which is primarily governed by hydrophobic interactions, is also influenced by the surface modification chemistry used to immobilize the stationary phase on the silica gel support [3]. The so-called slot model was proposed, in which the retention mechanism was described to be affected by the existence of cavities in the alkyl chain turf on the silica surface in which certain shape-suited analytes could penetrate better resulting in an increase in hydrophobic interactions [4]. Non-planar polycyclic aromatic hydrocarbon (PAH) solutes eluted before planar PAH solutes from certain columns even though these molecules did not differ notably in polarity. The shape of the solute (length-to-breadth ratio L/B) was found to be important for the separation process. These studies took place employing both monomeric and polymeric C_{18} chromatographic sorbents. It was revealed that the shape selectivity or shape recognition of chromatographic sorbents for solutes with a defined rigid structure such as PAHs was enhanced when the sorbents were synthesized according to a solution polymerization reaction [5-8]. The empirical slot model is in agreement with the statistical mechanical interphase concept used to describe retention of "blocklike" molecules [9-11].

4 SYNTHESIS AND CHARACTERIZATION OF POLY(ETHYLENE-*CO*-ACRYLIC ACID) CHROMATOGRAPHIC SORBENTS

RP sorbents based on different polymers were introduced before [12-19]. Poly(ethylene-*co*-acrylic acid) chromatographic sorbents with copolymers differing in chain lengths and polarity covalently bound via a spacer molecule on silica were developed earlier. They revealed different chromatographic performances [20]. Among three poly(ethylene-*co*-acrylic) copolymers, the longest and least polar copolymer with an acrylic acid mass fraction of 5 % proved to have superior shape selective properties [21, 22]. Before presenting the materials investigated in this work, a short general disquisition about the commonly employed strategies for the synthesis of chromatographic sorbents is given in the following paragraph.

4.1 Synthesis

4.1.1 Immobilization of RP stationary phases on silica gel

Covalently modified substrates and their use as LC column material dates back to the early 1970s [23-25]. The covalent bond ensures chemical stability in most organic solvents and the (usually) inorganic substrate assures pressure resistance. The

chromatographic capacity is dependent on the physical and chemical properties of both, the substrate and the immobilized stationary phase. Usually, silica gel is employed as support material with particle sizes ranging from 1 to 10 μm , and pore sizes from 60 \AA to 1000 \AA . Depending on the analyte mixtures, a careful selection of particle and pore sizes must be carried out when synthesizing novel sorbents. In order to have sufficient theoretical plates short diffusion pathways are necessary, therefore smaller particles are preferable. The backpressure, however, increases with decreasing particle size. Also, the smaller the pore size the greater the specific surface area leading to more interactions with the analytes and therefore to a higher retention factor. In this work, most analytes mixtures either consist of carotenoid isomers or PAHs for which a particle size of 3 μm and a pore size of 300 \AA are best suited, see Figure 2 for a visualization of the silica gel.

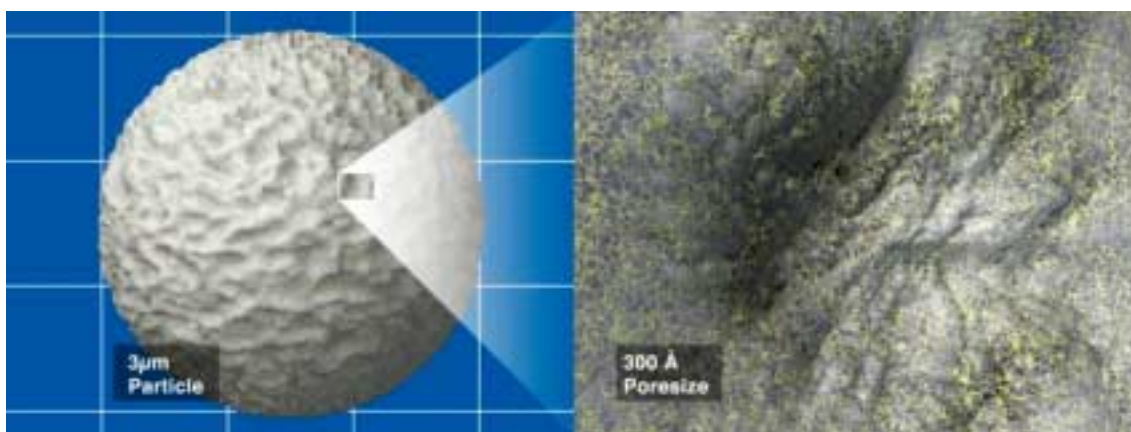


Figure 2 Visualization of porous spherical silica gel employed for the immobilization of stationary phases. The silica gel used in this work has a particle size of 3 μm and a pore size of 300 \AA

The possibility to modify the silica gel surface allows the synthesis of chromatographic sorbent materials tailored for specific separation problems. Polar, nonpolar, aromatic, chiral, and ionic sorbents can be prepared by appropriate modification reactions. Numerous publications, reviews, and books dealt with synthesis strategies for alkyl chain stationary phases modified silica gels [26]. Here the main and most commonly silanization reactions for microparticulate silica shall be recited. The condensation reaction of a monofunctional silane with silanol groups on the silica surface creates an individual siloxane bond and is specified as “monomeric synthesis”. In this case, possible undesired analyte silanol interactions can take place. By employing trifunctional silanes in the presence of water, however, polymerization occurs resulting in surfaces that differ from monomeric sorbents in their chemical composition and their chromatographic features. If a controlled amount of water is added and adsorbed onto the silica surface and this humidified silica gel is then reacted with a trifunctional silane in a dry solvent, polymerization occurs on the silica surface; thus a regular cross linked alkyl chain network is created. This reaction procedure is described as “surface polymerization synthesis”. If, however, a controlled amount of water is added to the solvent in which a trifunctional silane is dissolved, a silane polymer is formed. Subsequently added silica gel covalently binds these polymer clusters on the silica surface. This surface modification reaction is denoted as “solution polymerization synthesis”. Interactions between an analyte and silanol groups on the silica surface are less likely to occur when chromatographic sorbents are synthesized according to a polymeric synthesis approach since the crosslinking of the trifunctional silanes covers the non-reacted silanol groups.

4.1.2 Immobilization of poly(ethylene-co-acrylic acid) on silica gel

Three poly(ethylene-co-acrylic acid) copolymers, see Figure 3, with different chain lengths and different acrylic acid mass fractions were immobilized on porous silica gel (Table 1, chromatographic sorbents **A**, **B**, **C**, and **D**).

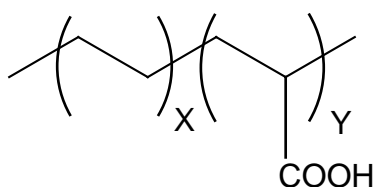


Figure 3 General structure of the poly(ethylene-co-acrylic acid) copolymer

Table 1 Properties of the chromatographic sorbents

sorbent	spacer	number of polymer chain moieties	x	y	acid mass fraction (%)	molecular weight (Da)	degree of immobilization*	polymer molarity on silica surface ($\mu\text{mol}/\text{m}^2$)
A	APS	119	2.4	5	3500	24	0.8	
B	APS	77	3.3	10	2400	12	0.44	
C	APS	33	2.3	15	1100	12	1.08	
D	GOPS	119	2.4	5	3500	7	0.18	

*carbon mass fraction (%)

Within the copolymers an average number of *co*-acrylic acid moieties (*y* denotes their number) are statistically incorporated in the ethylene backbone (*x* denotes the number of

ethylene moieties). The synthesis strategy of the attachment of the polymers to the silica support, that is the influence of different spacer molecules on the chromatographic behavior, is of interest. Therefore the copolymers were attached via an aminopropyltriethoxysilane (APS) linkage (sorbents **A**, **B**, and **C**), see Figure 4a; additionally a glycidoxypropyltrimethoxysilane (GOPS) linkage was used to attach the copolymer with the lowest acid mass fraction on the silica surfaces (sorbent **D**), see Figure 4b.

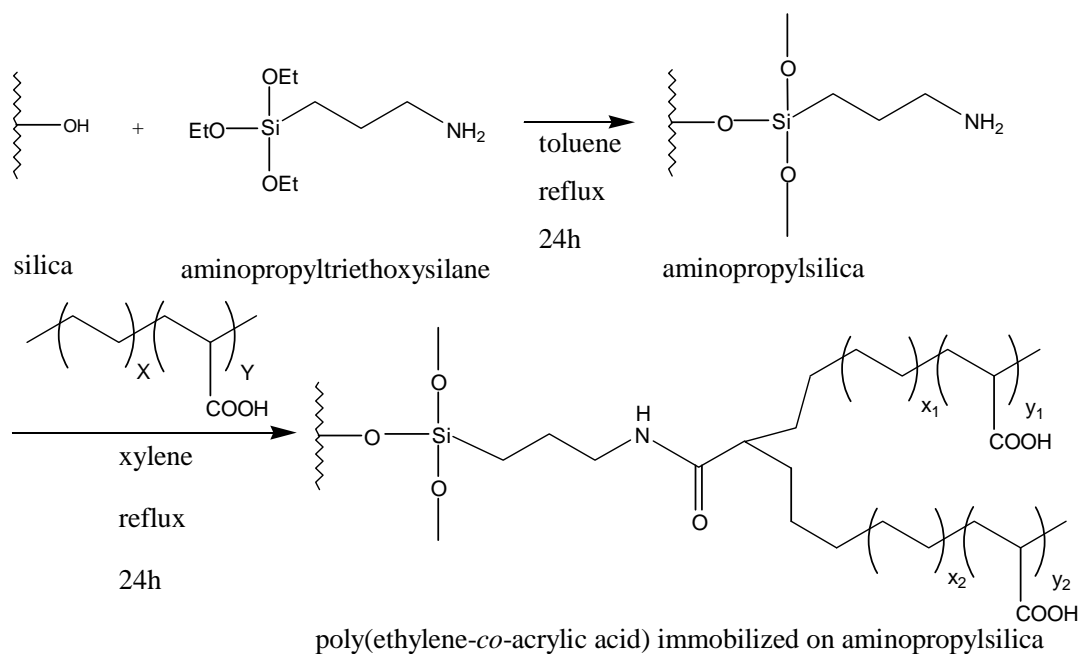


Figure 4a Reaction scheme for the synthesis of chromatographic sorbents **A**, **B**, and **C**

The first reaction step, the attachment of the silane spacer molecules, was undertaken using the surface polymerization reaction. This was done to obtain a preferably even spacer molecule layer. The obtained degrees of immobilization and surface coverages are given in Table 2, and are explained along with the results obtained from the ^{29}Si solid-

state NMR investigation in chapter 4.2.1.1. For the second reaction step, the acid groups within the copolymers were reacted with the reactive functional groups in the spacer molecules. Sorbents **A**, **B**, and **C** were synthesized via a peptide coupling reaction of the amino group in 3-aminopropylsilica and the acid groups of the respective copolymer

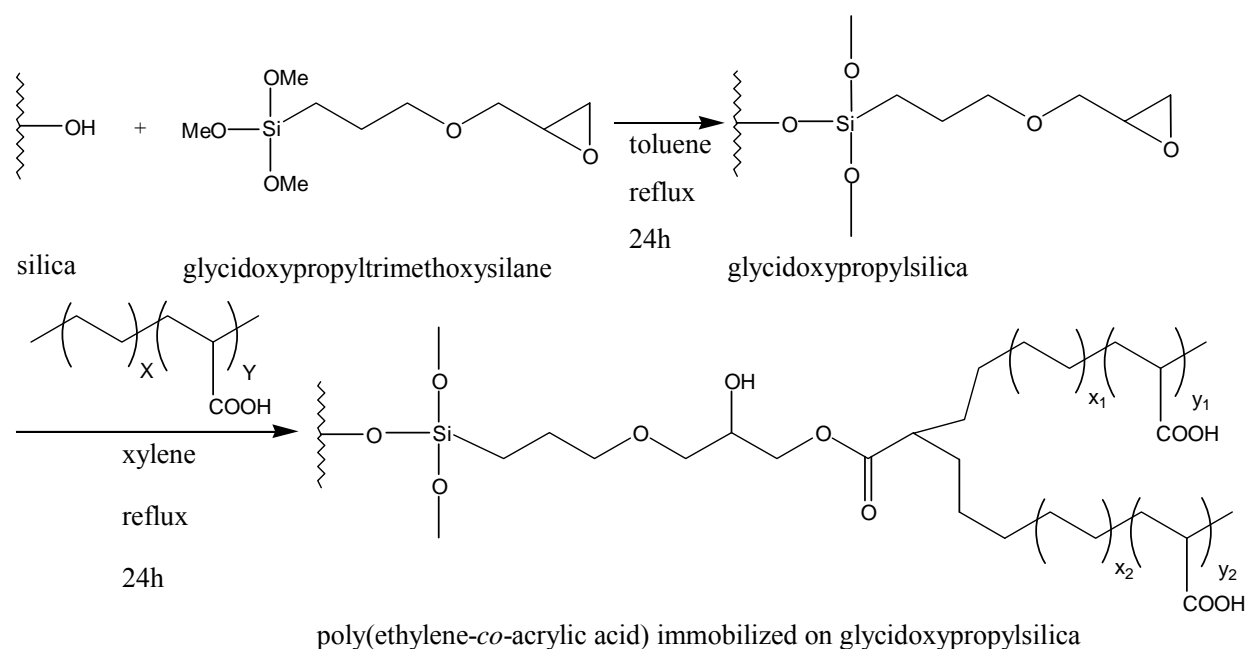


Figure 4b Reaction scheme for the synthesis of chromatographic sorbent **D**

using diisopropylcarbodiimide and hydroxybenzotriazole as catalysts. Sorbent **D** was synthesized by binding the copolymer with an acid mass fraction of 5 % to 3-glycidoxypropylsilica via an esterification reaction. Thus, the only difference between sorbent **A** and **D** in the synthesis is the use of a different spacer group. Elemental analysis of the corresponding chromatographic separation materials gave the carbon mass fraction, thus the degrees of immobilization. The employed silica gel with a particle size of 3 μm and a pore size of 300 \AA possesses a specific surface area of 200 m^2 per gram [27].

Thereby, the molarity of immobilized polymer on the silica gel surfaces was calculated, see Table 1. Sorbent **D** reveals the lowest immobilized polymer molarity, sorbent **C** the highest.

4.2 Characterization

The prime property of chromatographic sorbents is percent carbon loading determined by elemental analysis which allows for the calculation of surface coverages, and also helps to predict possible chromatographic behaviors. Yet, by reasonable choosing and separating certain analyte molecule systems one can surely provide direct experimental information about the behavior and properties of novel sorbent materials. For example, nitrogen groups containing molecules might interact with silanol groups, or analytes with the same polarity but different shapes are retarded differently. Nevertheless, such experiments provide only indirect indications about the potential morphology of chromatographic sorbents. The unambiguous elucidation and the profound understanding of the structure, conformation, and organization of alkyl-modified silica gel surfaces is requisite to, on the one hand a deeper understanding of the retention mechanism, on the other hand also the design of improved novel chromatographic sorbents and their expedient application. Lately, advances in modern analytical chemistry allowed for the establishment and routine implementation of spectroscopic tools which admit to gain direct evidence and sound insights into the molecular build-up and behavior of new materials. For example, Fourier transform infrared spectroscopy, Raman spectroscopy,

fluorescence spectroscopy, X-ray experiments, and neutron scattering studies yield information about alkyl chain conformations, motions, and cooperative associations. Certainly, results obtained from NMR spectroscopic experiments offer the richest and most comprehensive picture of the morphology in chromatographic sorbent materials. Therefore, a thorough ^{29}Si and ^{13}C solid-state NMR investigation was performed in order to characterize the novel polymer based chromatographic sorbent materials. Also, the results of another powerful spectroscopic method, ellipsometry, are presented which revealed a supplementary insight into the surface morphology of these polymer based sorbents. Also, contact angle measurements were performed to elucidate the surface polarity of the polymeric modified silica surfaces.

4.2.1 Solid-state NMR spectroscopy

As explained above to understand the chromatographic properties of chromatographic sorbents, an extensive investigation of the surface modification and alkyl chain order and morphology is of significance. Among the most powerful methods of investigating organic molecules bound to silica supports are solid-state ^{13}C and ^{29}Si cross polarization/magic angle spinning (CP/MAS NMR) spectroscopy. Especially solid-state ^{13}C and ^{29}Si CP/MAS NMR spectroscopy have earlier been used to obtain information about the surface chemistry and the alkyl chain arrangement of the stationary phase [28-30]. Molecular motion in alkylsilanes covalently bound to silica and different mobilities in polyethylene chains were revealed by ^{13}C solid-state NMR spectroscopy

before [31]. Different mobilities in alkylsilanes were also observed when they were covalently bound to different inorganic substrates than silica [32-34]. Besides NMR also IR methods revealed different mobilities in alkyl chains [35]. The fact that the order and mobility of alkyl chains in stationary phases play a major role in the retention mechanism was proved by ^{13}C NMR spectroscopy [36-45]. Two major types of alkyl chain arrangements in C_{30} stationary phases arising from different methylene group conformations were revealed by employing the 2D WISE NMR technique, mobile *gauche* and rigid *trans* aligned alkyl chains [46]. Earlier it was observed that increased shape selective properties were present in chromatographic sorbents when they were prepared according to a polymeric surface modification chemistry, and also when increasing bonding density and increasing alkyl chain lengths were employed [4, 7, 8]. When correlating these findings with the chromatographic performance one can generally state that the more rigid *trans* aligned alkyl chains are present the better the separation abilities for shape constrained solutes [45].

4.2.1.1 ^{29}Si solid-state NMR spectroscopy

The distinct chemical shifts of silyl species makes their assignment in ^{29}Si NMR spectra facile. Bare silica consist of bulk siloxane units (Q^4 group at -110 ppm), silanols (Q^3 groups at -101 ppm), and also geminal silanols (Q^2 groups at -92 ppm). Generally, the more crosslinking oxygens are present the more the chemical shift is high-field shifted. Covalently bound trifunctional silane species contain one oxygen atom less and are

therefore down-field shifted. Fully crosslinked T^3 groups appear at -65 ppm, T^2 groups at -56 ppm, and T^1 groups at -48 ppm. Figure 5a shows the structures and chemical shifts of the different silyl species. From a comparison of the solid-state ^{29}Si CP/MAS NMR spectra of bare silica and with 3-aminopropyltriethoxysilane respectively 3-glycidoxypropyltrimethoxysilane modified silica (see Figure 5b) two significant signals at -101 ppm and -110 ppm indicating the typical Q^3 and Q^4 groups were observed in all spectra. However, the signal at -92 ppm, representing the Q^2 groups, is significantly

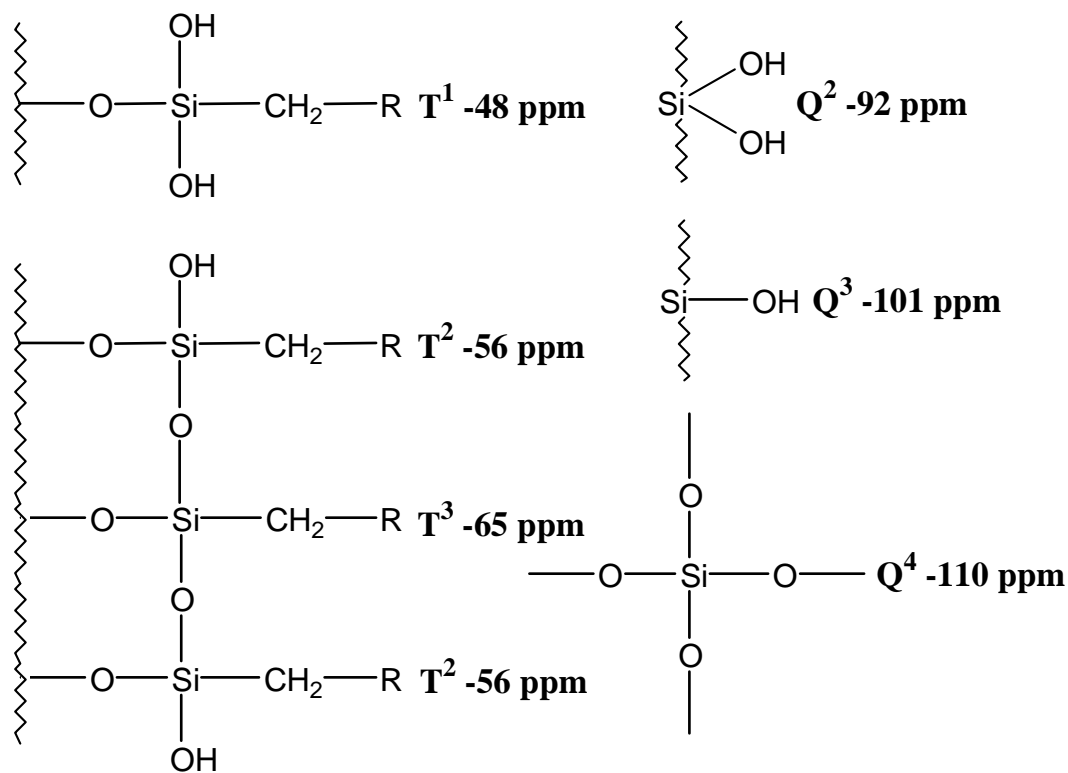


Figure 5a Nomenclature and chemical shifts of silyl species

reduced when the bare silica is modified with 3-aminopropyltriethoxysilane, respectively 3-glycidoxypropyltrimethoxysilane. Even though it is not possible to quantify the ratio of

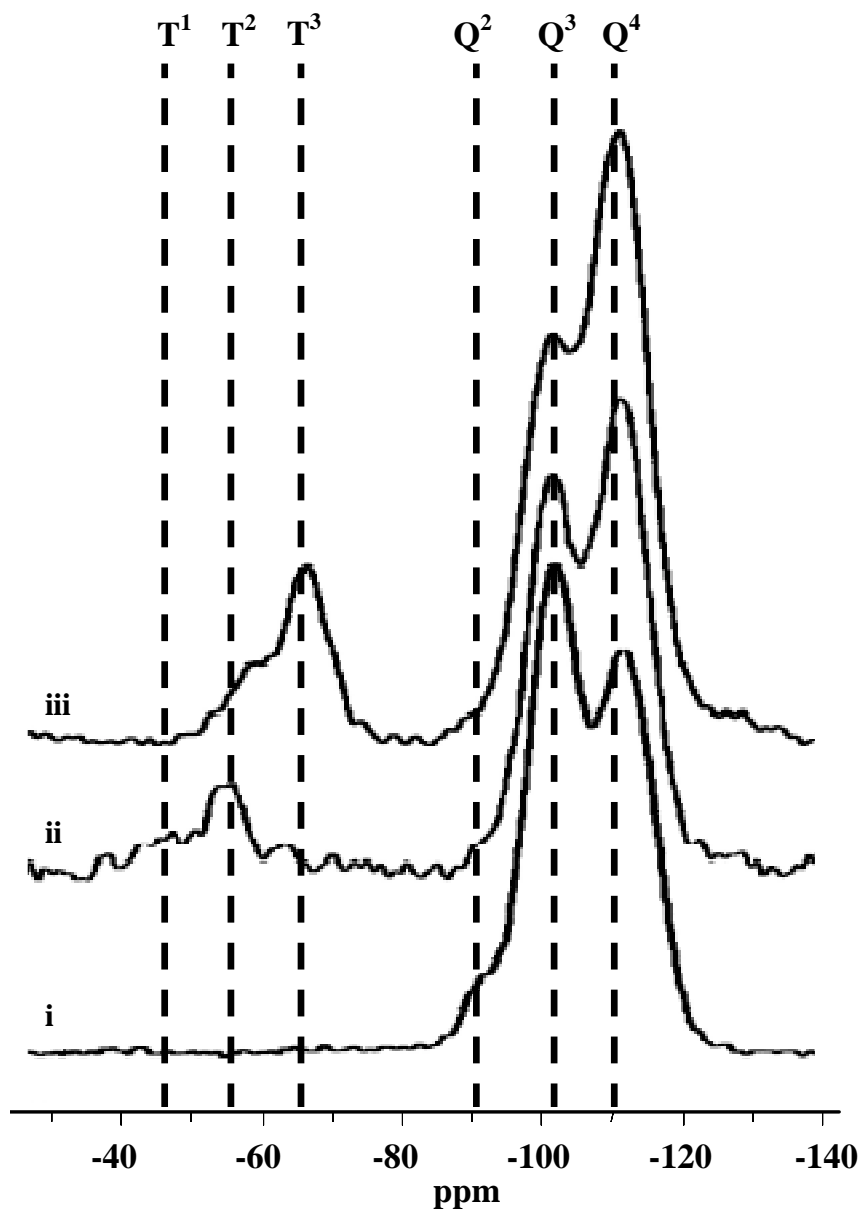


Figure 5b ^{29}Si CP/MAS NMR spectra. *i*: Bare silica. *ii*: Glycidoxypropylsilica. *iii*: Aminopropylsilica

Q^3 and Q^4 groups in a cross polarization NMR experiment, a quantification of the ratio of Q^2 and Q^3 groups is possible [30]. The build-up of ^{29}Si magnetization is carried out in a definite contact period in which the energy levels of abundant ^1H and rare ^{29}Si spins are

identical. The build-up of ^{29}Si magnetization then occurs at a rate defined by the cross relaxation constant T_{SiH} whereas the fall-off is a result of the decrease in the spin-locked ^1H magnetization which decays with the proton spin-lattice relaxation time in the rotating frame $T_{1\rho\text{H}}$. The contact time for a maximum magnetization is dependent upon the distance between protons and ^{29}Si nuclei and their mobility. For ^{29}Si species which are likewise mobile and have the same distance to protons the same contact time (thus the cross relaxation constant T_{SiH} and the proton spin-lattice relaxation time in the rotating frame $T_{1\rho\text{H}}$ are in the same order) can be used to transfer magnetization. Consequently, the signal intensity of similar ^{29}Si species (Q^2 and Q^3 groups) can be quantitatively compared. The absence of the most reactive Q^2 groups in the 3-aminopropylsilica and the 3-glycidoxypropylsilica indicates a low degree of residual silanol activity of all synthesized sorbents **A**, **B**, **C**, and **D**. Furthermore, from the solid-state ^{29}Si CP/MAS NMR spectra of the 3-aminopropylsilica eminent signals were observed at -56 ppm and -65 ppm (T^2 and T^3 groups) whereas no signal was detected at -48 ppm (T^1 group) pointing out the absence of mono attached 3-aminopropylsilyl species to the silica. By simulating Gaussian peaks over the T^2 and T^3 groups, a quantification of the corresponding signal area was made, i.e. peak deconvolution, showing 30 % and 70 % for the T^2 and T^3 groups, respectively. Here, similarities in contact times for T groups allow the quantitative evaluation of ^{29}Si CP/MAS NMR spectra. It is known that loss of stationary phase from a chromatographic sorbent can take place due to hydrolysis of the T groups binding the stationary phase to the support. Hence, in acidic and basic environment this would diminish the chromatographic performance from a sorbent with high amounts of T^1

groups. Therefore, the absence of T¹ groups present in the sorbents **A**, **B**, and **C** proves the successful surface polymerization and furthermore implies a high stability of these phases. The low intensity of T groups present in the ¹³C solid-state CP/MAS NMR spectrum of the 3-glycidoxypropylsilica made a quantification of the T groups impossible. However, it was clearly observed that an incomplete surface polymerization took place due to the presence of T¹ groups as well as the low concentration T³ groups. This data confirmed the low surface coverage found in the elemental analysis. From the degrees of immobilization along with the quantified silyl species the calculation of the surface coverages is possible (see Table 2).

Table 2 Properties of the chromatographic sorbents

	degree of immobilization	silyl species content (%)		surface coverage (μmol/m ²)
aminopropylsilica	2.9	T ¹	0	0
		T ²	30	1.66
		T ³	70	5.36
				} 7.02
glycidoxypropylsilica	1.5	T ¹	25	0.44
		T ²	66	1.04
		T ³	9	0.2
				} 1.68

4.2.1.2 ^{13}C solid-state NMR spectroscopy

In the solid-state ^{13}C CP/MAS NMR spectra (Figure 6a) one main signal at 30 ppm, corresponding to the methylene carbon units, is observed for sorbents **B** and **C** while two signals at 30 ppm and 32.8 ppm can be found for sorbents **A** and **D** (Figure 6b).

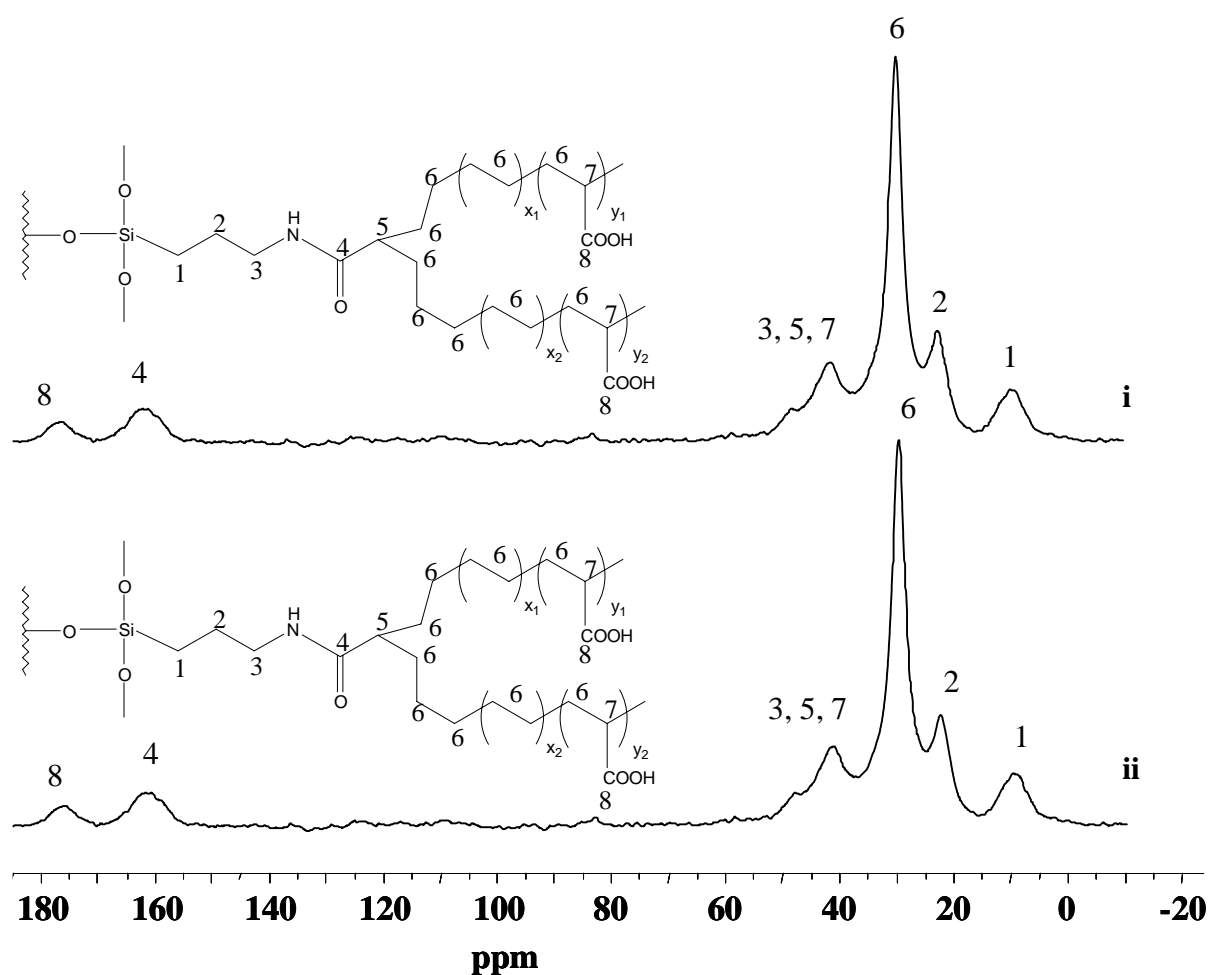


Figure 6a ^{13}C CP/MAS NMR spectra of chromatographic sorbents **B** (i) and **C** (ii)

Similar signal splitting occurs for the methylene moieties in C_{30} phases which were assigned via the solid-state 2D WISE experiment to disordered *gauche* (30 ppm) and more ordered *trans* (32.8 ppm) conformations [46]. A high degree of *trans* ordered conformations benefits the selectivity of *cis/trans* analytes; i.e. stationary phases that separate *cis/trans* analytes are shape selective in regard to shape constrained solutes [8].

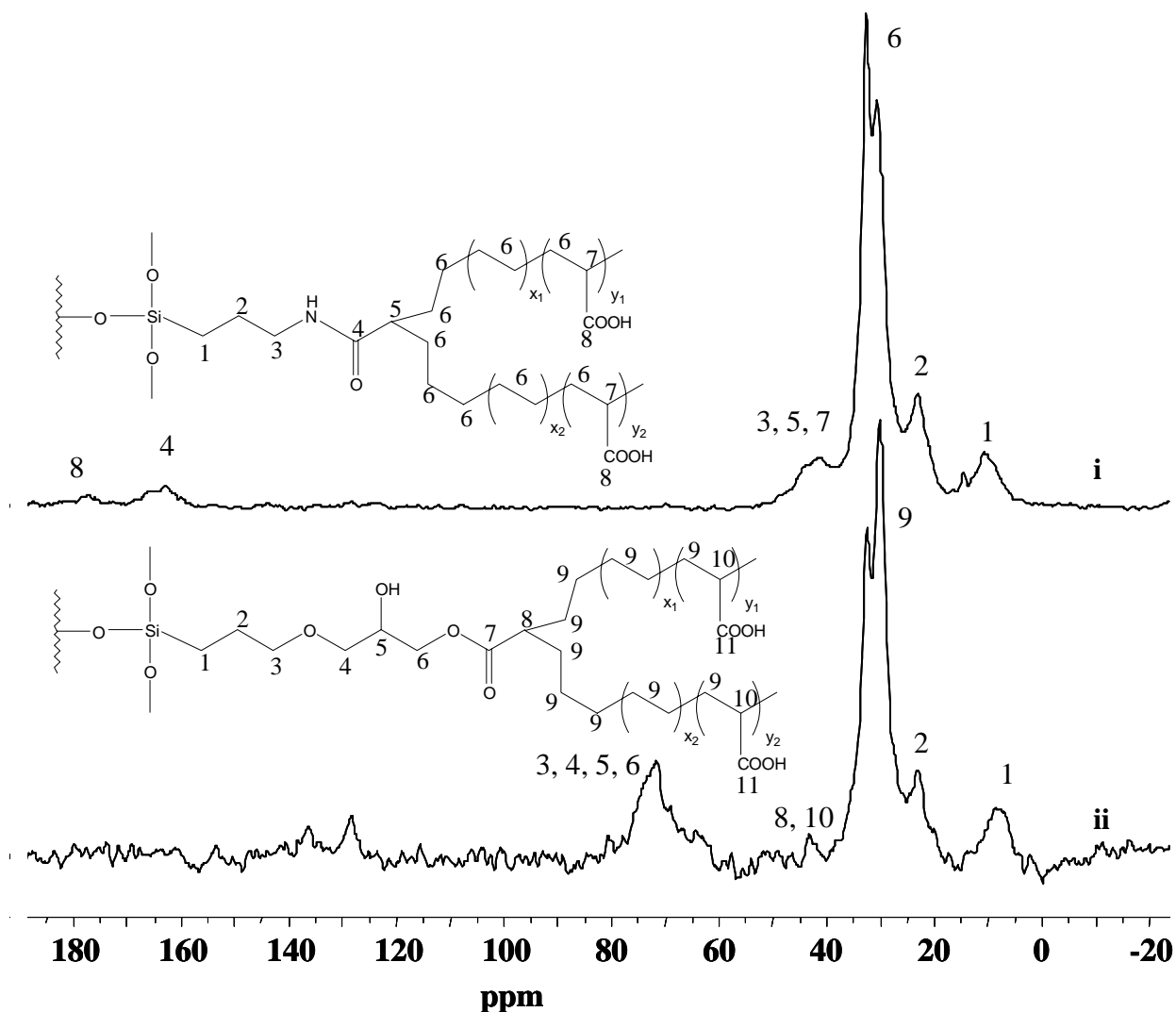


Figure 6b ^{13}C CP/MAS NMR spectra of chromatographic sorbents A (i) and D (ii)

In the solid-state ^{13}C CP/MAS NMR spectra of phases **B** and **C** only signals at 30 ppm were observed, implying that mobile alkyl chains in *gauche* conformation dominated. Figure 7 shows a visualization of the two different *trans* and *gauche* conformations. To quantify the *trans/gauche* ratio in sorbents **A** and **D**, which differ only in the spacer molecule used to attach the copolymer to the support, ^{13}C HPDEC solid-state MAS NMR spectra were recorded. Due to the magnetization transfer in a CP experiment, here from ^1H to ^{13}C , a general quantification of the carbon signals cannot be performed. In a HPDEC experiment the ^{13}C nuclei are directly excited and hence quantification is possible. However, more scans as well as longer pulse repetition times are needed in HPDEC measurements compared to the CP measurements due to the low abundance and long T_1 relaxation times of the ^{13}C species. From the peak deconvolution a *trans/gauche* ratio of 44/56 for sorbent **A** and of 48/52 for sorbent **D**, respectively, was calculated. Even

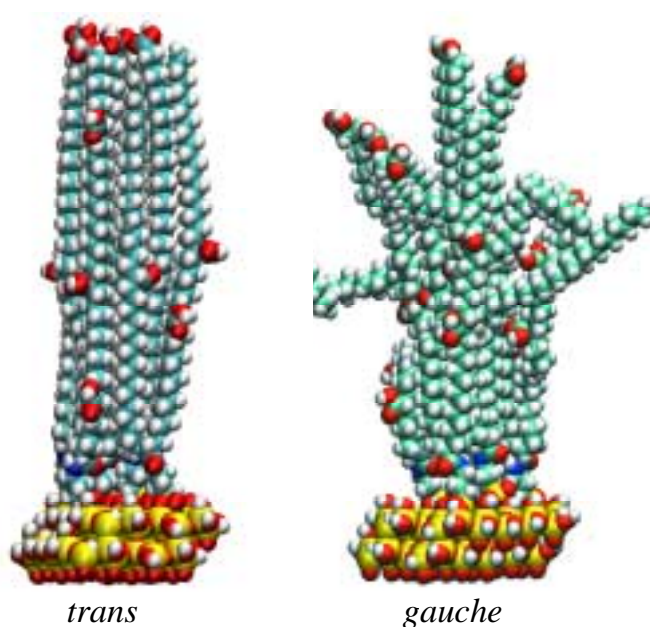


Figure 7 Visualization of rigid *trans* and mobile *gauche* aligned alkyl chains

though sorbent **D** has a significantly lower carbon content than sorbent **A**, both sorbents revealed similar amounts of mobile and rigid aligned alkyl chains. This proves that the effect of ligand density does not influence the alkyl chain conformation of the investigated copolymeric stationary phases. Previous studies, indeed, showed a dependence of the methylene moiety conformations from surface coverage, alkyl chain length, temperature and other conditions [7, 8, 44, 45]. The influence of various experimental factors on the retention mechanism, however, will be discussed later in chapter 5.

The distribution of the respective alkyl chain conformations *trans* and *gauche* on the silica surface was proven before to follow a certain pattern. The method employed was spin-diffusion, a solid-state NMR technique which has a large practical application for the determination of the homogeneity of polymers and has mainly been conducted to determine the phase structure of organic ligands [47-51]. When applied on C₃₀ stationary phases it was found that the two different conformations *trans* and *gauche* appear in distinct domains of certain sizes [52]. It was investigated before if the same mobility distribution, i.e. distinct domains, appeared in the polymer based stationary phase which displayed similar peak splitting in the ¹³C chemical shift of the main alkyl chains [53]. A strong fact also spoke for the existence of domains showing different mobilities on the silica surface. Assuming the case that an exchange process between *trans* and *gauche* conformations within one alkyl chain would take place, due to an NMR life time within the NMR time scale of approximately 1/75 MHz which equals 13.3 ns, the ¹³C solid-state

NMR spectrum would reveal only an averaged signal at 295 K. Thus the copolymeric stationary phase with the lowest acid mass fraction which revealed rigid and mobile aligned alkyl chains on the silica surface was investigated using ^{13}C spin-diffusion NMR spectroscopy to reveal whether the methylene moieties form distinct island clusters, as found for C_{30} sorbents, or whether there is a homogeneous distribution of the rigid respectively mobile aligned chains. To successfully perform this experiment, spheres of different mobilities must be present in the polymer. A pulse which saturates the mobile and rigid sphere is applied first, which is monitored in the spectrum where both parts are visible. Then due to a suitable pulse sequence (which makes use of different relaxation times), a selection of magnetization is conducted, which induces magnetization only in the mobile part resulting in just one signal in the ^{13}C NMR spectrum [54, 55]. However, dipolar interactions cause a transfer of magnetization in between neighboring nuclei, thus spin-diffusion is taking place. During a certain diffusion mixing time t_m , an increase in magnetization of the rigid component can be detected while the magnetization of the mobile component is decreasing. This effect can be monitored in the NMR spectrum and depending on t_m the corresponding signal intensity is increasing, respectively decreasing. At a certain mixing time an equilibrium state is reached. Depending on how fast the equilibrium is attained, one can draw a conclusion about the size of the different spheres, respectively domains. The smaller the spheres on the surface the faster spin-diffusion can take place. From the intensity course of the corresponding signals one can calculate the sizes of the domains making use of previously developed computer models [52]. A computer program developed earlier by Raitza et al. for the simulation of results obtained

by ^{13}C spin-diffusion solid-state NMR measurements was used. This program was also successfully applied for C_{30} chromatographic sorbents [52]. The time dependent course of the spin-diffusion effect which is subject to the size distribution of the domains and the diffusion coefficient can be simulated and visualized. The declining magnetization of the mobile component is compared with the experimental NMR parameters, then the relative size ratio is assessed. In order to accurately apply the computer model the size of the diffusion constant must be properly chosen. This issue was addressed earlier and diffusion constants in the range of 10 - 100 $\text{\AA}^2/\text{ms}$ were determined [56-58]. A diffusion constant of 15 $\text{\AA}^2/\text{ms}$ for the mobile component and 80 $\text{\AA}^2/\text{ms}$ for the rigid component were employed. These values were applied before to determine the domain sizes in pure polyethylene fibers [59]. Thereby, Wegmann et al. found a domain size of 16 (± 2) nm for the mobile component and a domain size of 3.2 (± 0.4) nm for the rigid component [53]. These results together with the ellipsometric measurements described in the following paragraph 4.2.2 were used to derive a refined model of the surface morphology of chromatographic sorbent **D**.

4.2.2. Ellipsometry

Ellipsometric spectroscopy is used to obtain information about the layer thickness of the alkyl chains [60, 61]. For example, the in-situ characterization of thin polymer films for applications in chemical sensing of volatile organic compounds is possible by spectroscopic ellipsometry [62, 63]. However, spherical silica particles cannot be used for

these measurements, therefore the copolymeric stationary phases were also immobilized on planar silica wafers using the same chemistry as to immobilize them on silica particles. The same nomenclature **A**, **B**, **C**, and **D** was used for the differently modified wafers. The layer thickness and alkyl chain conformation on both the silica wafers and the silica particles can be assumed to be similar [61]. The different copolymers were investigated by null ellipsometry which is a precise method to determine the thickness of organic polymeric layers on inorganic substrates. The thicknesses of the immobilized copolymers on silica wafers were measured by null ellipsometry as this method is very sensitive and highly accurate for the measurement of thin layers. The principle of ellipsometry is the following: A change in the polarization state of light is measured in order to characterize thin films. Therefore, a well defined polarization state of incident light is created. Then, the Fresnel coefficients r_p and r_s are calculated according to that change. This allows for the derivation of the optical constants of the surface. Figure 8 schematically shows the

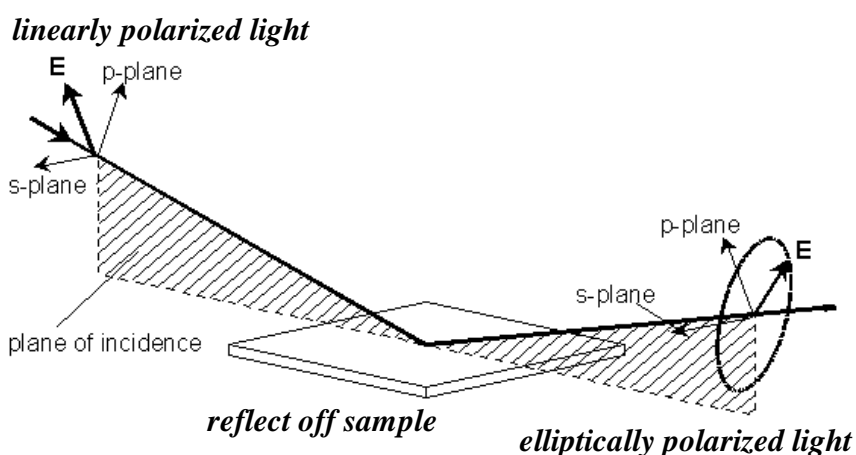


Figure 8 Schematic principle of ellipsometry

principle of ellipsometry.

The two ellipsometric angles Ψ and Δ are determined during the measurement and the changes upon reflection are described by these two parameters [62]. Thereby, $\tan \Psi$ describes the the change of the amplitude during reflection, and Δ is the difference of the retardation of the parallel (p) and perpendicular (s) polarized light before and after reflection. The thickness of polymeric layers can be determined by the evaluation of the complex ellipsometric parameter ρ , which is defined according to the following equation (1):

$$\rho = \tan \Psi \cdot e^{i\Delta} = r_p / r_s \quad (1)$$

where r_p and r_s denote the Fresnel reflection coefficients for the p- and s-polarized light. For the determination of the layer thickness with the null ellipsometer the refractive index of the polymeric layer must be fixed. A refractive index of 1.40 was estimated for the polymeric layers and the model for thickness was fitted to the measured ellipsometric angles. The layer thicknesses found by ellipsometry are plotted in Figure 9. The mean value and the standard deviation are also plotted. The measured copolymeric layer thicknesses on wafers **B** and **C** were in agreement with the empirical formula for the chain lengths and the mobile *gauche* alkyl chain conformation of the immobilized copolymers (Table 1, Figure 9). The mean value of the layer thickness on wafers **B** and **C** was found to be 6.5 (\pm 0.5) nm and 4.3 (\pm 0.3) nm. The layer thickness on wafer **A** was found to be 10.6 (\pm 0.3) nm, and on wafer **D** an average thickness of 9.9 (\pm 0.1) nm was measured.

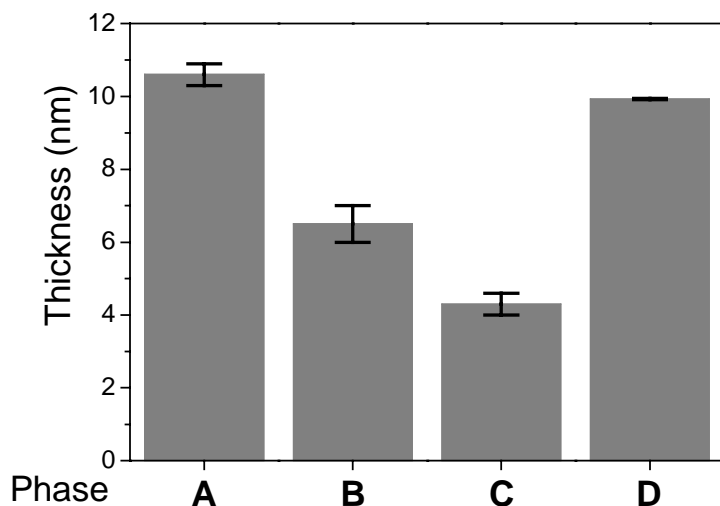


Figure 9 Phase thickness on the silica surface as determined from ellipsometric measurements on wafers **A**, **B**, **C**, and **D**. Mean value of thickness are plotted as bars and standard deviation as error bars

The maximum chain l_{\max} of an individual fiber, the contour length, corresponds to an overall all-*trans* conformation, and can be calculated according to the following formula (2) [46]:

$$l_{\max} = N l \sin (\Theta/2) \quad (2)$$

C-C bonds have a bonding length l of 0.154 nm, the complementary angle in alkane chains in all-*trans* conformation is $\Theta = 111.5^\circ$ [51]. $N = 245$ is the number of bonds derived from the mean molecular weight of the copolymer with the lowest mass fraction

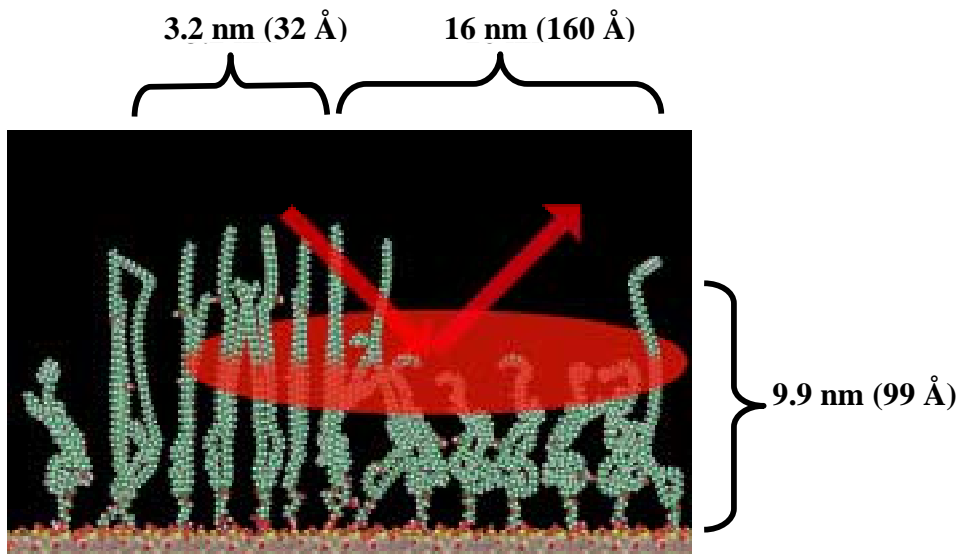


Figure 10 Visualization of the surface morphology of chromatographic sorbent **D**. Due to the existence of domains, the ellipsometric measurements reveal just mean layer thicknesses. The red circle visualizes the measuring spot; the incoming laser and the outgoing elliptical polarized light after interacting with the copolymeric layer are shown as red arrows

of acid. Thus, a contour length of $l_{\max} = 31.2$ nm was calculated. The measured layer thicknesses on wafers **A** and **D**, however, are threefold smaller than the calculated value for an alkyl chain in all-*trans* conformation. Assuming that any carboxylic acid group (which are randomly distributed along the copolymer) can bind to the glycidoxypropyltrimethoxysilane modified silica surface respectively aminopropyltriethoxysilane modified silica, still a fiber length of approximately 15 nm can be expected. Therefore we presume that a coverage of at most 70 % is estimated as a result of gaps between the alkyl chain clusters with different mobilities on the silica surface. This confirms the results obtained from the ^{13}C spin-diffusion experiments.

Domains with only all-*trans* conformed chains and domains with more mobile *gauche* aligned alkyl chains exist on the silica surface. Thus, a model of the surface morphology can be derived. The ellipsometric measurements revealed a polymer layer thickness of 9.9 nm (99 Å) in sorbent **D**. Along with the above described results obtained from the spin-diffusion measurements the surface morphology of chromatographic sorbent **D** is visualized which is shown in Figure 10. The size of the rigid *trans* domain is the predominant factor for superior separation abilities of the chromatographic sorbent **D** towards complex mixtures of stereoisomers as proven before for C₃₀ sorbents. The similarity of the surface morphology of C₃₀ sorbents and the investigated poly(ethylene-*co*-acrylic acid) sorbent **D** is therewith proven.

4.2.3 Contact angle measurements

The shape and size of a sessile drop resting on a horizontal surface allows for the determination of the surface polarity [64, 65]. Figure 11 shows a water droplet on a polar and on a non-polar surface.

Contact angle measurements on all wafers **A**, **B**, **C**, and **D** were performed. Valuable information about the surface polarity could be derived. A dependence of the surface polarity on the acid mass fraction in the polymer was found. A reduced contact angle of wafer **B** compared to wafer **C**, thus an increase in the surface polarity indicates the influence of the acid mass fraction in the copolymer (Table 3). Both wafers **A** and **D**

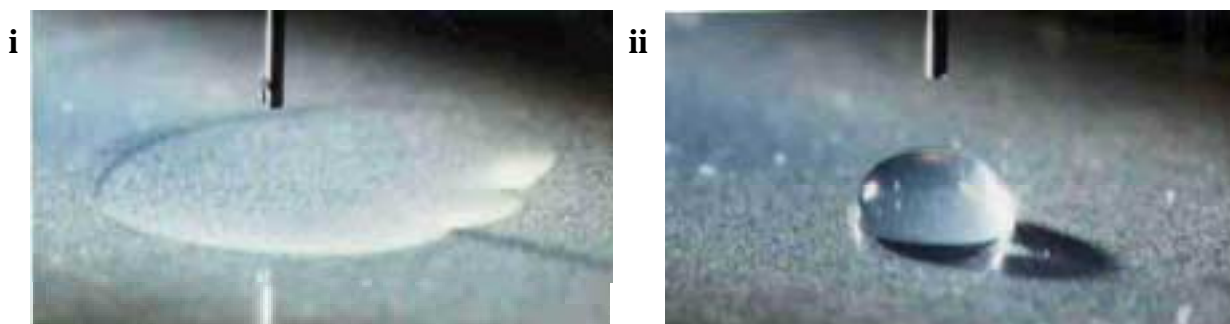


Figure 11 Deposition of a water droplet on a horizontal surface to measure the surface polarity revealing a polar (**i**) and a non-polar (**ii**) surface

revealed, however, a contact angle between the angles measured for wafer **B** and **C**. The rigid *trans* aligned alkyl chains in the copolymer with the lowest acid mass fraction must therefore have an impact on the surface polarity. Due to the rigid conformation the water droplet is in contact with the more nonpolar part of the polymer backbone resulting in an intermediate contact angle for wafers **A** and **D**.

Table 3 Properties of the modified SiO_2 species

chromatographic sorbent (respectively wafer)	spacer	alkyl chain conformation	contact angle
A	APS	<i>trans/gauche</i>	67.7 (± 1.0) °
B	APS	<i>gauche</i>	103.4 (± 8.1) °
C	APS	<i>gauche</i>	54.8 (± 2.6) °
D	GOPS	<i>trans/gauche</i>	80.0 (± 1.0) °

5 APPLICATION IN HPLC AND DEPENDENCE OF THE SEPARATION MECHANISM

Chromatography gives direct experimental proof of conclusions drawn by spectroscopic investigations on the stationary phase morphology. The interactions of various kinds of solutes with the stationary phases as foreseen by NMR and other techniques are confirmed. Early theoretic explanation in chromatography described retention to be caused by hydrophobic effects excluding solute shape effects [66-68]. Then, the United States Environmental Protection Agency (EPA) described method 610 for the separation of priority pollutant PAHs by specifying the use of a particular C₁₈ column with which one was able to achieve a separation of these in terms of hydrophobicity alike compounds [69]. Later the term “shape selectivity” was created to describe the ability of chromatographic sorbents to differentiate between solutes based on their shape [3]. Numerous publications described the retention mechanism to be affected by the alkyl chain morphology [70]. An important group of compounds that was difficult to separate with RP chromatographic sorbents were provitamin A isomers which differ significantly in their biological activity [71]. For quantitative evaluation of these effects the development of an efficient separation method was a matter of great importance. The knowledge derived from the research on shape selectivity led to the development of a tailored chromatographic sorbent material for the separation of *cis/trans* β-carotene isomers [72]. This “carotenoid column” contains long alkyl chains and has widely been

applied for the described separation problems [73, 74]. The successful separation mechanism was proven to be caused by a distinctive distribution of rigid and mobile aligned C₃₀ alkyl chains on the silica surface. Extensive research regarding the influence of different variables on the retention mechanism of C₃₀ based chromatographic sorbents was done [45].

The results obtained from investigations on poly(ethylene-*co*-acrylic acid) copolymeric stationary phases are presented in this study. In addition to the characterization of the to C₃₀ sorbents alike surface morphology obtained by using different spectroscopic methods, which was described in chapter 4, the influence of several factors on the retention mechanism was investigated. A direct correlation of spectroscopic evidence with practical chromatographic separations of analyte systems is given.

5.1 Influence of different acrylic acid mass fractions in the copolymer

Figure 12 shows the structure formulas of the xanthophylls isomers lutein and zeaxanthin and of the main geometric isomers of β -carotene [75, 76]. The only difference between lutein and zeaxanthin is the position of the double bond in the cyclohexene rings, which, however, affects the polarity of the neighboring hydroxyl group making zeaxanthin more hydrophobic.

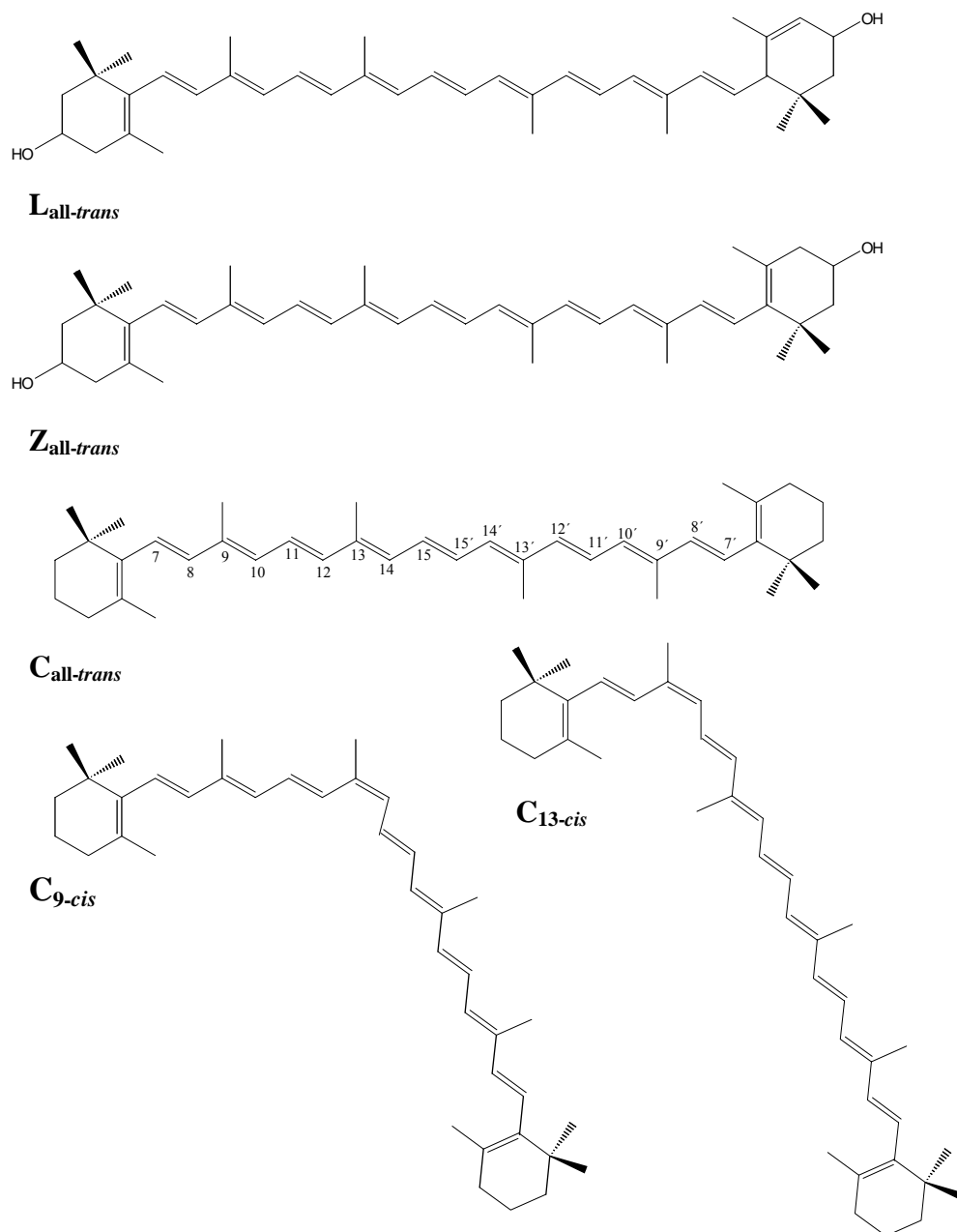


Figure 12 Schematic diagram of the structures of all-trans lutein ($L_{all-trans}$) and all-trans zeaxanthin ($Z_{all-trans}$); and of 13-cis (C_{13-cis}), 9-cis (C_{9-cis}), and all-trans β -carotene ($C_{all-trans}$)

Significant differences in the retention behavior are obvious comparing the chromatograms obtained from the sorbents **A**, **B**, and **C** from the elution of either the

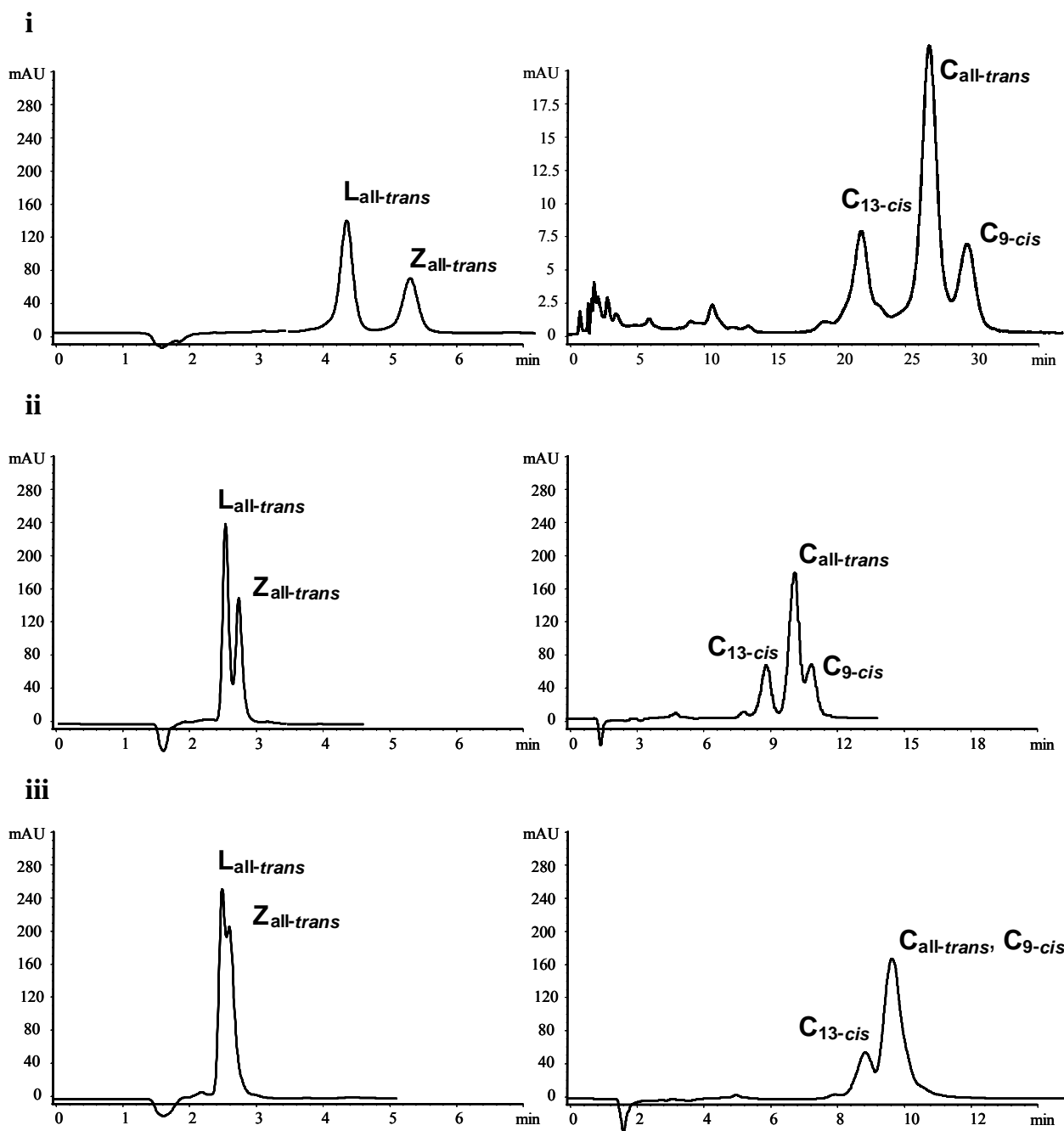


Figure 13 Chromatograms of all-trans lutein ($L_{all-trans}$) and all-trans zeaxanthin ($Z_{all-trans}$) as well as of 13-cis (C_{13-cis}), 9-cis (C_{9-cis}), and all-trans β -carotene ($C_{all-trans}$) eluted from chromatographic sorbents A (i), B (ii), and C (iii) using a mobile phase composition of methanol/water 97.5/2.5 (v/v)

xanthophylls isomers lutein and zeaxanthin or the *cis/trans* β -carotene isomers with a mobile phase composition of methanol/water (97.5/2.5, v/v), see Figure 13. The elution times were significantly longer when the β -carotene *cis/trans* isomers C_{13-cis} , $C_{all-trans}$, and C_{9-cis} were eluted from sorbent **A** compared to sorbents **B** and **C**. This is evident in view of the higher degree of immobilized stationary phase for phase **A** as well as the lower amounts of polar carboxylic acid residues, see Table 1. All the sorbents separated analytes C_{13-cis} and $C_{all-trans}$ which is believed to be caused mainly by the differences in hydrophobic interactions between the analytes and the stationary phases. Sorbent **C** was not able to separate analytes $C_{all-trans}$ and C_{9-cis} . From a comparison of the selectivity between analytes $C_{all-trans}$ and C_{9-cis} obtained from sorbents **A**, **B**, and **C** the best selectivity was obtained from the sorbent **A**. Hence the best selectivities were obtained from the stationary phase with the lowest mass fraction of acrylic acid and the highest content of *trans* conformed alkyl chains in the copolymer, see chapter 4 for the characterization of the stationary phase alkyl chain conformation of the synthesized sorbents. Thus, the separation of the *cis/trans* analytes C_{13-cis} , C_{9-cis} and $C_{all-trans}$ is evidently dependent both on strong hydrophobic interactions as well as on a high degree of rigid *trans* conformed alkyl chains in the stationary phase. From a comparison of the separations of the structure analogues **L** and **Z** (see Figure 13) it can be seen that the analytes were separated when they were eluted with a mobile phase composition of methanol/water (97.5/2.5, v/v) from all the sorbents **A**, **B**, and **C**. These analytes were baseline separated when eluted from sorbent **A** ($\alpha = 1.35$). The selectivity factors

obtained when the analytes were eluted from sorbents **B** and **C** were significantly lower, 1.21 and 1.10, respectively.

5.2 Influence of the spacer molecule

5.2.1 Separation of carotenoid isomers

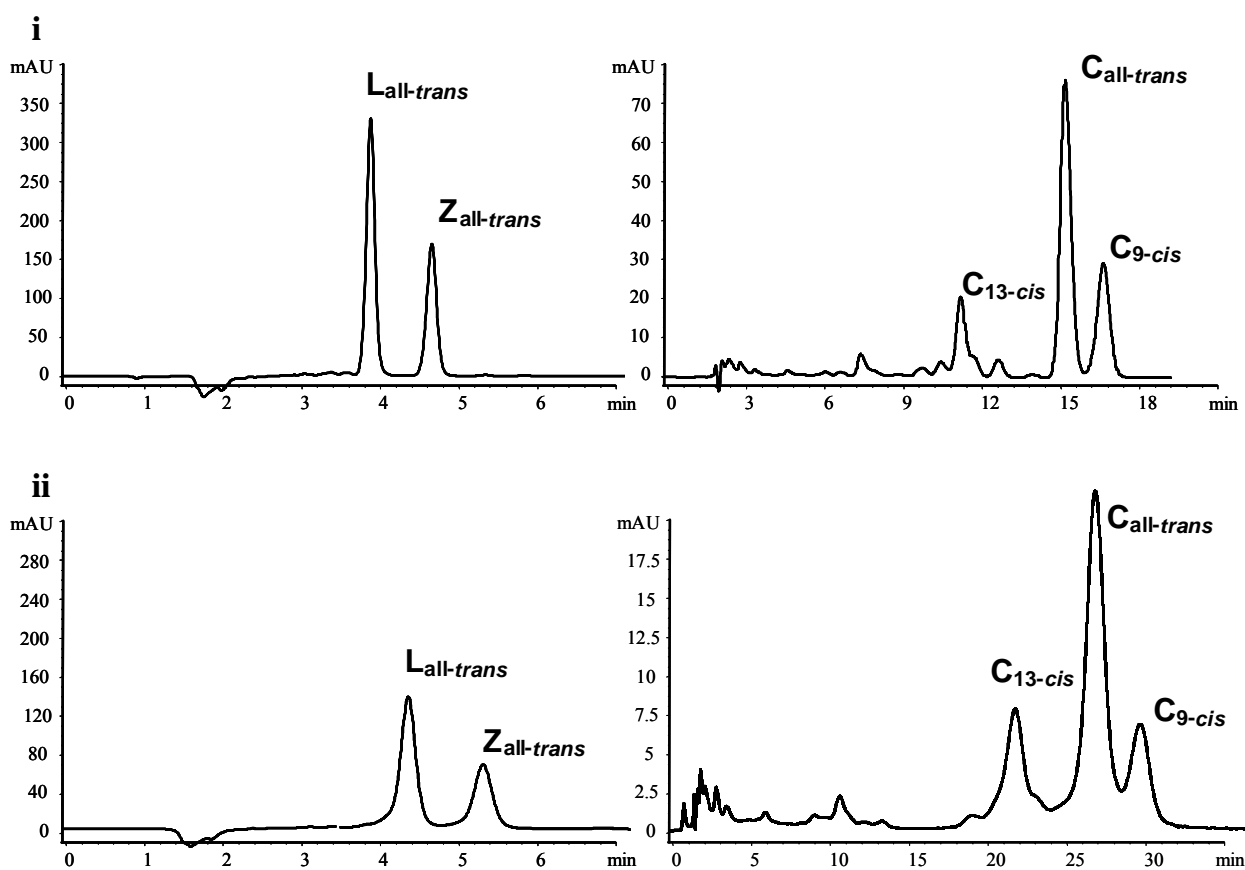


Figure 14 Chromatograms of all-trans lutein ($L_{all-trans}$) and all-trans zeaxanthin ($Z_{all-trans}$) as well as of 13-cis (C_{13-cis}), 9-cis (C_{9-cis}), and all-trans β -carotene ($C_{all-trans}$) eluted from sorbent **A** (i) and **D** (ii) using a mobile phase of methanol/water 97.5/2.5 (v/v)

From a comparison of the selectivity between analyte **C**_{13-*cis*} and **C**_{all-*trans*} obtained from sorbents **A** and **D**, it was observed that the selectivity obtained from sorbent **D** ($\alpha = 1.41$) was superior compared to sorbent **A** ($\alpha = 1.25$), see Figure 14. This is most likely due to unfavorable interactions with the nonreacted amino groups present on the silica surface in sorbent **A**. These significant differences in selectivity between the analytes proved that the change of spacer caused a change of the retention mechanism as well. Both sorbents **A** ($\alpha = 1.35$) and **D** ($\alpha = 1.33$) baseline separated analytes **L** and **Z**. Even if the selectivity was slightly better from sorbent **A**, the resolution (R_S) was significantly better for sorbent **D**, $R_S = 2.7$ compared to $R_S = 1.9$, see Figure 14. This is most likely due to the absence of the interactions taking place between the free amino groups present in the sorbent **A** and the analytes.

5.2.2 Separation of SRM 869

Standard reference material (SRM) 869 consists of three planar and non-planar polycyclic aromatic hydrocarbons (PAHs) and was developed to assess the shape selective properties of C_{18} chromatographic sorbents [77]. Figure 15 shows the structures of the three analyte molecules: SRM 869 is composed of phenanthro[3,4-*c*]phenanthrene (**PhPh**), tetrabenzonaphthalene (**TBN**), and benzo[α]pyrene (**BaP**). Non-planar **PhPh** elutes before non-planar **TBN** and planar **BaP**. If **BaP** is retarded longer than **TBN** a

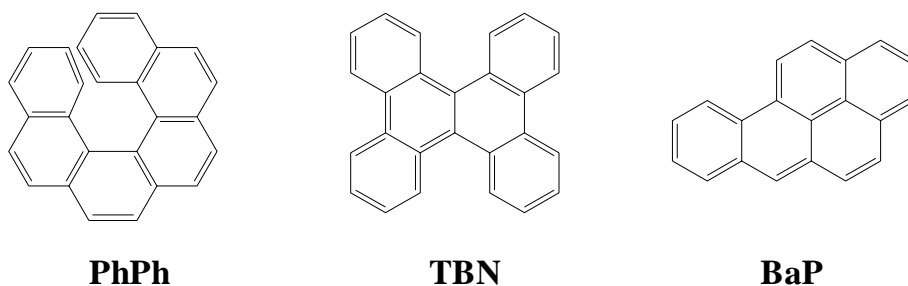


Figure 15 Schematic diagram of the structures of benzo[a]pyrene (**BaP**), phenanthro[3,4-c]phenanthrene (**PhPh**), and 1,2:3,4:5,6:7,8-tetrabenzonaphthalene (**TBN**) of SRM 869

polymeric C₁₈ sorbent with a higher shape selectivity than a monomeric C₁₈ sorbent is indicated. Therefore low values for $\alpha_{\text{TBN/BaP}}$ typically indicate “polymeric-like” retention

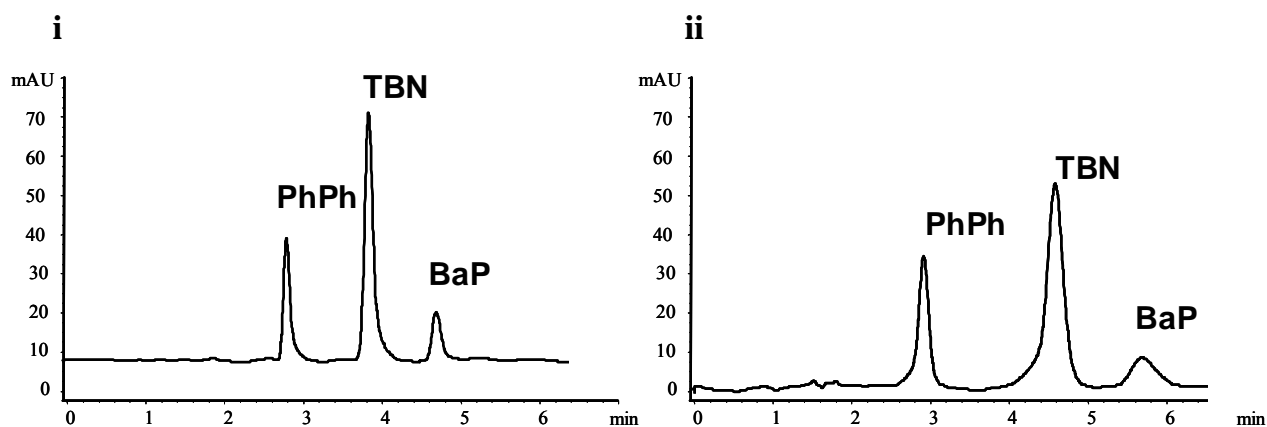


Figure 16 Chromatograms of SRM 869 consisting of phenanthro[3,4-c]phenanthrene (**PhPh**), 1,2:3,4:5,6:7,8-tetrabenzonaphthalene (**TBN**), and benzo[a]pyrene (**BaP**) eluted from the chromatographic sorbents **D** (i) and **A** (ii) using a mobile phase composition of methanol/water 95/5 (v/v)

behavior and high values of $\alpha_{\text{TBN/BaP}}$ indicate “monomeric-like” retention behavior. The “polymeric-like” retention behavior was observed when SRM 869 was eluted from both sorbents **A** and **D**, see Figure 16. Also in this case, the influence of non-reacted amino-groups is evident from the chromatograms. At comparable selectivities the resolution was better for sorbent **D** ($\alpha = 0.73$) compared to sorbent **A** ($\alpha = 0.7$). Since the degree of immobilization of both sorbents **A** and **D** differs, the retention times and thus the retention factors are higher in the case of sorbent **A** ($k_{\text{BaP}}' = 1.91$) compared to sorbent **D** ($k_{\text{BaP}}' = 1.1$). The decrease in resolution of **TBN** and **BaP** in sorbent **A** ($R_s = 1.5$) might be due to the higher surface coverage of this phase compared to sorbent **D** ($R_s = 2.8$). However, the fact that this was also observed for the separation of carotenoids and xanthophylls, it is assumed that the nonreacted amino groups caused the loss of resolution.

5.3 Influence of the mobile phase composition

5.3.1 Separation of xanthophylls and geometric β -carotene isomers

When the analytes $\text{C}_{13\text{-cis}}$, $\text{C}_{\text{all-trans}}$, and $\text{C}_{9\text{-cis}}$ were eluted from sorbent **D** the selectivity of analyte $\text{C}_{13\text{-cis}}$ and $\text{C}_{\text{all-trans}}$ increased. The selectivity between analytes $\text{C}_{\text{all-trans}}$ and $\text{C}_{9\text{-cis}}$, on the other hand, decreased when the water content in the mobile phase was increased, see Tables 4a and 4b. For this reason analyte $\text{C}_{\text{all-trans}}$ is proportionally

Table 4a Retention factor of 13-cis and the corresponding selectivity vs. all-trans (β -carotene) eluting from chromatographic sorbents **A**, **B**, **C**, **D**, and the C_{18} based sorbent with different methanol/water mobile phase compositions

chromatographic sorbent	C₁₈		A		B		C		D	
% MeOH in H ₂ O	k'	α	k'	α	k'	α	k'	α	k'	α
100	10.2	1	6.4	1.25	2.6	1.15	2.4	1.1	3.04	1.38
97.5	22.3	1.04	13.2	1.25	5	1.16	4.6	1.1	5.6	1.41
95	53	1.06	28.5	1.25	10.1	1.17	9.23	1.09	10.7	1.46
92.5			61.7	1.25	21.4	1.17	18.9	1.09	21.9	1.48
90							40.3	1.09		

Table 4b Retention factor of all-trans and the corresponding selectivity vs. 9-cis (β -carotene) eluting from chromatographic sorbents **A**, **B**, **C**, **D**, and the C_{18} based sorbent with different methanol/water mobile phase compositions

chromatographic sorbent	C₁₈		A		B		C		D	
% MeOH in H ₂ O	k'	α	k'	α	k'	α	k'	α	k'	α
100	10.17	1	8	1.12	3	1.1	2.65	1	4.2	1.12
97.5	23.2	1	16.5	1.11	5.8	1.1	5.1	1	7.9	1.11
95	56.2	1	35.3	1.1	11.8	1.09	10.1	1	15.6	1.09
92.5			77.3	1.08	24.95	1.08	20.7	1	32.5	1.08
90							43.7	1		

more retarded than analyte C_{9-cis} when the mobile phase strength is decreased resulting in a decrease in selectivity between analyte $C_{all-trans}$ and C_{9-cis} . This proportionally higher

increased retention for analyte $C_{\text{all-trans}}$ will of course benefit the separation of analyte C_{13-cis} and $C_{\text{all-trans}}$. This behavior was observed for sorbents **A** and **D**, which contained rigid domains, but not for **B** and **C**, which did not contain rigid domains. Therefore, this behavior was consistent with the slot model, earlier introduced [3], where the stationary phase alkyl chains can retain solutes in the space present between the alkyl chains. This space is more likely to be available if a high amount of ordered *trans* alkyl chain domains are present compared to the case in which domains with more flexible *gauche* conformed alkyl chains appear in the chromatographic sorbent. Thus, if a high amount of flexible *gauche* domains is present in the sorbent, they will hinder the analyte from penetrating between the alkyl chains. According to this model, linear solutes are more likely to penetrate deeper into the rigid *trans* alkyl domains of the stationary phase, thus having increased interactions, compared to the more bulky non linear solutes [3]. Hence, this shape discriminating effect is canceled if a low amount of rigid *trans* alkyl chain domains is present in the chromatographic sorbent, see the visualization in Figure 17. When the analytes C_{13-cis} , $C_{\text{all-trans}}$, and C_{9-cis} were eluted from the sorbents **A** and **D** with different mobile phase compositions of methanol/TBME, however, a significant change in retention behavior was obtained. Here it was observed that the selectivity between analyte C_{13-cis} and $C_{\text{all-trans}}$ increased as well as the selectivity between $C_{\text{all-trans}}$, and C_{9-cis} when the TBME content in the mobile phase was reduced. Hence, in the polar organic mode both phases **A** and **D** apparently have lost the shape selective effect to a certain extent. Also, the analytes C_{13-cis} , $C_{\text{all-trans}}$, and C_{9-cis} were eluted from a C_{30} sorbent using the same mobile phase compositions of methanol/TBME. Here it was observed, however, that the

selectivity between analyte C_{13-cis} and $C_{all-trans}$ increased while the selectivity decreased between analyte $C_{all-trans}$, and C_{9-cis} when the TBME content in the mobile phase was reduced. Consequently, the C_{30} sorbent showed shape selective properties in the polar organic mode.

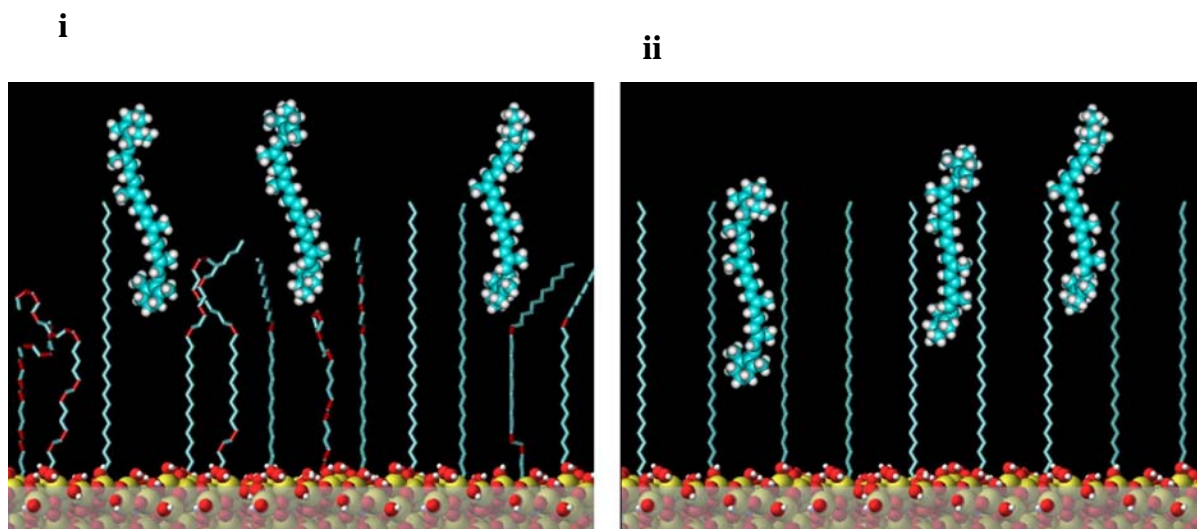


Figure 17 Visualization of the slot model; **i**: gauche conformed alkyl chains prevent the analytes to penetrate deeper between the alkyl chains, **ii**: trans conformed alkyl chains allow a deeper penetration thus a better interaction between the analytes and the stationary phase is possible (gauche kinks are marked in red, silica network oxygens are plotted as red balls)

The retention behavior of analytes **L** and **Z** was compared when they were eluted with different methanol/water mobile phase compositions from sorbents **A**, **B**, **C**, **D**, a C_{18} sorbent, and a C_{30} sorbent. Table 5 reveals that the selectivity factors for analytes **L** and **Z** eluting from sorbents **A** and **D** increased when the water content in the mobile phase was

Table 5 Retention factor of lutein and the corresponding selectivity vs. zeaxanthin eluting from chromatographic sorbents **A**, **B**, **C**, **D**, and the C_{18} based sorbent with different methanol/water mobile phase compositions

chromatographic sorbent	C_{30}	C_{18}		A		B		C		D		
% MeOH in H_2O	k'	α	k'	α	k'	α	k'	α	k'	α	k'	α
100	3.2	1.37	0.66	1	0.89	1.34	0.38	1.21	0.4	1	1.02	1.31
97.5	5.3	1.35	1.6	1	1.48	1.35	0.64	1.21	0.63	1.1	1.54	1.33
95	10.8	1.34	2	1	2.5	1.35	0.99	1.21	0.95	1.1	2.6	1.36
90	37.3	1.34	6.99	1	7.75	1.37	2.76	1.22	2.6	1.1	7.6	1.39
85			28.2	1	28.8	1.37	8.27	1.21	8.49	1.1	23.6	1.39

increased. This indicates that hydrophobic interactions contribute to their separation. The slightly better selectivity factors obtained from sorbent **D** compared to phase **A** must be due to the competing analyte amino interactions present when sorbent **A** instead of **D** is used. The selectivity factors did not change when the analytes **L** and **Z** were eluted from phases **B**, **C**, and the C_{18} sorbent when the water content in the mobile phase was increased. Furthermore, when the water content in the mobile phase was increased from 0 % to 10 % a slight decrease in selectivity was observed when analytes **L** and **Z** were eluted from the C_{30} sorbent. This indicates that not only hydrophobic interactions are responsible for the separation of analytes **L** and **Z** but also the ratio of *trans/gauche* alkyl

chains in the stationary phase. Hence, from a comparison at likewise retention factors ($k' = 7-11$) the selectivity obtained from phase **D** was superior to all the other sorbents, including the C_{18} and C_{30} sorbents, under these experimental conditions.

5.3.2 ^{13}C suspended-state HPDEC NMR spectroscopy

Suspended-state NMR allows one to gain an unique insight into the stationary phase conformational behavior in the presence of a mobile phase by mimicking the chromatographic system in the NMR rotor [78-80].

A series of ^{13}C suspended-state HPDEC MAS NMR spectra of sorbents **A**, **D**, and C_{30} suspended in mixtures of methanol/water was recorded in order to investigate if the *trans/gauche* ratio was affected by the mobile phase composition [81]. Different *trans/gauche* ratios were observed in the ^{13}C suspended-state HPDEC MAS NMR spectra, and quantified by peak deconvolution, see Table 6. No differences in the

Table 6 *trans/gauche* ratios of sorbents **A**, and **D**, and the C_{30} sorbent at 298 K

% MeOH in H_2O	sorbent A	sorbent D	C_{30} sorbent
100	40/60	38/62	59/41
50	47/53	44/56	60/40

trans/gauche ratio could be noticed between phase **A** and **D** when they were suspended in 100% methanol. Yet, a significantly higher *trans/gauche* ratio was observed for the C_{30} phase, 59/41, compared to the *trans/gauche* ratio obtained from phase **A** and **D**, 40/60

respectively 38/62. These results imply that the C_{30} sorbent has a better shape selectivity at a high organic content in the mobile phase compared to phase **A** and **D**. This was confirmed from the chromatographic evaluation of the analytes C_{13-cis} , $C_{all-trans}$, and C_{9-cis} eluted from the sorbents **A**, **D**, and C_{30} using different mobile phase compositions of methanol/TBME.

A significant increase in the *trans/gauche* ratios was observed for phase **A** and **D** in the ^{13}C suspended-state HPDEC MAS NMR experiments when the sorbents were suspended in a mixture of methanol/water (50/50), compared to the *trans/gauche* ratios obtained in pure methanol. This is exemplified in Figure 18 for sorbent **A**. Therefore, a

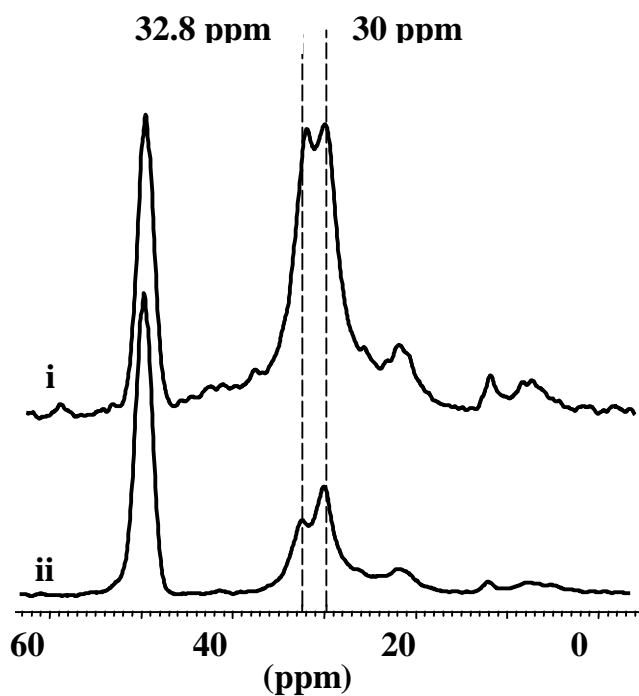


Figure 18 Suspended-state ^{13}C HPDEC NMR spectra of chromatographic sorbent **A**. *i*: In methanol/water 50/50 (v/v). *ii*: In methanol

greater amount of *trans* domains at a higher water content which was observed for phase **A** and **D** explains the retention behavior for the analytes C_{13-cis} , $C_{all-trans}$, and C_{9-cis} . The increase in selectivity between analytes C_{13-cis} and $C_{all-trans}$ as well as the decrease in selectivity between analytes $C_{all-trans}$ and C_{9-cis} , eluted from phase **A** or **D**, is most likely caused by a relative better fit between the hydrophobic chains of the rigid parts of the stationary phase. Hence, analyte $C_{all-trans}$ has a higher surface exposure to the stationary phase compared to analyte C_{9-cis} which will foster the separation of analytes $C_{all-trans}$ and C_{9-cis} . This effect is most pronounced in the case of the more linear analyte $C_{all-trans}$ compared to analyte C_{13-cis} and C_{9-cis} , in view of the differences in geometrical shape of the analytes. No change in the *trans/gauche* ratio, however, took place for the C_{30} sorbent when the solvent composition changed. Therefore, the increase in the *trans/gauche* ratio of the alkyl chains for phase **A** and **D** leads to an increase in selectivity between the analytes **L** and **Z**. So, the reduction of the selectivity between analytes **L** and **Z** obtained from the C_{30} sorbent is due to the fact that no increase in the *trans/gauche* ratio of the alkyl chains in the C_{30} sorbent was observed. Hence, the suspended-state ^{13}C HPDEC MAS NMR experiments imply that an increase in water content in the mobile phase composition should increase the shape selectivity obtained from phase **A** and **D** to a larger extent compared to the C_{30} sorbent. A visualization of these effects is presented in Figure 19. These results were confirmed from the chromatographic results shown in Table 5.

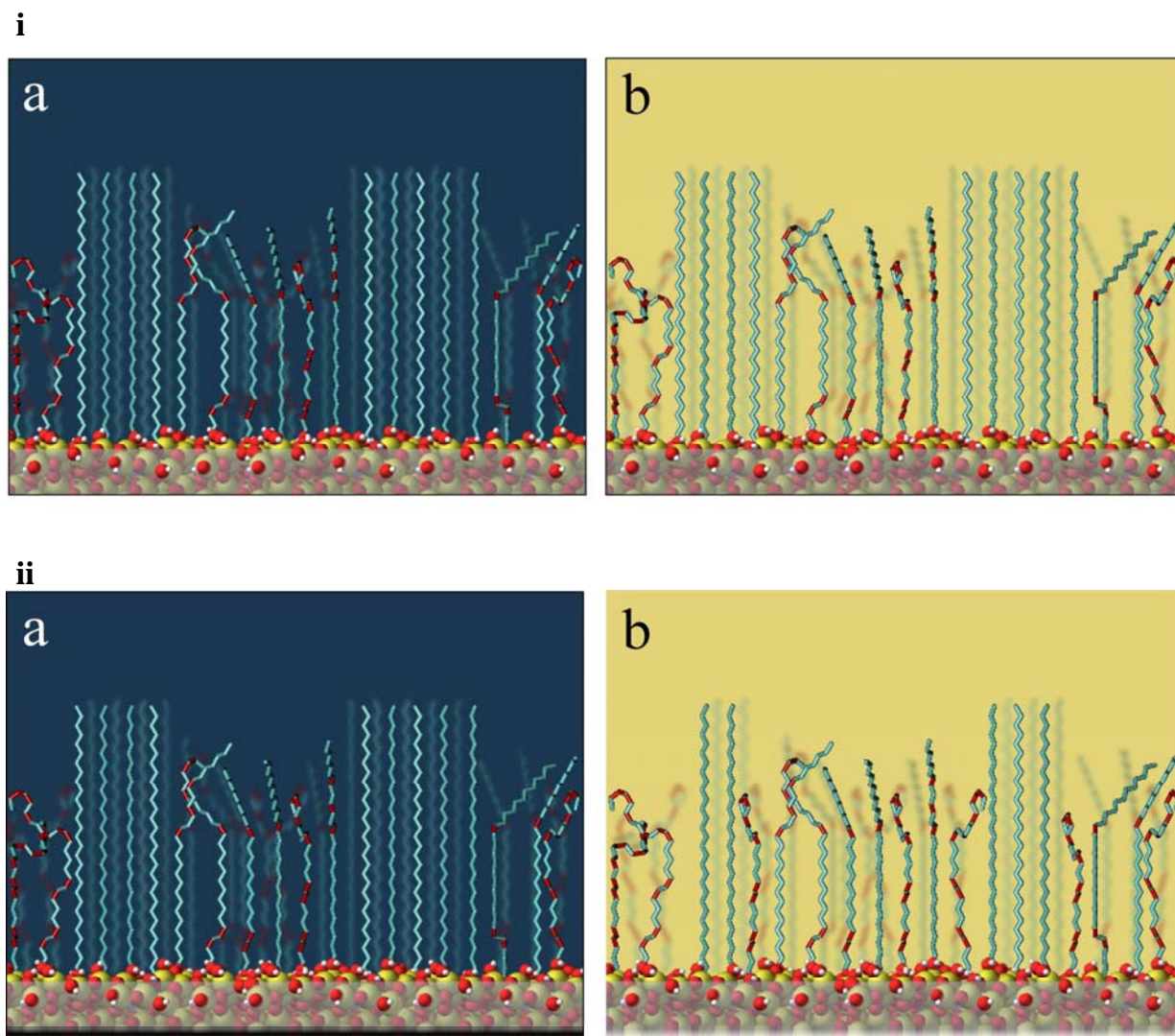


Figure 19 Visualization of alkyl-chain conformations in different solvents. **a:** C_{30} sorbent. **b:** Sorbents A and D. **i:** In methanol/water (50/50 v/v). **ii:** In methanol (gauche kinks are marked in red, silica network oxygens are plotted as red balls)

5.4 Influence of the surface coverage

Surface coverages differ significantly for conventional alkyl stationary phases synthesized by either a monomeric or a polymeric covalent attachment of alkylsilanes on

silica gel. Mostly, C₁₈ columns are prepared according to a monomeric modification with bonding densities of approximately 3 μmol/m². Solution polymerized C₁₈ columns reveal a bonding density of approximately 5 μmol/m² and surface polymerized C₁₈ column approach the limit of self-assembled monolayers (8 μmol/m²). Thereby it was proven that shape selectivity in C₁₈ sorbent material is strongly correlated with surface density. Better shape discriminating effects were observed for more ordered stationary phases with a higher bonding density [26].

Here, three polymer based chromatographic sorbents were synthesized by immobilizing three different amounts of the poly(ethylene-*co*-acrylic acid) with the lowest *co*-acrylic acid mass fraction of 5 % and the longest alkyl chains on the same batch of glycidoxypropylsilica. This polymer revealed both rigid *trans* and mobile *gauche* aligned alkyl chains in the ¹³C solid-state CP/MAS NMR characterization described in chapter 4. The aim of this investigation was to figure out if the selectivity behavior in these kinds of sorbent materials is affected by surface density and also spectroscopic evidence was necessary to explain the obtained chromatographic results. Therefore, the three copolymeric stationary phases were also characterized by ¹³C solid-state NMR spectroscopy to reveal any polymer alkyl chain conformational differences which dependent on the bonding density.

5.4.1 Separation of shape constrained solutes

Three chromatographic sorbents with different degrees of immobilized polymer

were synthesized. Table 7 constitutes the degrees of immobilization (carbon mass fraction) and the calculated polymer bonding densities on the glycidoxypopylsilica surfaces (polymer molarity on the silica surface). The separation of SRM 869 and of the main *cis/trans* β -carotene isomers is shown in the chromatograms of Figure 20. Along with decreasing carbon mass fraction, the hydrophobic interactions resulted in shorter retention times and retention factors. This holds true for all solutes. Interestingly, for analytes **BaP** and **TBN**, the selectivity is lowest for the intermediate chromatographic sorbent ($\alpha = 0.61$). The selectivity behavior of these solutes is indicative for the shape selective properties. The smaller the selectivity the better the shape discriminating

Table 7 Retention factors and selectivities of shape constrained solutes eluting from chromatographic sorbents **D** synthesized with different degrees of immobilization with a methanol/water mobile phase composition of 95/5 (v/v)

degree of immobilization ⁱ	polymer molarity on silica surface ($\mu\text{mol}/\text{m}^2$)	k' ⁱⁱ		k' ⁱⁱⁱ		k' ^{iv}	
		α	α	α	α	α	α
7	0.18	1.16	0.85	14.8	1.35	16.8	1.14
4.5	0.084	2.88	0.61	12.6	1.39	15.1	1.19
2	0.018	2.37	0.73	3	1.36	3.8	1.27

i carbon mass fraction

ii retention factor of BaP and selectivity vs. TBN

iii retention factor of 13-*cis* and selectivity vs. all-*trans* (β -carotene)

iv retention factor of all-*trans* and selectivity vs. 9-*cis* (β -carotene)

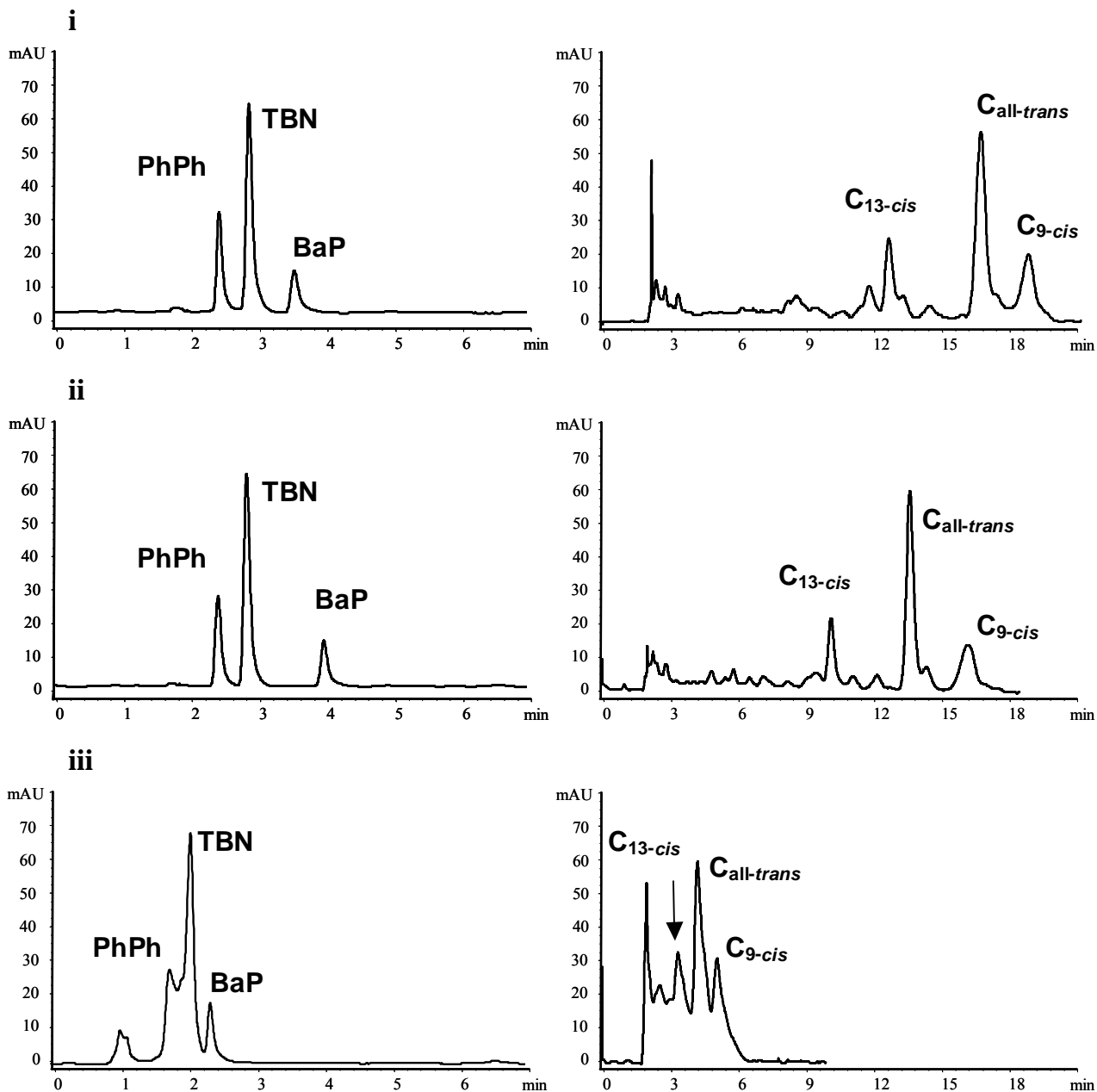


Figure 20 Chromatograms of SRM 869 consisting of phenanthro[3,4-*c*]phenanthrene (**PhPh**), 1,2:3,4:5,6:7,8-tetrabenzonaphthalene (**TBN**), and benzo[*a*]pyrene (**BaP**) as well as 13-*cis* (**C_{13-cis}**), 9-*cis* (**C_{9-cis}**), and all-*trans* β -carotene (**C_{all-trans}**) eluted from different chromatographic sorbents **D** synthesized either with a high (**i**), medium (**ii**), or low surface coverage (**iii**) using a mobile phase composition of methanol/water 95/5 (v/v)

properties of C_{18} columns [26]. Here, in the case of the polymer based sorbents, we found that an intermediate coverage resulted in better selectivities. This is most probably caused by the fact that a coverage that is too dense prevents the planar PAH **BaP** to penetrate deeper in between the cavities of the polymer alkyl chain turf on the silica surface. The hydrophobic interactions are thus reduced. This observation is substantiated by the longer retention factor ($k' = 2.88$) compared to the sorbent with a higher carbon content ($k' = 2.37$). This proves the influence of the shape of **BaP** and thus the influence of the surface morphology. Another striking feature is the fact that even though the sorbent with the lowest surface coverage contains an extremely low amount of polymer (surface molarity of $0.018 \mu\text{mol}/\text{m}^2$) is still able to reveal the properties comparable to a polymeric chromatographic sorbent by eluting **BaP** after **TBN**. Furthermore, this sorbent still separated the three β -carotene isomers C_{13-cis} , $C_{all-trans}$, and C_{9-cis} . This separation was achieved in a timeframe of only 7 min. Even though the analytes are not baseline separated, this proves the influence of the stationary phase conformational behavior. Not only hydrophobic interactions are responsible for the separation of analytes $C_{all-trans}$, and C_{9-cis} which are not different in polarity. Therefore, the three sorbents were also investigated by ^{13}C solid-state NMR spectroscopy.

5.4.2 ^{13}C solid-state NMR spectroscopy

Figure 21 shows the ^{13}C CP/MAS NMR spectra of the polymer based chromatographic sorbents synthesized by immobilizing different amounts of

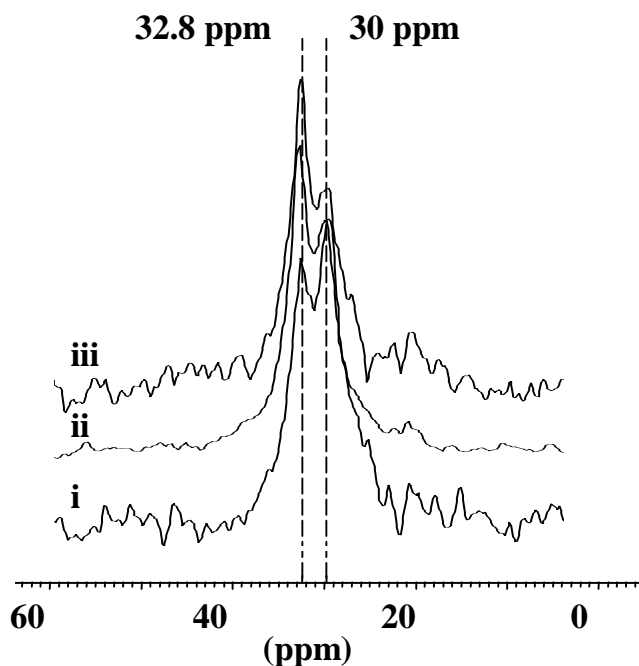


Figure 21 ^{13}C CP/MAS NMR spectra of different chromatographic sorbents **D** synthesized either with a high (**i**), medium (**ii**), or low surface coverage (**iii**)

poly(ethylene-*co*-acrylic acid) on glycidoxypypylsilica from the same batch. Even though the carbon content, thus the surface coverage differed significantly, still a peak splitting in a chemical shift of 30 ppm and 32.8 ppm of the main alkyl chains of all sorbents could be observed. This proves that in the case of this copolymer the bonding density does not influence the conformational behavior. Both, rigid *trans* and mobile *gauche* conformed alkyl chains are present. This also explains the selectivity behavior towards shape constrained solutes as described in the previous paragraph. These results imply, that it is generally possible to synthesize extremely low density polymer based chromatographic sorbents with which highly selective separations of, in terms of polarity

alike compounds, can be achieved. The low carbon content reduces the hydrophobic interactions, whilst the shape selective properties of the polymeric stationary phases are still available. Thus rapid separations of such compounds are possible without losing selectivity. This will be very helpful for practical application in preparative chromatography, also because polymer based chromatographic sorbents generally have a higher loading capacity [20-22]. Rapid separations of large quantities of compounds are therefore achievable.

5.5 Influence of the temperature

The effect of temperature in RP-HPLC in terms of thermodynamics was studied in previous research work [82-85]. Compared to investigations concerning the influence of different stationary phases and different mobile phase compositions, the effect of temperature is underrated. The influence on the selectivity is ample [77]. IR spectroscopy on chromatographic sorbents contributed to the understanding of RP-HPLC at different temperature ranges [86]. The correlation of the retention behavior with the alkyl chain conformation at various temperatures was, however, most successfully done by ^{13}C NMR spectroscopy with the sorbent either in the solid-state or suspended in a mobile phase [78, 87, 88]. Here, ^{13}C solid- and suspended-state NMR was used to monitor the mobility behavior of the *trans* and *gauche* aligned alkyl chains of the polymer based sorbent at various temperatures. Furthermore, advanced solid-state NMR experiments to determine the residual dipolar couplings were applied to explore the mobility and molecular motion

of proteins. Torsion angles in peptides were ascertained by investigating heteronuclear dipolar couplings earlier [89-92]. Here, the application of a separated-local field NMR experiment (dipolar and chemical shift correlation experiment, DIPSHIFT) to analyze the molecular motion and dynamics in a chromatographic sorbent is reported. Quantitative information about the order degree in the alkyl chains of the polymer based chromatographic sorbent at different temperatures by the correlation of the C-H heteronuclear dipolar coupling with the carbon chemical shift was gained in collaboration with Dr. Detlef Reichert and Dr. Ovidiu Pascui (University of Halle, Germany).

The temperature dependence of the retention behavior of both geometric carotenoid isomers and also SRM 869 on a variety of RP sorbents was previously investigated [93, 94]. The selectivity and retention of these two different analyte mixtures in regard to the molecular dynamics and alkyl chain conformational behavior in the copolymer based stationary phase at various temperatures was systematically investigated.

5.5.1 Temperature dependent ^{13}C NMR investigations

5.5.1.1 ^{13}C solid- and suspended-state CP/MAS NMR spectroscopy

From the solid-state ^{13}C CP/MAS NMR spectra in Figure 21 one can observe that the signal intensity at 32.8 ppm increased with decreasing temperature, implying that rigid alkyl chain domains in *trans* conformation dominate at 298 K compared to 318 K. A

direct estimation of the *trans* versus *gauche* population could not be done because the applied CP technique does not provide quantitative spectra. It is clearly observable that with decreasing temperature, however, the resonances broaden, indicating a decrease in

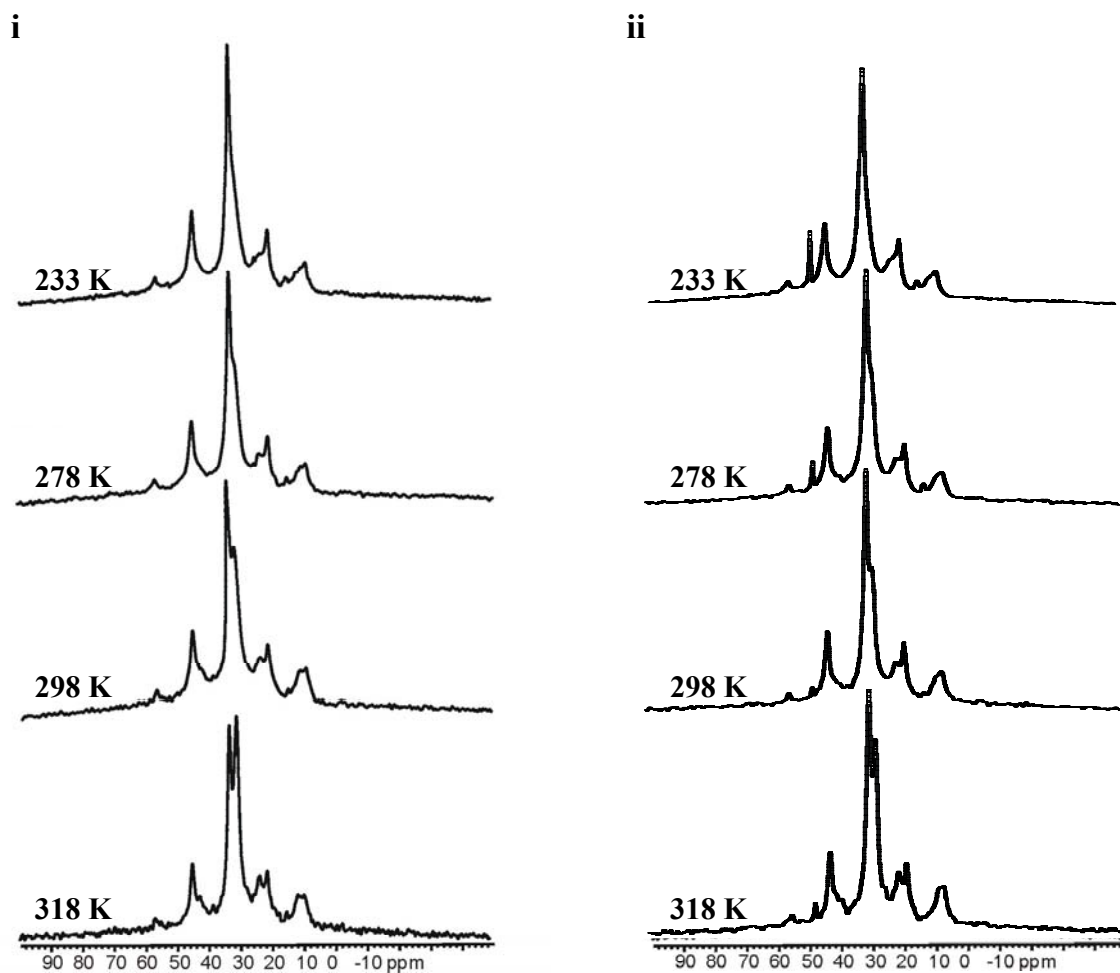


Figure 22 ^{13}C CP/MAS NMR spectra of chromatographic sorbent **D** in the solid-state (i) and suspended in methanol/water (95/5, v/v) (ii) at various temperatures

mobility. Here, the ^{13}C CP/MAS spectra revealed an increasing fraction of *gauche* conformation with increasing temperature. Therefore, these data do not support the

existence of a sudden phase transition in the polymer based sorbent. Rather, the temperature dependence of *trans* versus *gauche* populations is a more gradual process, which proceeds during a wide temperature interval. This supports the review of Wheeler et al. on phase transitions where they concluded that this phenomena can be viewed as a diffuse change, going from a solid-like to a liquid-like state over a broad temperature range [95]. A series of ^{13}C CP/MAS NMR spectra of the polymer based sorbent suspended in methanol/water (95/5, v/v) was also recorded in order to investigate if the *trans/gauche* ratio was affected by the mobile phase, see Figure 22. Previous reports proved a dependence of the alkyl chain conformation on the mobile phase composition [22]. The stationary phase of the polymer based sorbent in the suspended-state showed an increased mobility compared to the solid-state, however, the same trend of constantly increasing mobility with increasing temperature was observed.

5.5.1.2 Solid- and suspended-state ^{13}C DIPSHIFT NMR spectroscopy

Using the DIPSHIFT experiment, that is the correlation of the ^{13}C - ^1H heteronuclear dipolar coupling with the carbon chemical shift, further information about the alkyl chain mobility could be revealed. The strength of the ^{13}C - ^1H dipolar couplings was measured using the DIPSHIFT pulse sequence, see Figure 23. The reduced dipolar coupling in the fast exchange limit ($\tau_c \ll T_2$) contains information about the geometry of motion, that is the ratio between the reduced versus the full coupling which can be interpreted as an order parameter S with values between 0 and 1. For a number of motional geometries,

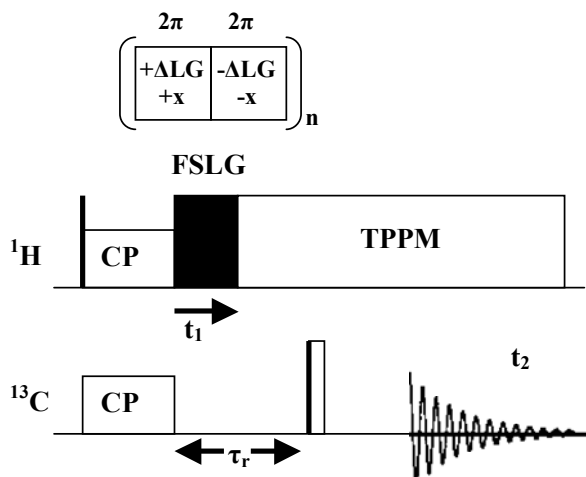


Figure 23 Constant time dipolar and chemical shift (DIPSHIFT) pulse sequence

relations of the order parameter S versus angles can be derived. Thereby, 0 means isotropic motion and 1 no motion. Values between 0 and 1 can be interpreted as an increasing opening angle of a motion with a decreasing order parameter. Figure 24 shows a visualization of models of internuclear vector reorientation. The order parameter S was derived in the work of Lipari and Szabo in 1982 [92]. Experimentally, this parameter can be obtained from the ratio of the reduced (fast anisotropic movement) dipolar coupling and the full coupling (no motion). Both, the sorbent in the solid-state as well as suspended in the mobile phase were measured, and the peak intensities at different temperatures and ^1H decoupling pulse lengths t_1 of the resonances corresponding to *trans* and *gauche* conformed alkyl chains were determined. The results for the sorbent in the solid-state and the suspended-state are shown in Figure 25. The depicted lines are simulations and the

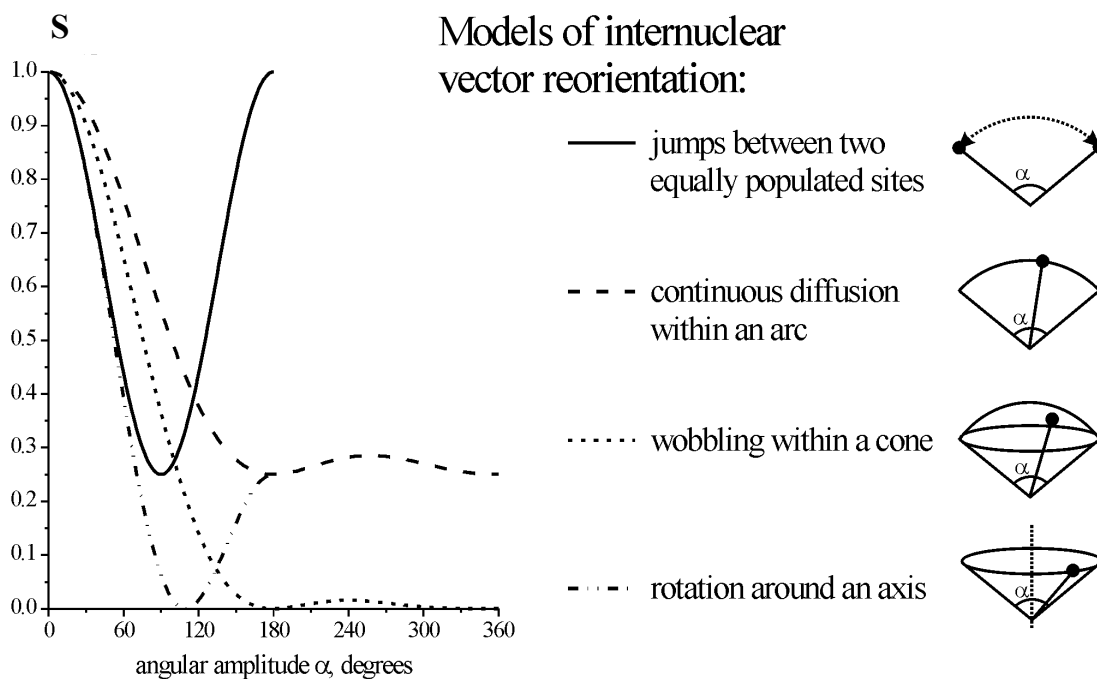


Figure 24 Models of internuclear vector reorientation

extracted dipolar couplings diverge slightly from the actual values since the theory used to obtain the data is for CH groups and not for CH₂ groups. Here, the acquired values are compared with a rigid CH₂ group, however, and discussed are only the relative ratio. The CH₂ group of glycine, which does not exhibit any molecular motion, was used as a reference. Therefore, the presented results comprehend valuable information about the molecular motion behavior of the alkyl chains in the investigated chromatographic sorbent material. The fitting yields an apparent dipolar coupling and a spin-spin relaxation time T_2 which stems from experimental parameters, as well as from exchange broadening. Consequently, by dividing the apparent dipolar coupling presented in Figure 25 by the glycine data we obtain a diagram of the order parameter S versus the temperature T

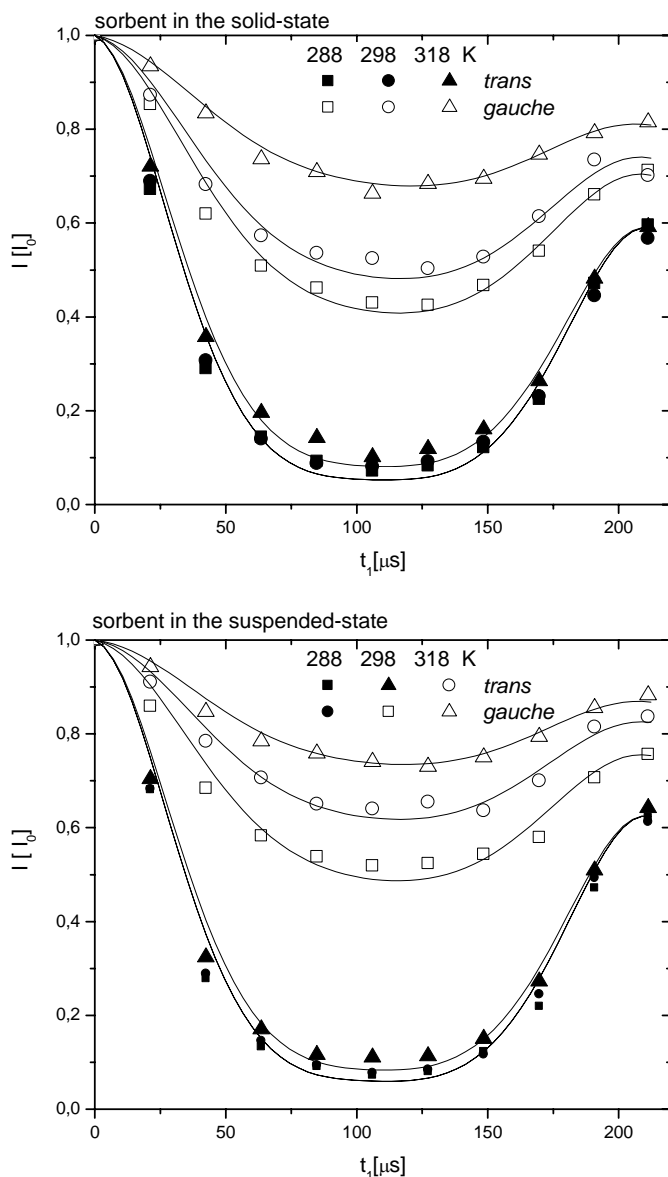


Figure 25 Peak intensities of the ^{13}C chemical shifts corresponding to *trans* respectively *gauche* conformed alkyl chains of chromatographic sorbent **D** in the solid-state and in the suspended-state at various temperatures at different 1H decoupling pulse lengths t_1

displayed in Figure 26. It shows that there is not much dynamic in the *trans* aligned alkyl chains whereas there is dynamic for the *gauche* aligned alkyl chains. Furthermore, the

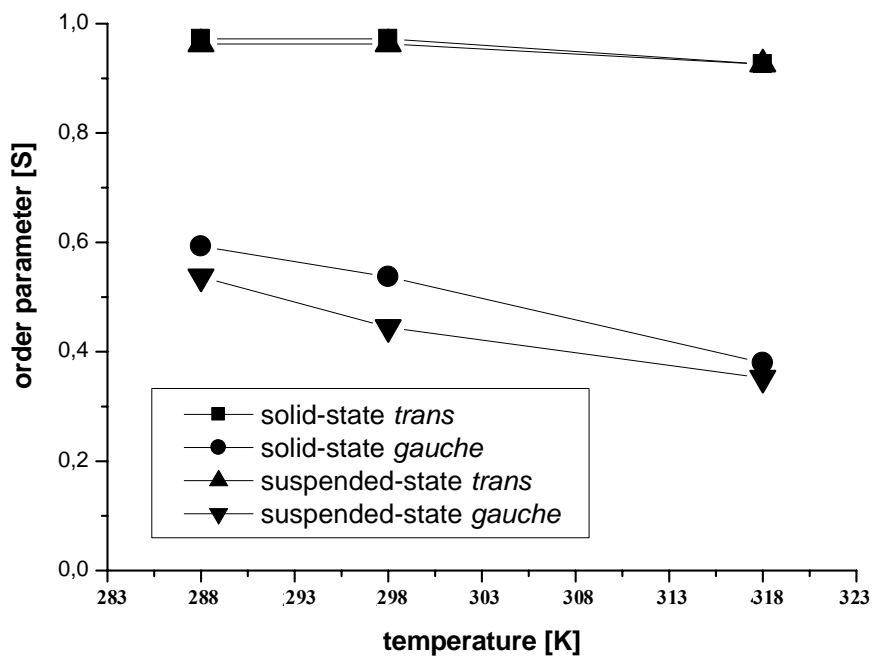


Figure 26 Plot of the order parameter S versus the temperature T (Kelvin)

Table 8 Spin-spin relaxation time T_2 (in ms) of the signals corresponding to *trans* respectively *gauche* aligned alkyl chains at different temperatures (in K)

	288	298	318
solid-state <i>trans</i>	0.4	0.4	0.4
solid-state <i>gauche</i>	0.6	0.7	1
suspended-state <i>trans</i>	0.45	0.45	0.45
suspended-state <i>gauche</i>	0.75	1.1	1.5

molecular motion becomes more intense at elevated temperatures with a decreasing order parameter S which stands for larger amplitude of motion. Also, the molecular motion in

the alkyl chains is more intense (the dynamics covers wider reorientation angles) for the sorbent in the suspended-state. Additional qualitative information can be extracted from the spin-spin relaxation time (T_2) values (Table 8). While the T_2 values of the *trans* resonances did not change with increasing temperature, the spin-spin relaxation time of the *gauche* resonance increased with increasing temperatures. Taking into consideration that with increasing temperature, not only the amplitude of a dynamic process but in particular the rate increases and that T_2 might contain a contribution of exchange broadening, it is reasonable to assume that the increase of T_2 with temperature is due to a decreasing of $+\delta\nu^{exchange}$. Hence, this is a clear indication for an increased motional rate at elevated temperatures:

$$1/T_2^* = 1/T_2 + \delta\nu^{exchange} \quad (3)$$

5.5.2 Temperature dependent separation of shape constrained solutes

The fact that temperature changes affect the *gauche* conformed alkyl chains to a greater extent compared to the *trans* conformed alkyl chains leads to the conclusion that the order degree of the *gauche* conformed alkyl chains contributes to the chromatographic properties besides the overall *trans/gauche* ratio. Generally, the order degree is higher at decreased temperatures which should implicate better shape selective properties. It must be mentioned, however, that the retention mechanism for different classes of compounds is not the same because of different interaction sites due to structural differences.

Currently under discussion are retention mechanisms that involve partition theory, adsorption theory, and the solvophobic theory with their privileged area of validity depending on the operating conditions [96]. PAHs and carotenoids can be compared in view of their similar retention mechanism as both classes of compounds penetrate into cavities in the stationary phase by their cyclohexenic part [87]. All analytes could be separated from each other with selectivities comparable to highly shape selective C_{30} sorbents, in agreement with the conformational behavior of the polymer based sorbent at ambient conditions as described above. Also, the chromatographic evaluation of the analytes C_{13-cis} , $C_{all-trans}$, and C_{9-cis} eluted from the sorbent at different temperatures confirms the selectivity dependence for these analytes on the temperature and thus on the alkyl chain conformation in the stationary phase. A higher selectivity between analytes C_{13-cis} and $C_{all-trans}$ compared to the selectivity between analytes $C_{all-trans}$ and C_{9-cis} at 298 K can be observed, thus $C_{all-trans}$ and C_{9-cis} are both more interacting with the stationary phase compared to analyte C_{13-cis} . This is most likely caused by a relative better fit of analytes $C_{all-trans}$ and C_{9-cis} between the hydrophobic chains of the rigid parts in the stationary phase. With respect to the above described slot-model, we have to mention the following: Regarding the L/B ratio of analytes and the thereby derived model of retention with more linear analytes being retarded longer compared to “blocklike” analytes, and the fact that analyte $C_{all-trans}$ exhibits the highest L/B ratio, analyte C_{9-cis} should be eluted before analyte $C_{all-trans}$. From Figure 27, with some exceptions, however, which will be explained later, can be seen that the retention time of all analytes decreases with

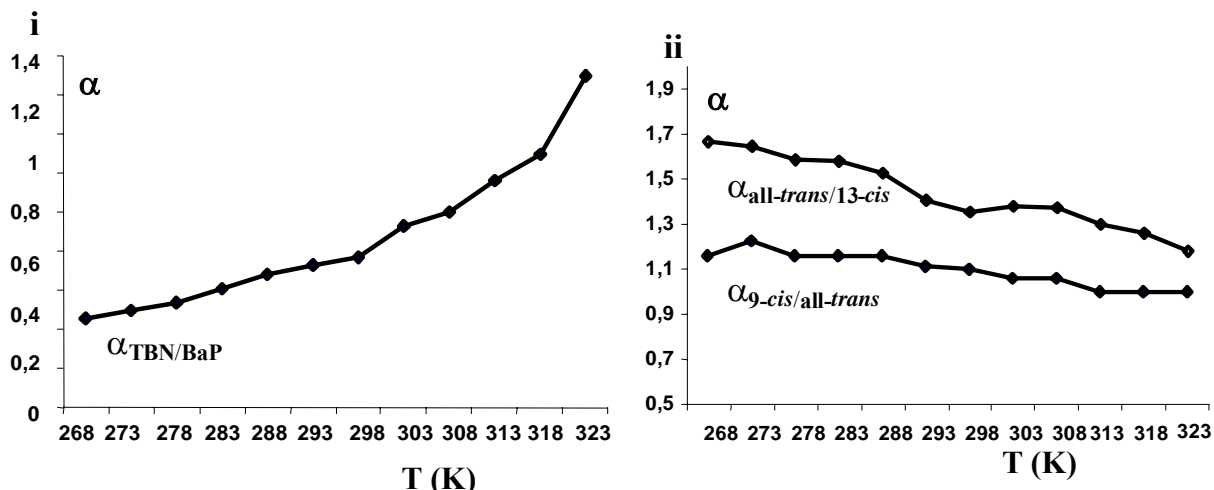


Figure 27 Plot of the selectivity $\alpha_{TBN/BaP}$ of SRM 869 consisting of phenanthro [3,4-c] phenanthrene (**PhPh**), 1,2:3,4:5,6:7,8-tetrabenzonaphthalene (**TBN**), and benzo[a]pyrene (**BaP**) (i) and plot of the selectivities $\alpha_{all-trans/13-cis}$ and $\alpha_{9-cis/all-trans}$ of 13-cis (C_{13-cis}), 9-cis (C_{9-cis}), and all-trans β -carotene ($C_{all-trans}$) (ii) eluting from chromatographic sorbent **D** with a methanol/water mobile phase composition of 95/5 (v/v) at different temperatures

increasing temperature; therefore, the interacting strength between the stationary phase and the analytes decreases. Also, it can be noticed that an increase in temperature comes along with a decrease in selectivity for both $\alpha_{all-trans/13-cis}$ and $\alpha_{9-cis/all-trans}$. This correlated with the decreasing order parameter of the *gauche* population, as revealed by the DIPSHIFT experiments. The relative larger decrease in selectivity between analytes C_{13-cis} and $C_{all-trans}$ compared to the relative slighter decrease in selectivity between analytes $C_{all-trans}$ and C_{9-cis} is most likely caused by the fact that analytes $C_{all-trans}$ and C_{9-cis} are both equally affected by the conformational change in the stationary phase with changing temperature which impacts the retention of analyte C_{13-cis} to a lesser extent. The greater amount of *gauche* domains at higher temperatures explains the retention behavior for the

analytes C_{13-cis} , $C_{all-trans}$, and C_{9-cis} . We assume that analytes $C_{all-trans}$ and C_{9-cis} are likewise affected by an increase in mobility in the stationary phase thus preventing the penetration into cavities of the stationary phase, whereas the earlier eluting analyte C_{13-cis} is less affected by the phenomena of increase in mobility. The similar trends in retention and selectivity behavior revealed for the geometric β -carotene isomers were also observed for PAH isomers. SRM 869 was developed to evaluate the shape selective properties of C_{18} sorbents and consists of planar and non-planar PAHs, see also paragraph 5.2.2 [77]. The “polymeric-like” retention behavior was observed when SRM 869 was eluted from the polymer based sorbent at 298 K, see Figure 27. By decreasing the temperature, $\alpha_{TBN/BaP}$ decreased further. The more rigid conformation in the stationary phase were present the larger the retardation of **BaP** relative to **TBN**. Therefore, the hydrophobic interactions of **BaP** with the stationary phase increased to a relative larger extent in the case of **BaP** compared to **TBN**, thus **BaP** is able to penetrate into cavities of the stationary phase present at temperatures below 308 K. It must be mentioned that for the separation of 16 priority pollutant PAHs of SRM 1647 a selectivity $\alpha_{TBN/BaP}$ in the range of 0.65-0.9 is necessary when working with C_{18} sorbent material [97]. Nevertheless, the polymer based sorbent was not able to separate the benz[α]anthracen/chrysene critical pair in SRM 1647, also not at lower temperatures down to 263 K. When the temperature was increased compared to ambient conditions, a selectivity behavior resembling a monomeric C_{18} phase was observed. From Figure 27 can be seen that **TBN** and **BaP** coelute at a temperature of 308 K, and at higher temperatures **BaP** eluted before **TBN**. The eminent impact of the temperature on the retention of **BaP** is a significant evidence for the

influence of the stationary phase alkyl chain conformation and thus for the applicability of the above described slot-model for the polymer based chromatographic sorbent.

In order to further examine the temperature effect in view of thermodynamics, van't Hoff plots of both separated analyte mixtures were derived. The van't Hoff equation is the thermodynamic relationship between the retention factor k' and the temperature (T):

$$\ln k' = -\Delta H / RT + \Delta S / R + \ln \Phi \quad (4)$$

ΔH is the enthalpy of transfer of the solute from the mobile phase to the stationary phase, ΔS is the entropy of transfer of the solute from the mobile phase to the stationary phase, R is the ideal gas constant, and Φ is the volume phase ratio of the stationary and mobile phases. A plot of $\ln k'$ versus $1/T$ gives a slope of $-\Delta H/R$ and an intercept of $\Delta S/R + \ln \Phi$. Enthalpies of transfer can thus be determined, however an exact calculation of the phase ratio is challenging as the volume of the stationary phase contributing to the retention of the analyte must be estimated. Therefore, the determination of the absolute entropies of transfer is difficult. A ΔH which is invariant with temperature gives a linear van't Hoff plot [98-101]. A change in the nature of the interactions between the solute and the mobile phase or stationary phase, or both results in non-linear van't Hoff plots. Both, the enthalpy and the entropy can be a function of temperature and thus the relative contribution of these factors to the retention may be changed. It was shown before that at low temperatures in highly aqueous systems where the retention mechanism is mainly governed by hydrophobic effects entropic forces are the general factor as both ΔH and ΔS

are positive, however, at higher temperatures ΔH is negative and also the enthalpy contributes [102]. Changes in the retention mechanism are often ascribed to conformational changes in the stationary phase [103]. Generally, for C_{18} and C_{30} sorbents the rigidity in the alkyl chains increases, as described above. Also, from the NMR results of the poly(ethylene-*co*-acrylic acid) sorbent, a clear conformational change in the alkyl chains was observed, as expatiated above. In Figure 28 the derived van't Hoff plots from the separations of geometric carotenoid isomers and SRM 869 are depicted. The van't Hoff plots for the analytes C_{13-cis} and $C_{all-trans}$ diverge when 308 K are reached while reducing the temperature. At this temperature also an inflection point for the slope of the enthalpy can be observed for all β -carotene isomers to the region between 288 K and 293 K, where the retention of all analytes stagnates. At 298 K the slope again upswings. In between 288 K and 293 K the interaction with the stationary phase of analytes C_{13-cis} and $C_{all-trans}$ increases whereas for the interaction with the stationary phase of analyte C_{9-cis} decreases as the temperature increases. The difference of behavior between analyte C_{13-cis} and $C_{all-trans}$ on the one side and analyte C_{9-cis} on the other side was in agreement with the above described observation of similar retention behavior in regard to their retardation at different temperatures. For planar **BaP** the van't Hoff plot is slightly non-linear with similarities to analyte **3**. The non-planar **TBN** gave a van't Hoff plot resembling analytes C_{13-cis} and $C_{all-trans}$. The slope for **TBN** indicates a lesser influence of the temperature on the retention. A greater slope can be observed for **BaP**. This is in agreement with a study

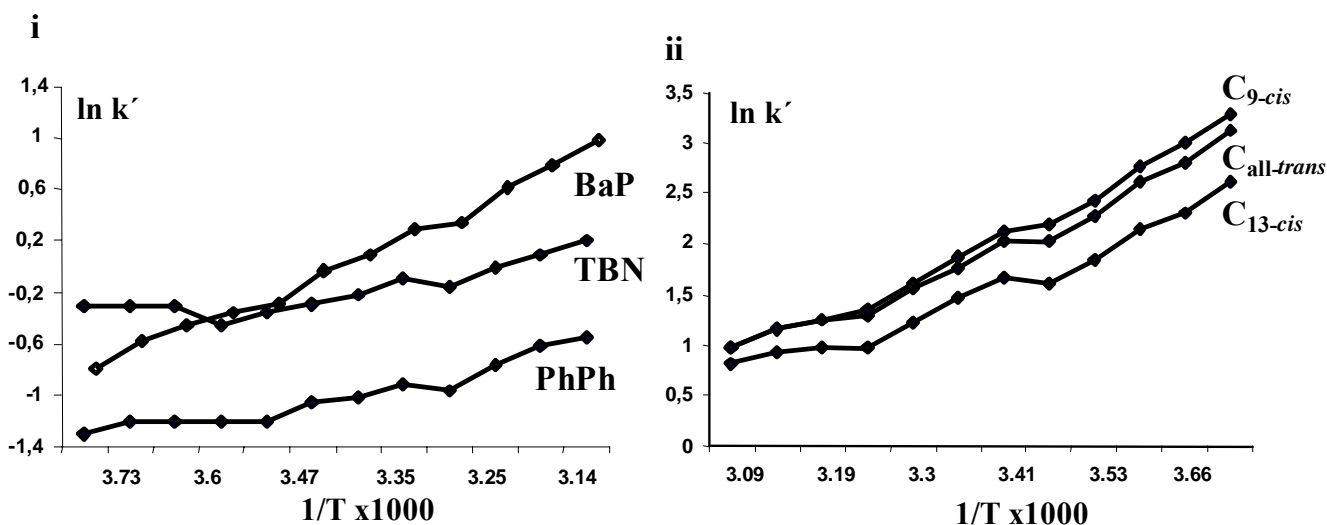


Figure 28 Van't Hoff plots of SRM 869 (i) and of 13-cis (C_{13-cis}), 9-cis (C_{9-cis}), and all-trans β -carotene ($C_{all-trans}$) (ii) eluting from chromatographic sorbent **D** with a methanol/water mobile phase composition of 95/5 (v/v) at different temperatures

conducted earlier, which proved that bulkier solutes gave increased retention (relative to other solutes) [104]. Here, however, this phenomenon was not observed in the case of the β -carotene isomers. Interestingly, at a temperature range between 288 K and 293 K the retention of all analytes slightly decreased; this was more pronounced for analyte C_{9-cis} , **TBN** and **PhPh** than for analytes C_{13-cis} , $C_{all-trans}$ and **BaP**. This observation was found to be more pronounced in a study on a C_{30} sorbent of these analyte mixtures conducted by Bell et al. [73]. Thereby, they observed a decrease of retention at this temperature range of bulkier solutes and attributed this to the retention model of Dill and Sentell/Dorsey [105, 106].

6 APPLICATION IN CAPILLARY HPLC-NMR

HYPHENATION

The increased demand of chromatographic materials that are able to achieve fast and well-resolved separations of large quantities of structure analogues is a challenge. Figure 29 shows the chromatographic triangle illustrating the most important criteria in chromatography.

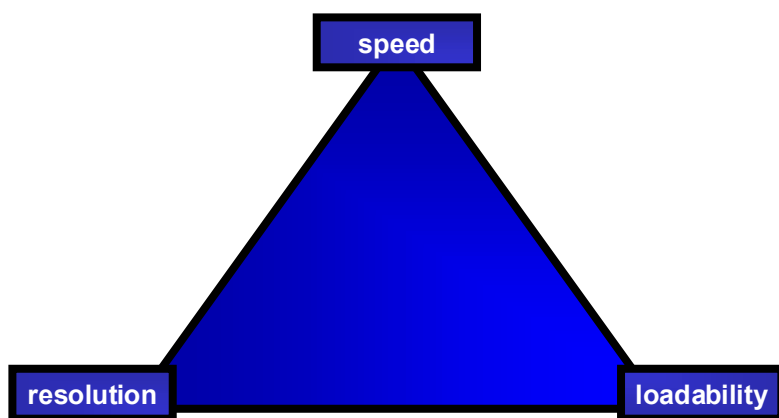


Figure 29 The chromatographic triangle

Polymer based chromatographic materials are known to have a high loadability, compared to silica based sorbent materials [1]. Unfortunately these polymer materials cannot be used under high pressure that is necessary in order to obtain a high flow, and hence performing a separation takes a long time. By immobilizing a polymer on a mechanically stable porous silica core this problem can be circumvented and it should be possible to achieve a higher flow on these materials. Especially for capillary HPLC-NMR

a high loadability is of great importance in order to obtain sharp, well-resolved, and highly concentrated peaks, thus, to have a good signal to noise ratio in the subsequent NMR experiment since NMR sensitivity is still an issue [107, 108]. Approaches like the development of cryogenic flow-probes have been undertaken to achieve better signal-to-noise ratios [109]. Also, a reduction in size of the radio frequency coil in order to be able to measure mass-limited samples was achieved: These microcoils are well size-matched to capillary HPLC columns [110]. The geometrical build-up of the probe is achieved either in the saddle-type arrangement [111] or in the solenoidal-type with the radio frequency coil directly wrapped around the capillary column [112] and placing this set-up perpendicular to the magnetic field. A several times better sensitivity is achieved using the microcoil solenoidal arrangement [113].

For the separation and analysis of mass limited, nanoliter-volume samples miniaturized systems such as capillary HPLC have the advantage of higher efficiencies resulting in a higher concentration at the eluting peak maxima. The low solvent consumption makes the usage of fully deuterated solvents possible thus no solvent suppression in the NMR experiments is needed. The capillary HPLC-NMR system was applied, for example, for the detection of biologically active compounds like carotenoids (provitamin A isomers) and retinyl acetate dimers [114, 115]. The shape selectivity of C₃₀ sorbents accounted for the successful separation of tocopherol homologues, which is not possible using C₁₈ sorbents [116-118]. Recently, this engineered stationary phase was also employed by Krucker et al. in capillary HPLC-NMR hyphenation experiments [107]. The separation and on-line ¹H NMR spectroscopic identification of tocopherol homologues

was achieved. Thereby, the C_{30} sorbents prove to have the high loading capacity described before. Tocopherol homologues are known to have antioxidative effects [119]. These antioxidant vitamins showed beneficial effects in the prevention of cardiovascular diseases and the aging process in general [120]. Tocopherols, however, can be sensitive to air in the presence of light [121]. The usage of a closed system build-up such as capillary HPLC-NMR hyphenation prevents the degradation of tocopherol homologues during their analysis.

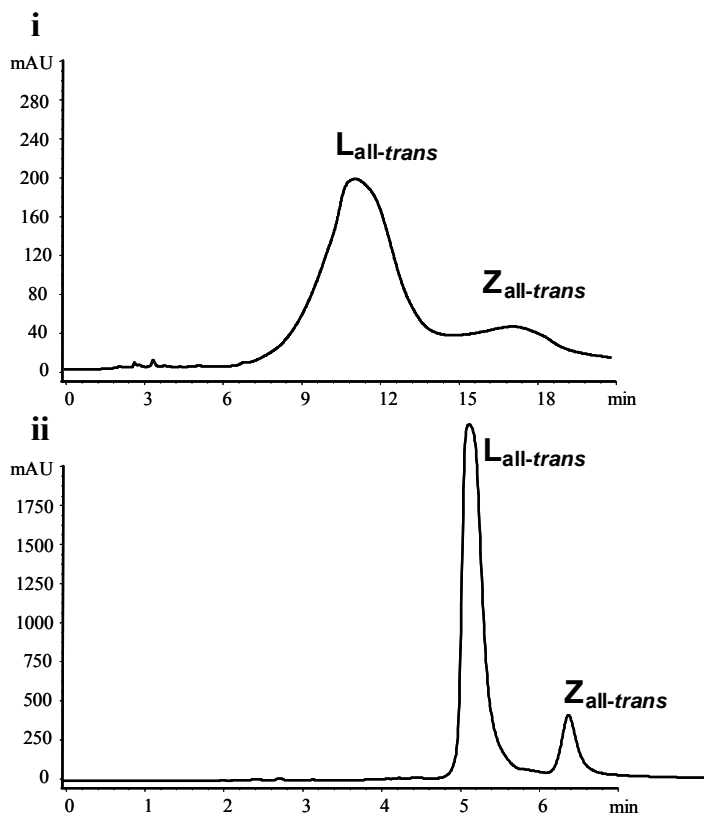


Figure 30 Chromatograms of a highly concentrated solution of all-trans lutein ($L_{all-trans}$) and all-trans zeaxanthin ($Z_{all-trans}$) eluting from a C_{30} sorbent (i) and sorbent D (ii) using acetonitrile as mobile phase, $[c_L] = [c_Z] = 100 \mu\text{g/mL}$, injected $100 \mu\text{L}$

In addition to the commercially available C₃₀ sorbent material, chromatographic sorbent **D** was also successfully employed in the hyphenation of capillary HPLC to microcoil ¹H NMR spectroscopy by the separation and identification of a highly concentrated solution of tocopherol homologues.

First, the suitability of this polymer based sorbent in regard to better loadability was demonstrated by the separation of xanthophyll isomers compared to a C₃₀ sorbent. The xanthophyll isomers **L** and **Z**, refer to Figure 11 for the structure formulas, were dissolved in acetonitrile to yield a concentration of 100 µg/mL of each analyte. Acetonitrile was employed as mobile phase to elute these analyte molecules from the polymer based chromatographic sorbent and the C₃₀ sorbent. Depicted in Figure 30 are the chromatograms from each sorbent material. Acetonitrile is an easy to evaporate mobile phase. This is important in regard to possible applications of this polymer based chromatographic sorbent in preparative chromatography, which requires highly loadable sorbent materials to achieve fast separations of large sample amounts. Acetonitrile can be removed rapidly from the separated target molecules. Therefore, we employed this organic modifier without the addition of water (therefore the retention times are not the same). Even though the selectivity of the C₃₀ sorbent is higher, no baseline separation could be achieved using these conditions; moreover the column lost resolution due to column overloading. The polymer based sorbent, in contrast, still gave sharp, baseline resolved, well-shaped peaks, even though the selectivity was lower, see also Table 9.

Table 9 Selectivities, retention factors, and height equivalents of a theoretical plate of the HPLC separation of xanthophyll isomers eluting from chromatographic sorbent **D** and a C_{30} sorbent; $[c] = 100 \text{ mg/mL}$, injected $100 \mu\text{L}$; * = not baseline separated

	α		k'		HETP (10^{-5}m)	
	D	C_{30}	D	C_{30}	D	C_{30}
lutein			3.02	6.2	6.08	*
zeaxanthin	1.38	1.64	4.17	10.17	3.25	*

These results make the application of the polymer based sorbent **D** in capillary HPLC-NMR apparent. Figure 31 shows the experimental set-up. The depicted

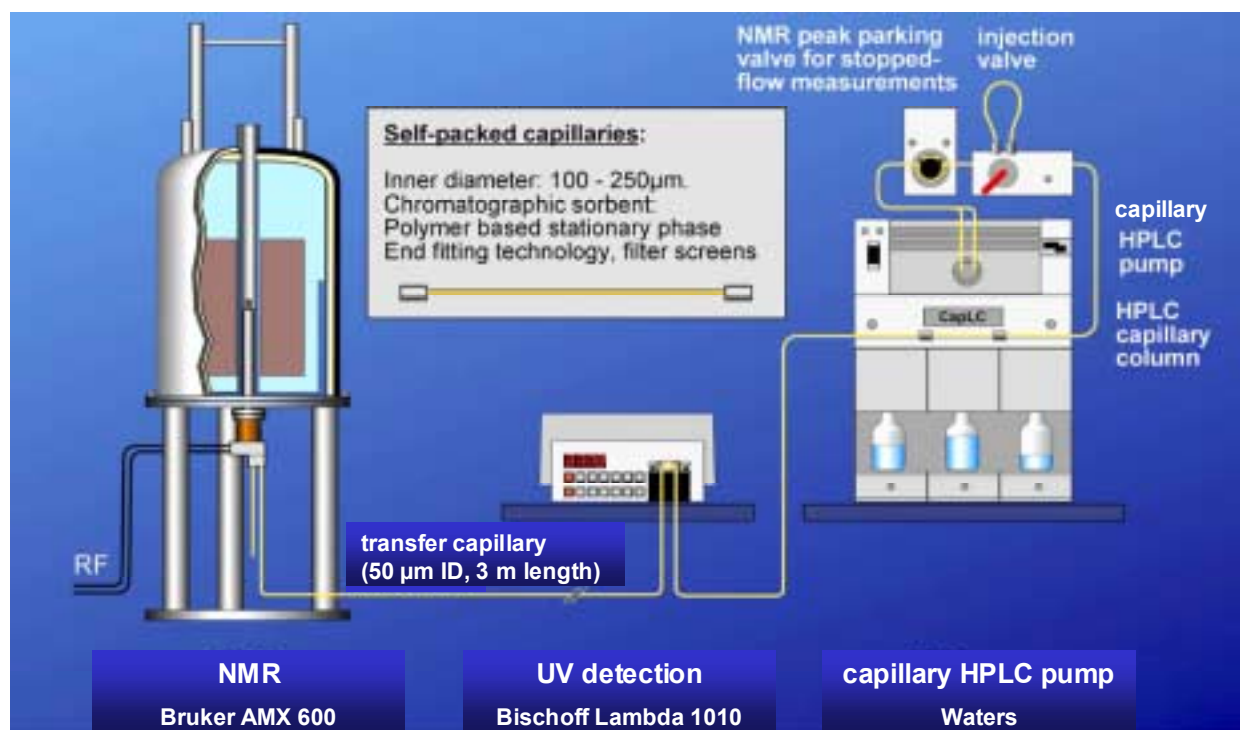


Figure 31 Capillary HPLC-NMR system

miniaturized chromatographic system allows flow rates of 1- 10 μL . The minimal amount of 20 mg of sorbent **D** was slurry packed into the capillary. Generally, in capillary HPLC, diffusion is minimized, thus the efficiency of separations is increasing. A transfer capillary to the NMR detection system of 3 m length was employed to prevent possible interference of the NMR magnetic stray field with the HPLC system. The NMR detection cell needs a high analyte concentration as described above. Figure 32 shows a photograph

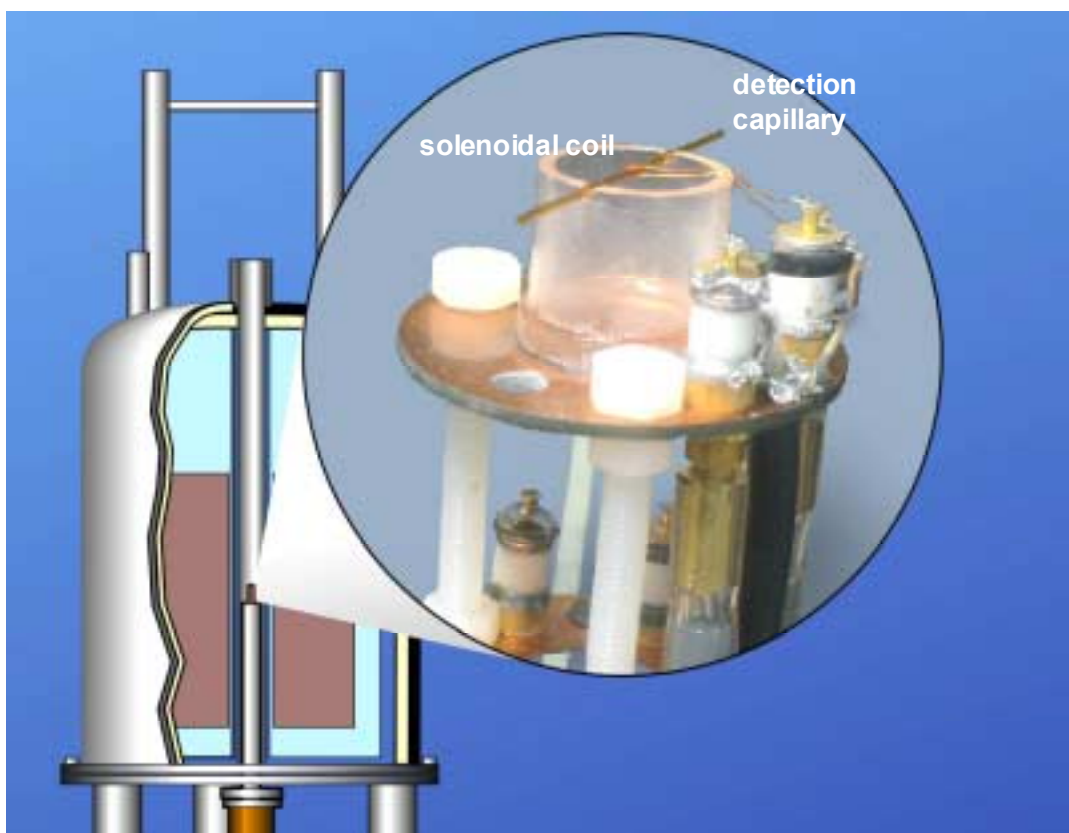


Figure 32 Solenoidal microprobe for on-line NMR coupling

of the solenoidal microprobe for on-line NMR coupling which was developed by Klaus Albert, Manfred Krucker, and Karsten Putzbach (University of Tuebingen) in cooperation

with Professor Andrew Webb (Penn State University). In contrast to conventional double-saddle-Helmholtz NMR probes, a perpendicular arrangement to the outside magnetic field B_0 is realized. The sending and detecting coil is wrapped directly around the capillary. To prevent susceptibility broadening by the copper coil, the whole arrangement is placed in a fluorocarbon solution, see Figure 33. This set-up generates a 3-

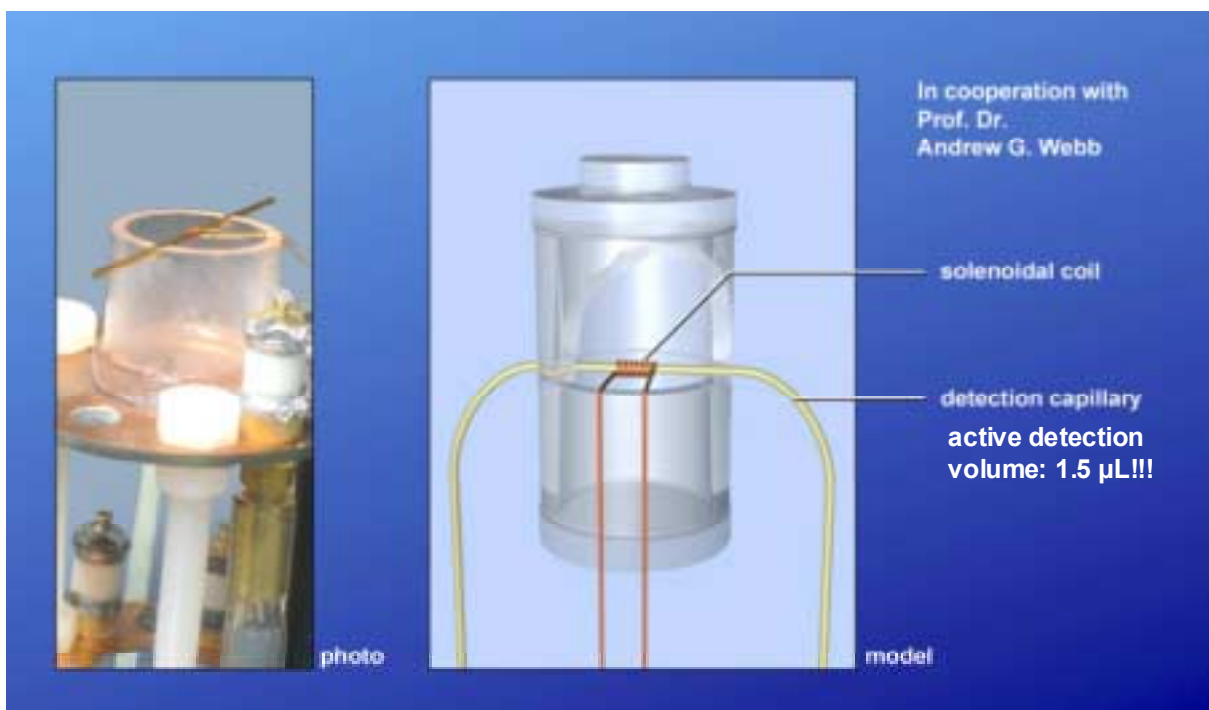


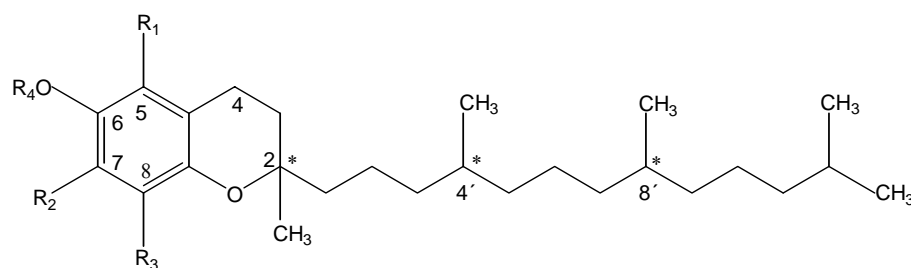
Figure 33 Close-up of the assembly of the capillary column and the solenoidal coil

fold increase in ^1H sensitivity compared to conventional NMR probes [122]. The residence time of the analyte in the detection cell is limited when working in the continuous flow mode. The active detection volume of this cell is extremely small, only 1.5 μL compared to 500 μL in conventional NMR tubes. Therefore, measurements in the

low nanogram range are possible. However, in order to obtain a good signal-to-noise ratio in the NMR experiments, large concentrations are needed.

6.1 Capillary HPLC separation of tocopherol homologues

With respect to these findings and owing to the system requirements of the hyphenation of capillary HPLC to NMR, described above, the polymer based sorbent was



	R ₁	R ₂	R ₃	R ₄
δ-tocopherol	-H	-H	-CH ₃	-H
γ-tocopherol	-H	-CH ₃	-CH ₃	-H
β-tocopherol	-CH ₃	-H	-CH ₃	-H
α-tocopherol	-CH ₃	-CH ₃	-CH ₃	-H
α-tocopherol acetate	-CH ₃	-CH ₃	-CH ₃	-COCH ₃

Figure 34 Chemical structure of the tocopherol homologues and α-tocopherol acetate; * denotes chiral C-atoms

applied for the capillary HPLC separation and microcoil ¹H NMR structure elucidation of tocopherol homologues. Figure 34 shows the structures of the tocopherol homologues. It must be noted that each homologue contains three chiral centers resulting in 8

stereoisomers which can not be separated when eluting them from the polymer based sorbent. The separations of tocopherol homologues, depicted in the chromatograms in Figure 35, present The loadability property of the polymer based sorbent material by comparing the elution of a low concentrated with a highly concentrated solution of these analytes. The

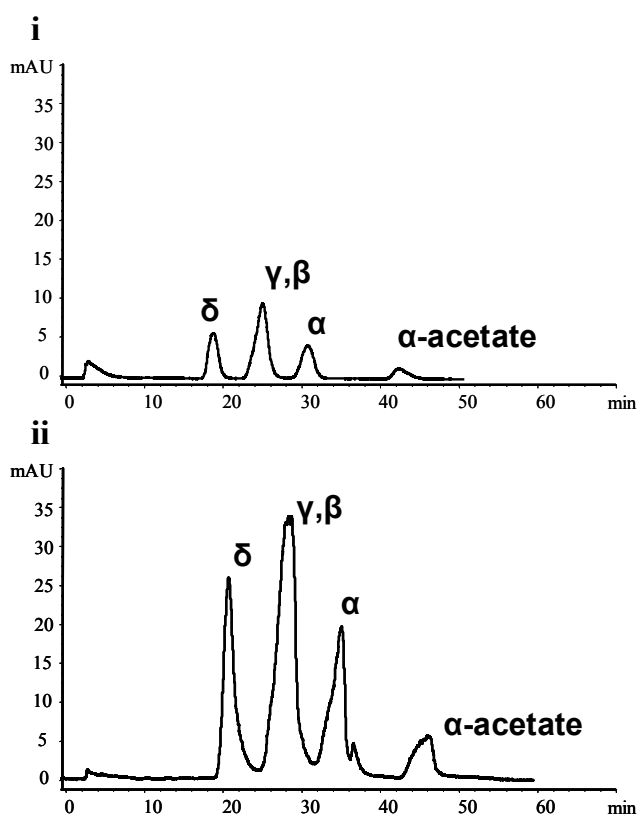


Figure 35 Chromatograms of the capillary LC separation of the tocopherol homologues eluted from the polymer based chromatographic sorbent using a mobile phase composition of methanol/water 85/15 (v/v) with a flow rate of 5 μ L/min. **i:** $[c_1] = 1.6$ mg/mL, injected 200 nL; **ii:** $[c_2] = 5.66$ mg/mL, injected 500 nL

injection volume was also increased when the high concentrated solution was injected. Even then the widths of the peaks increased minimal, which means that the desired high concentration in the NMR probe can indeed be achieved. Table 12 shows a comparison of the HETP values proving the loadability capability of this sorbent.

Table 10 Selectivities, retention factors, and height equivalents of a theoretical plate of the capillary LC separation of the tocopherol homologues eluting from chromatographic sorbent **D**; $[c_1] = 1.6 \text{ mg/mL}$, injected 200 nL; $[c_2] = 5.66 \text{ mg/mL}$, injected 500 nL

	α [c ₁]	α [c ₂]	k' [c ₁]	k' [c ₂]	HETP [c ₁]	(10 ⁻⁵ m) [c ₂]
δ -tocopherol				7.4		13.29
γ -tocopherol		1.37		10.2	*	*
β -tocopherol		1		10.2	*	*
α -tocopherol		1.24		12.6		12.97
α -tocopherol		1.38		17.4		16.66

6.2 Identification of tocopherol homologues using on-line capillary

HPLC-NMR hyphenation

It must be stated that the sorbent was not able to separate β -tocopherol and γ -tocopherol, therefore the UV-detection could not distinguish them. Mass spectrometry can distinguish α -tocopherol, δ -tocopherol, and α -tocopherol acetate from each other and also from β -tocopherol and γ -tocopherol; however the β - and γ - homologues have the same

fragmentation pattern. The only method to differentiate between γ -tocopherol and β -tocopherol is NMR spectroscopy. Despite the fact that these analytes co-eluted, the front of the peak contained more of γ -tocopherol, whereas the end of the peak contained more of β -tocopherol (the elution order of these tocopherol homologues on RP stationary phases was revealed before [102]). Thus, by creating a pseudo 2D NMR contour plot of the continuous-flow NMR spectra of the tocopherol homologues, it is possible to distinguish between γ -tocopherol and β -tocopherol by their different chemical shifts. The substitution of the aromatic ring of γ -tocopherol and β -tocopherol differs only in the position of the methyl group either in position 2 (γ -tocopherol) or position 1 (β -tocopherol). The contour

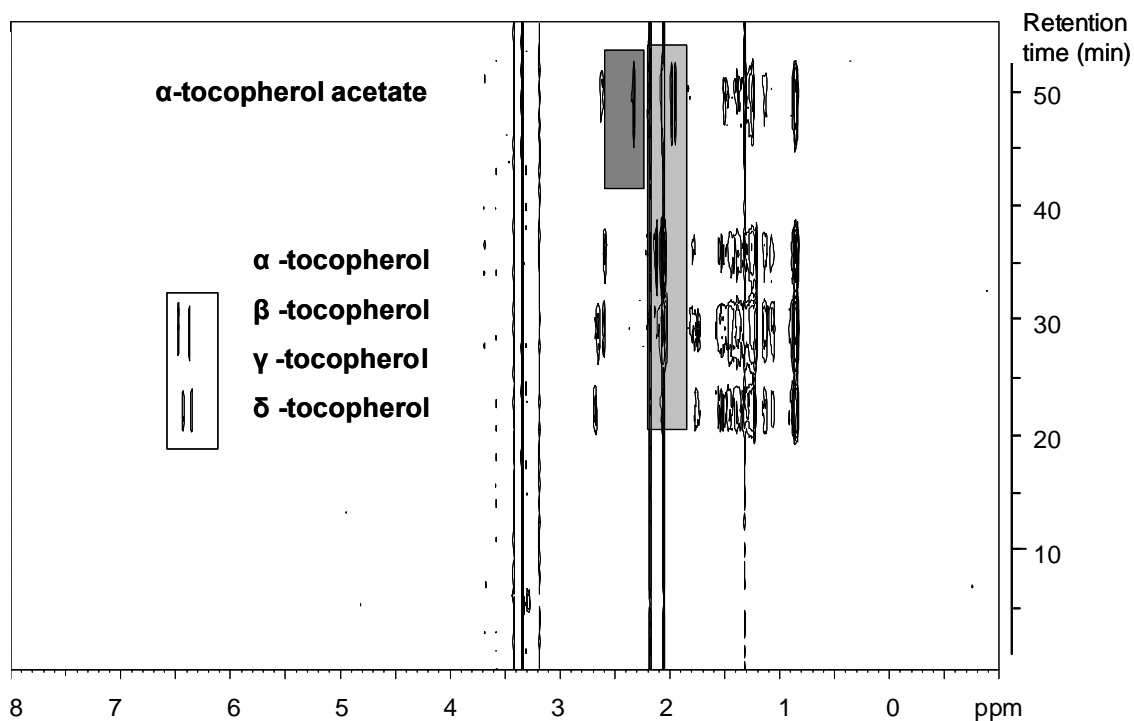


Figure 36 Pseudo 2D plot of the continuous-flow capillary LC NMR measurement of tocopherol homologues

plot depicted in Figure 36 contains the ^1H chemical shift axis and the retention time. As can be seen in the aromatic chemical shift region the signal for the aromatic proton of γ -tocopherol ($\delta = 6.4$ ppm) overlaps with the one of β -tocopherol ($\delta = 6.5$ ppm), displaying the co-elution of these analytes. It is clearly visible, however, that the aromatic signal corresponding to γ -tocopherol appears earlier than the one of β -tocopherol.

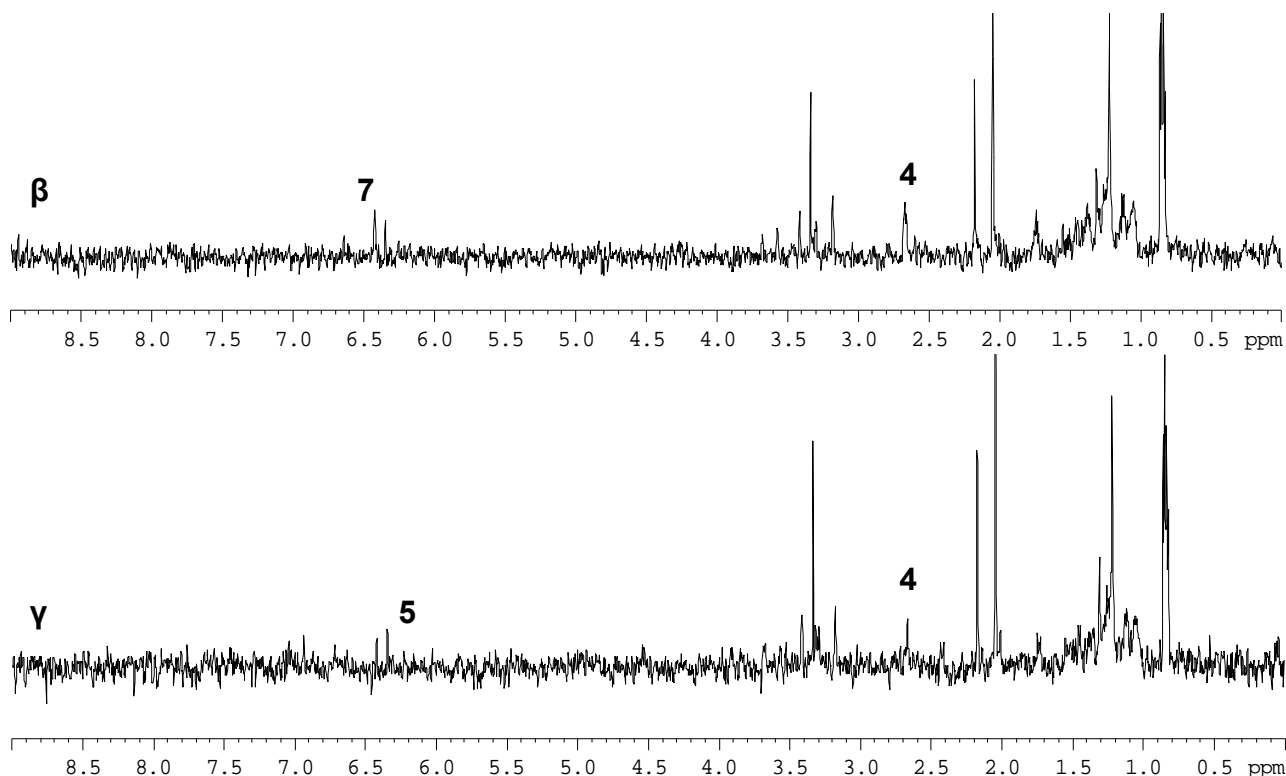


Figure 37 Extracted ^1H NMR spectra of the tocopherol homologues at the corresponding peak maxima

In order to obtain a more detailed interpretation, conventional ^1H NMR spectra of these two analyte molecules were extracted at the peak maxima of the capillary HPLC-

NMR separation, see Figure 37. Even though the signal-to-noise ratio is moderate (due to the fact that only 16 scans account for each spectrum), all resonance signals can be identified. The signal of proton 7 of β -tocopherol is superimposed with the shift at 6.4 ppm rising from the previously eluted γ -tocopherol. The same applies for γ -tocopherol where the signal of proton 5 is superimposed from the signal arising from the later eluting β -tocopherol. Furthermore, the signal of the proton at position 4 at 2.7 ppm experiences an upfield shift in β -tocopherol due to the neighboring methyl group attached to the aromatic ring in position 5.

7 CHIRAL POLY(ETHYLENE-CO-ACRYLIC ACID) CHROMATOGRAPHIC SORBENTS

The scope of the research described in this chapter was to unify the advantages of the highly shape selective and highly loadable poly(ethylene-*co*-acrylic acid) stationary phases with the enantiomeric selectivity of a Pirkle type chiral selector in a single sorbent material. The separation of geometric as well as enantiomeric carotenoid isomers (e.g. astaxanthin) by using only one column prompted this synthesis approach. Therefore, a Pirkle type chiral selector was immobilized on the silica support using the same linkage molecule as to attach the copolymeric poly(ethylene-*co*-acrylic acid) stationary phases.

The first separations of the enantiomers of sulfoxides, amines, amino acids, alcohols, hydroxy acids, lactones, and mercaptans by means of chiral fluoroalcoholic stationary phases were reported by Pirkle et al. [123]. The development of the (*S*)-(+)-*N*-(3,5-dinitrobenzoyl)- α -phenylglycine selector employed in this investigation is based on the fact that chiral recognition is a reciprocal event, thus fluoroalcohols could be separated using the previously separated analyte enantiomers as stationary phases immobilized on silica [124]. Early models of the chiral recognition mechanism describing face-to-edge π - π interactions were developed [125]. Other investigations were emphasizing on non-specific adsorption processes influencing the enantioselectivity, where the effect of polar groups either diminished or enhanced the chiral separation process [126]. A mechanistical rationalism for the separation of underivatized naproxen

was achieved by employing an improved chiral stationary phase [127]. The general principles of chiral recognition were also discussed in regard to the fact that chiral solvating agents cause non-equivalent NMR signals to arise from enantiomers [128]. ^1H NMR was first employed to ascertain the preferential retention of a certain enantiomer [129].

Pirkle type stationary phases were employed by Abu-Lafi et al. to achieve the separation of configurational isomers of astaxanthin [130]. Interestingly the same authors, two years later, also reported the fact that even columns packed from the same batch of produced sorbent material revealed different selectivity behavior towards enantiomers such as configurational isomers of astaxanthin [131]. A Pirkle type L-leucine column was also employed to separate the configurational astaxanthin isomers [132].

Another approach to separate these kind of isomers was reported by Grewe et al. using a cellulose tris-(3,5-dimethylphenylcarbamate) column [133]. Another group reported on the separation of naturally derived enantiomers of astaxanthin as dicamphanates [134]. Also, an amylose tris-(3,5-dimethylcarbamate) column was successfully employed previously for the separation of the astaxanthin enantiomers [135].

Here, the synthesis strategy followed to obtain the novel polymer based chiral chromatographic sorbents is presented, an elaborate characterization using solid-state NMR spectroscopy of the new material is described and prove the successful

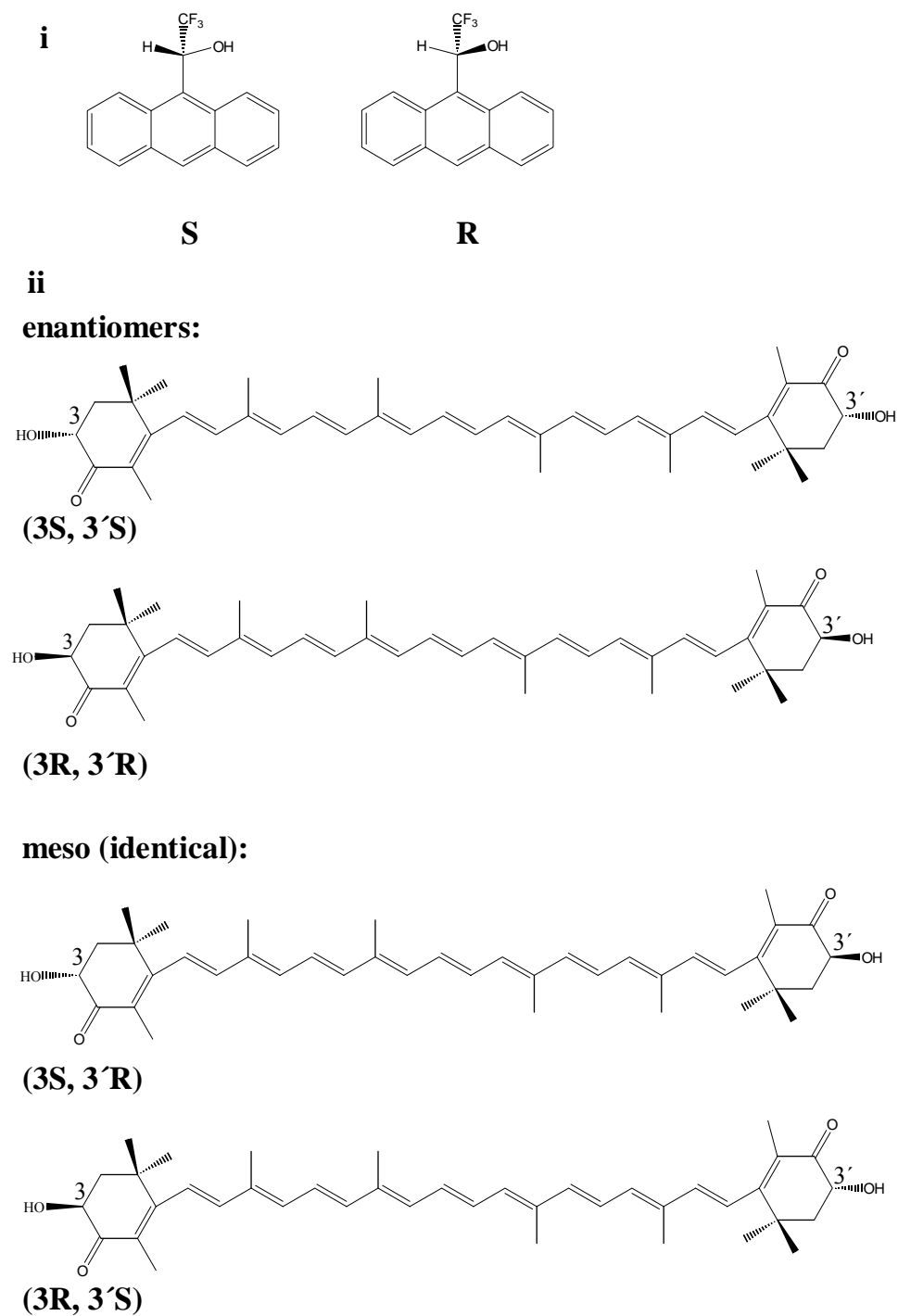


Figure 38 Scheme of the structures of (*S*) and (*R*) 2,2,2-trifluoro-(9-anthryl)ethanol (**i**) and (*3S, 3'S*), (*3R, 3'R*), (*3S, 3'R*) and (*3R, 3'S*) all-trans astaxanthin (**ii**)

immobilization of the stationary phases. The separation of 2,2,2-trifluoro-(9-anthryl)ethanol enantiomers employing the novel chiral polymer based chromatographic sorbents in the NP, and also the separation of geometric β -carotene isomers in the RP mode was successfully accomplished. The enantiomers and the meso forms of astaxanthin were slightly separated in the NP mode. Figure 38 shows the structures of the employed enantiomers.

7.1 Synthesis strategy

The chiral selector (*S*)-(+)-*N*-(3,5-dinitrobenzoyl)- α -phenylglycine was covalently immobilized on silica, using either a 3-aminopropyltriethoxysilane or a 3-glycidoxypropyltrimethoxysilane spacer molecule. Consecutively, also the copolymer poly(ethylene-*co*-acrylic acid) with an acrylic acid mass fraction of 5% (that featured highly shape selective properties) was covalently attached using the same immobilization chemistry. Sorbent **E** was synthesized by consecutively attaching the respective stationary phases (Figure 39a), whereas sorbent **F** was successfully synthesized by a joint immobilization reaction (Figure 39b). Numerous different reaction pathways were carried out in order to obtain the desired reaction products. It must be mentioned, that also a contiguous reaction would yield sorbent **E**, respectively a consecutive reaction would yield sorbent **G**. The results presented, however, indicate the synthesis strategies which gave the highest yields and highest stationary phase surface coverages.

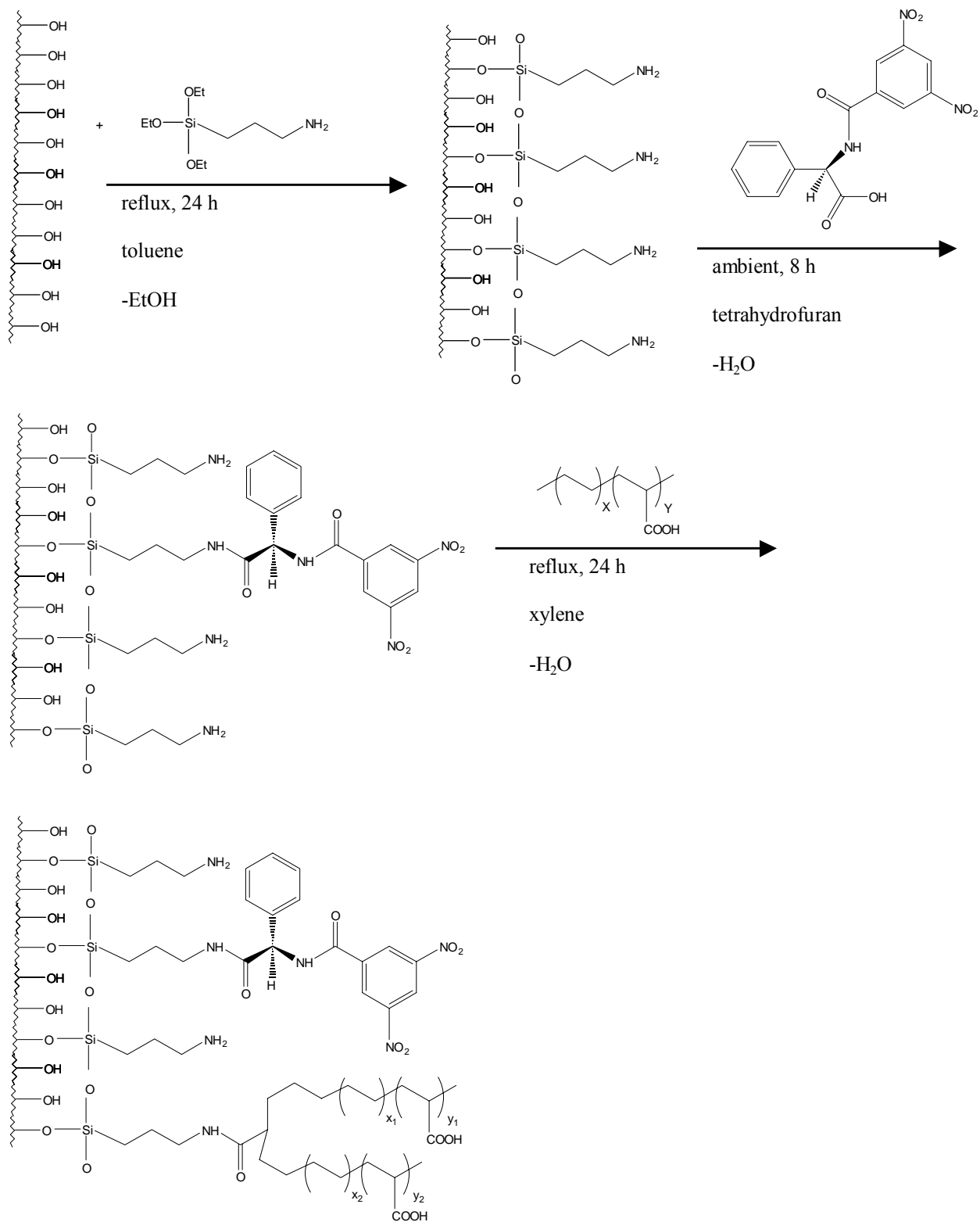


Figure 39a Reaction scheme for the synthesis of the chiral polymer based sorbent **E**

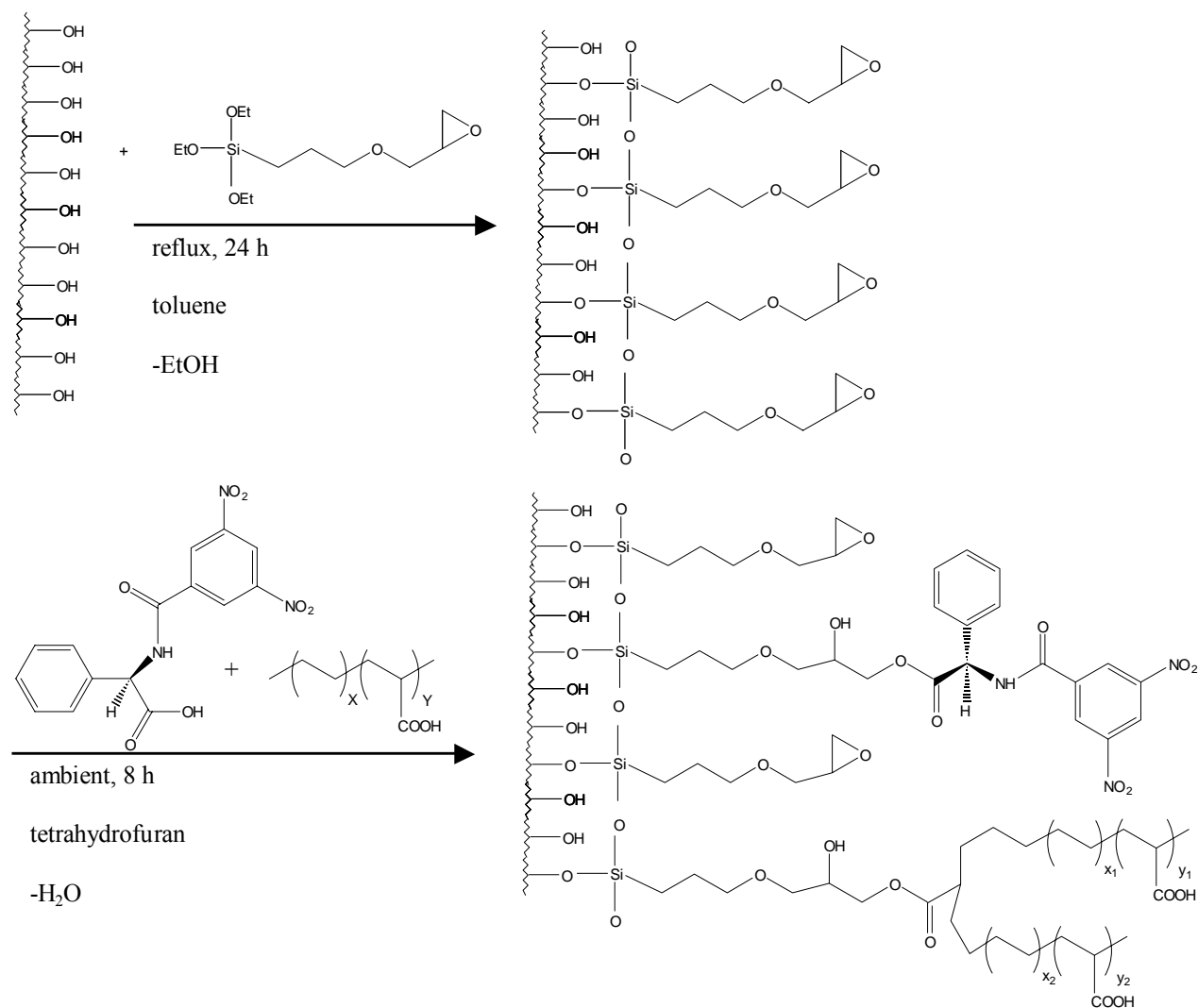


Figure 39b Reaction scheme for the synthesis of the chiral polymer based sorbent **F**

7.2 Characterization

In order to characterize the synthesized materials, elemental analysis, ²⁹Si and ¹³C solid-state NMR spectroscopy was performed. Table 11 shows the nitrogen and carbon content and the stationary phase surface coverages calculated therewith, or stationary phase surface molarities. Compared to the surface coverages obtained from the sorbents only containing the polymer (see chapter 4) a reduced polymer degree of immobilization

Table 11 Surface coverages of the chiral polymer based sorbents ($\mu\text{mol}/\text{m}^2$)

chiral polymer based sorbent	carbon content (%)	nitrogen content (%)	selector molarity on silica surface ($\mu\text{mol}/\text{m}^2$)	polymer molarity on silica surface ($\mu\text{mol}/\text{m}^2$)
E	15.9	1.2	1.1	0.26
F	5.7	0.2	0.3	0.12

is existent. This is due to steric effects since the chiral selector competes for available binding sites of the spacer molecules. These binding sites were available in a much higher concentration in the case of aminopropylsilica compared to glycidoxypropylsilica. To attach the silane spacer molecules, the surface polymerization reaction was carried out. The degree of immobilization for the aminopropyltriethoxysilane was higher compared to glycidoxypropylsilica (carbon mass fraction 2.9 % compared to 1.5 %). Therefore, also the amount of immobilized chiral selector molecule is lower in the case of sorbent **F**. Furthermore, the degree of cross-linking was higher in the case of aminopropylsilica (see also chapter 4 for the interpretation of the corresponding ^{29}Si CP/MAS NMR spectra) compared to glycidoxypropylsilica. In the case of glycidoxypropylsilica, this retrieves the risk of unwanted analyte silanol interactions. Furthermore, loss of sorbent material due to hydrolysis must be worried about. The described drawbacks in this material are due to the fact that moderate conditions must be chosen in the attachment reaction of the glycidoxypropylsilane to prevent opening of the oxirane ring. Therefore, the temperature must be low which prevents the silane to completely polymerize at the silica surface. Nevertheless, the chromatographic results presented in paragraph 7.3 show the better

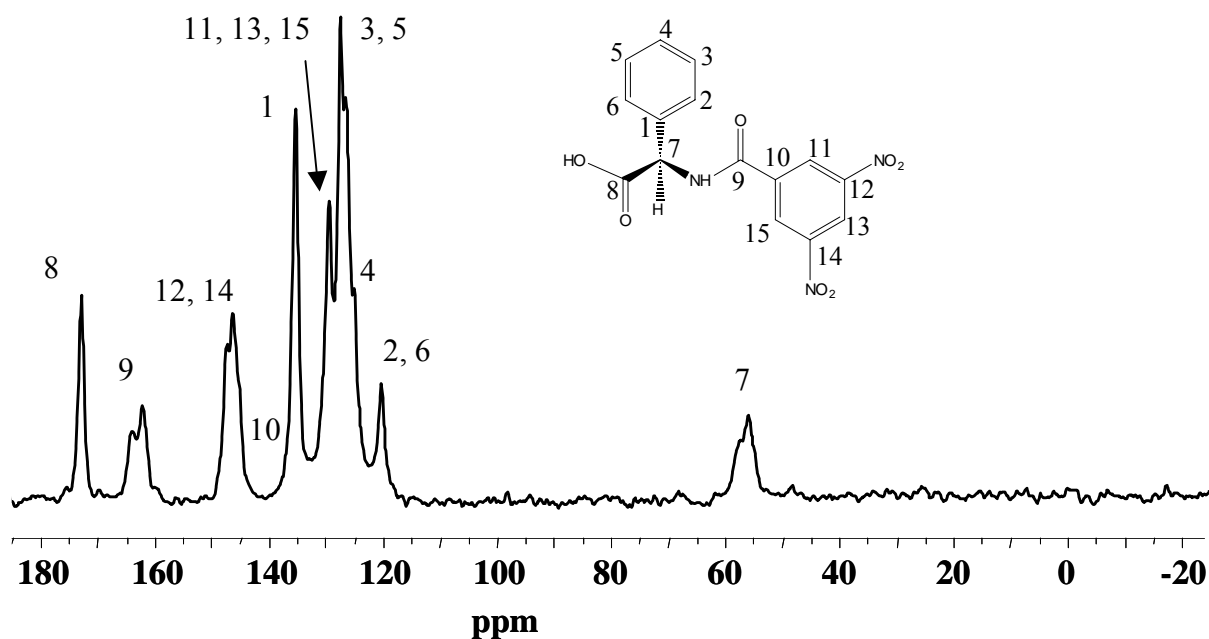


Figure 40a ^{13}C CP/MAS NMR spectra of *(S)*-(+)-*N*-(3,5-dinitrobenzoyl)- α -phenylglycine

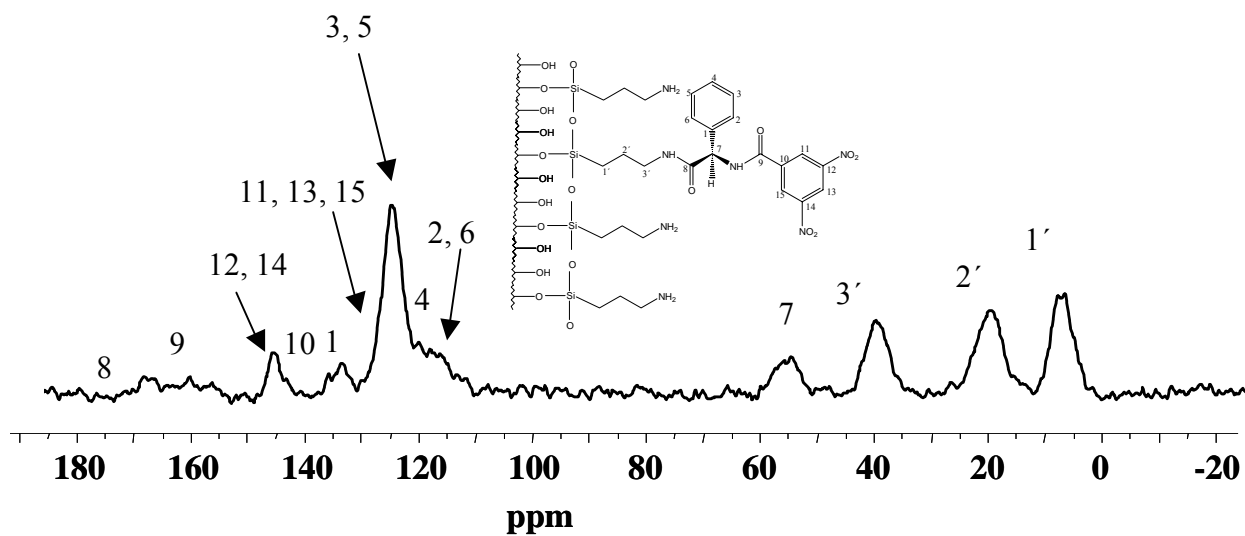


Figure 40b ^{13}C CP/MAS NMR spectra of *(S)*-(+)-*N*-(3,5-dinitrobenzoyl)- α -phenylglycine
3-aminopropylsilica

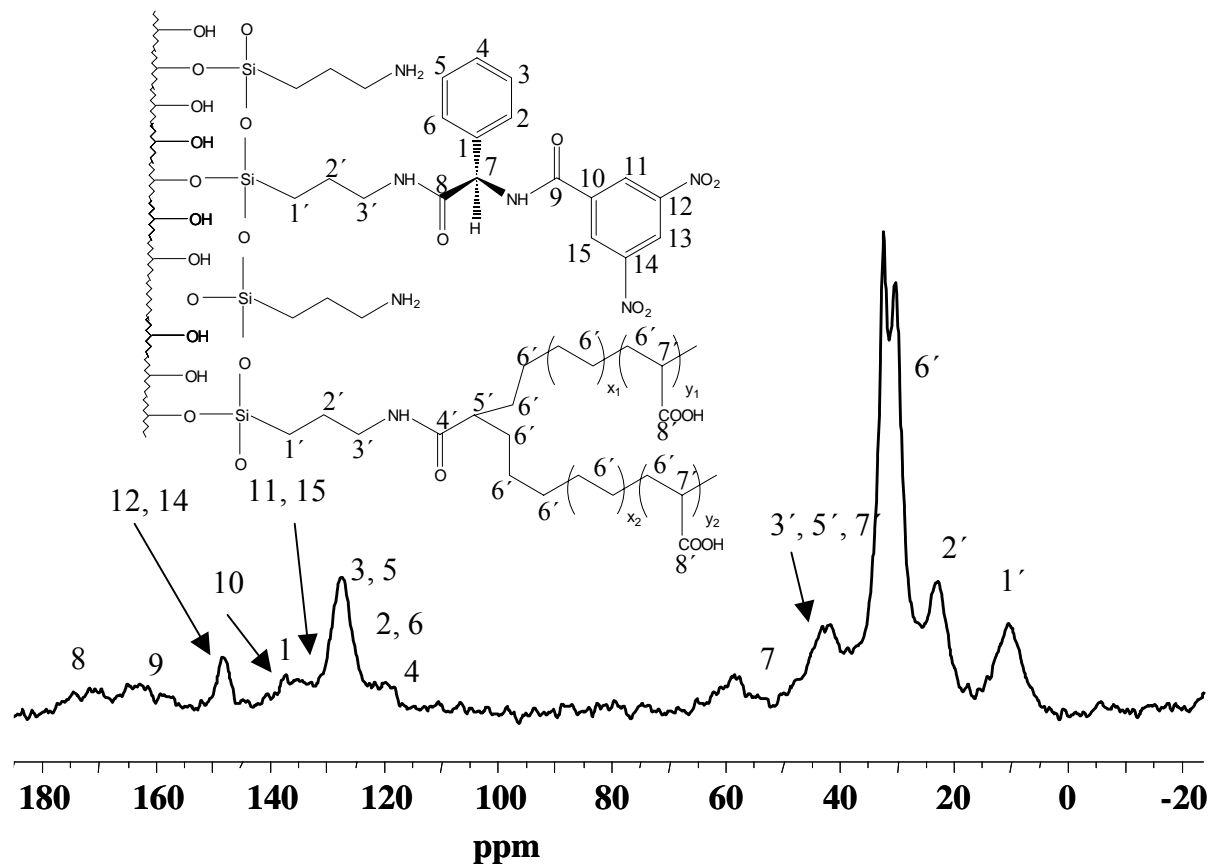


Figure 40c ^{13}C CP/MAS NMR spectra of sorbent *E*

chromatographic performance of sorbents synthesized using the glycidoxypyrilsilane linkage strategy due to the absence of possible amino group analyte interactions. In Figure 40a the ^{13}C solid-state CP/MAS NMR spectrum of the free chiral selector molecule (*S*)-(+)-*N*-(3,5-dinitrobenzoyl)- α -phenylglycine is given. The chemical shift of the acid group appears in the down-field region at 175 ppm (C-8). The amide group signal C-9 is at 165 ppm. High-field shifted therefrom are the carbon atoms of the aromatic ring. The chemical shift of the chiral carbon atom C-7 of the selector molecule appears at 57 ppm. Figure 40b shows the ^{13}C solid-state CP/MAS NMR spectrum of the chiral selector

molecule (*S*)-(+)-*N*-(3,5-dinitrobenzoyl)- α -phenylglycine immobilized on aminopropylsilica. In addition to the carbon chemical shifts of the

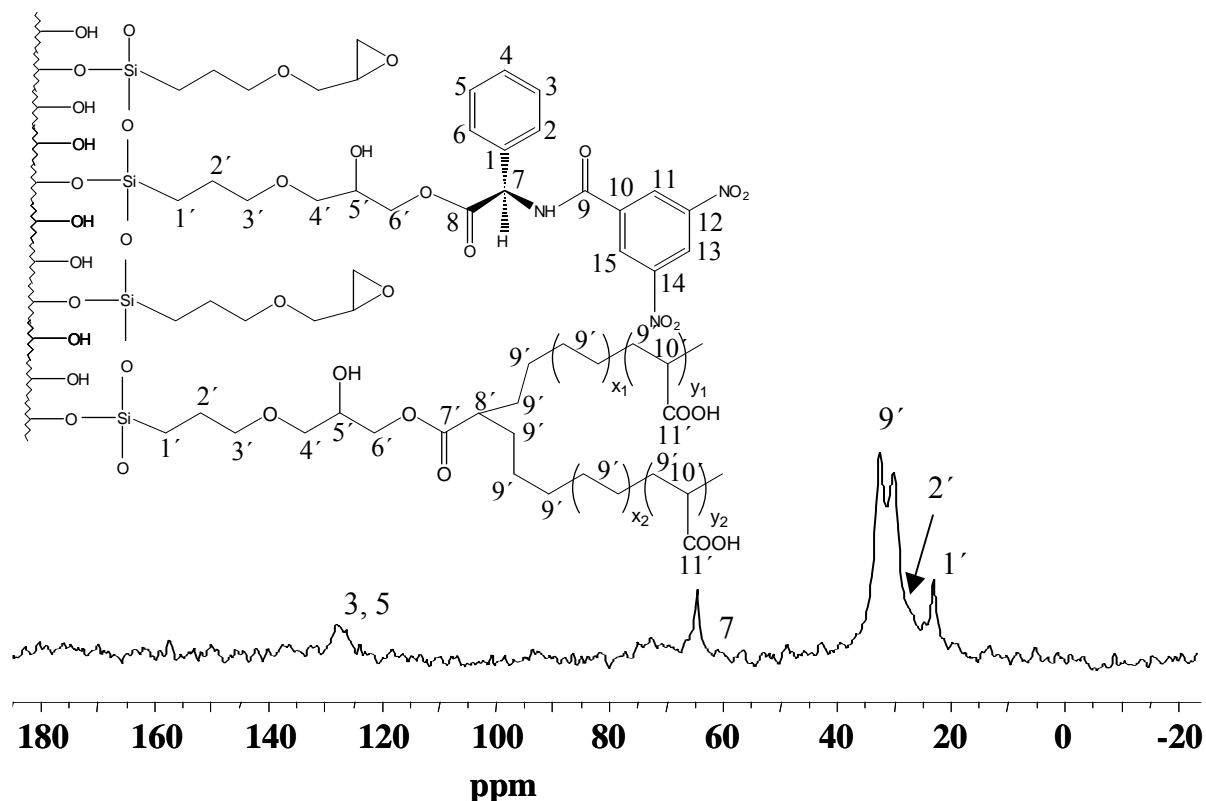


Figure 40d ^{13}C CP/MAS NMR spectra of sorbent *F*

selector molecule the three shifts of the immobilized linker molecule aminopropyltriethoxysilane appear in the high-field region between 0 and 50 ppm. The next step was the subsequent immobilization of the poly(ethylene-*co*-acrylic acid). Due to the huge molecular weight of this polymer ($M = 3500$ Da) compared to the chiral selector ($M = 345$ Da) the carbon mass fraction rose (see Table 11) and also the signal-to-noise ratio of the carbon chemical shift corresponding to the main alkyl chains is higher than the one of the chiral selector molecule. Also here, a signal splitting into a shift at 30 ppm

and 32.8 ppm, as expected, was observed indicating mobile *gauche* and rigid *trans* aligned alkyl chains. The combined immobilization of both stationary phases, the chiral selector and the polymer, on glycidoxypropylsilica yielded sorbent **F**. Due to the minor degree of immobilization, the signal intensity of the chiral selector is low. However, the elemental analysis clearly proved the successful immobilization with the existence of nitrogen that stems from the chiral selector. Also the carbon chemical shifts between 125 ppm and 130 ppm correspond to the aromatic carbon atoms of the immobilized chiral selector. Clearly visible is the signal splitting in the carbon chemical shift corresponding to the main alkyl chain of the immobilized polymer.

7.3 Application in the RP and NP mode

In order to test the synthesized sorbents, the enantiomers **R** and **S** of 2,2,2-trifluoro-(9-anthryl)ethanol were eluted from sorbent **E**. The enantiomers were separated with a selectivity $\alpha_{S/R} = 1.28$. Also sorbent **F** separated the isomers **R** and **S** of 2,2,2-trifluoro-(9-anthryl)ethanol with a selectivity of $\alpha_{S/R} = 1.1$.

Even though the enantioselectivity was found to be better when these solutes were eluted from sorbent **E** under these experimental conditions, the peak shape was better on sorbent **F** due to the absence of interfering analyte amino interactions. The influence of amino groups was observed before when sorbent **D** was compared to sorbent **A** (see chapter 5). Sorbent **E** was also employed to separate the enantiomers of all-*trans*

astaxanthin. The obtained selectivities were $\alpha_{3S, 3'S/3S, 3'R}$ and $3R, 3'S = 1.1$ and $\alpha_{3S, 3'R}$ and $3R, 3'S / 3R, 3'R = 1.1$. All chiral separations were performed in the NP mode. By applying RP

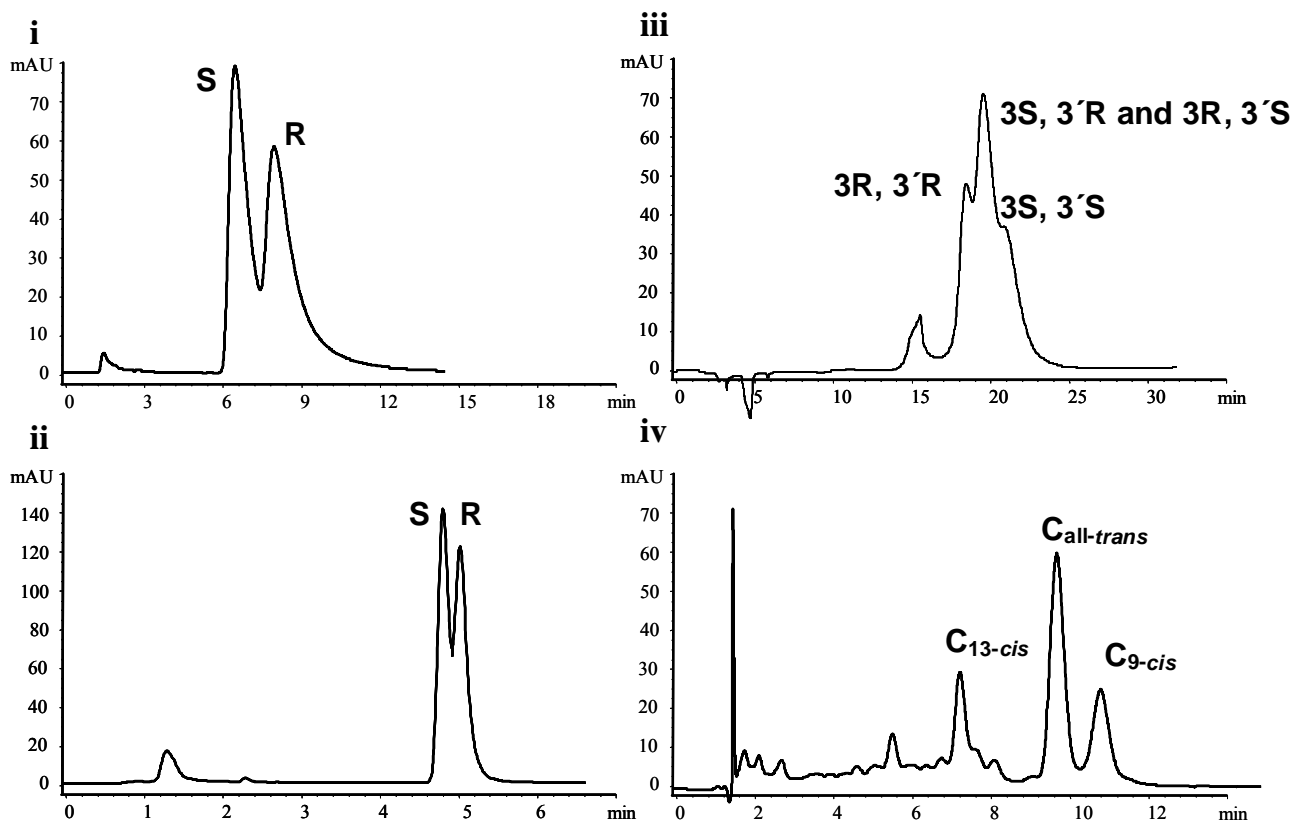


Figure 41 Chromatograms of **i**: *S* and *R* 2,2,2-trifluoro-(9-anthryl)ethanol eluted from sorbent **E** using a mobile phase composition of *n*-heptane/2-propanol 95/5 (v/v); **ii**: *S* and *R* 2,2,2-trifluoro-(9-anthryl)ethanol eluted from sorbent **F** using a mobile phase composition of *n*-heptane/2-propanol 95/5 (v/v); **iii**: (3*S*, 3'*S*), (3*R*, 3'*R*), (3*S*, 3'*R*) and (3*R*, 3'*S*) all-trans astaxanthin eluted from sorbent **E** using a mobile phase composition of *n*-heptane/methylene chloride/2-propanol 70/25/5 (v/v/v); **iv**: 13-cis (C_{13-cis}), all-trans (C_{all-trans}), and 9-cis (C_{9-cis}) β-carotene eluted from sorbent **F** using a mobile phase composition of methanol/water 95/5 (v/v)

conditions geometric β -carotene isomers were separated on sorbent **F** with selectivities of $\alpha_{2/1} = 1.5$ and $\alpha_{3/2} = 1.1$.

7.4 Discussion

Two novel chiral polymer based sorbents were synthesized and characterized by ^{29}Si and ^{13}C solid-state NMR spectroscopy, and elemental analysis. Sorbent **E** separated 2,2,2-trifluoro-(9-anthryl)ethanol and also slightly separated the enantiomers of all-*trans* astaxanthin in the NP mode. The chiral polymer based glycidoxypropylsilica

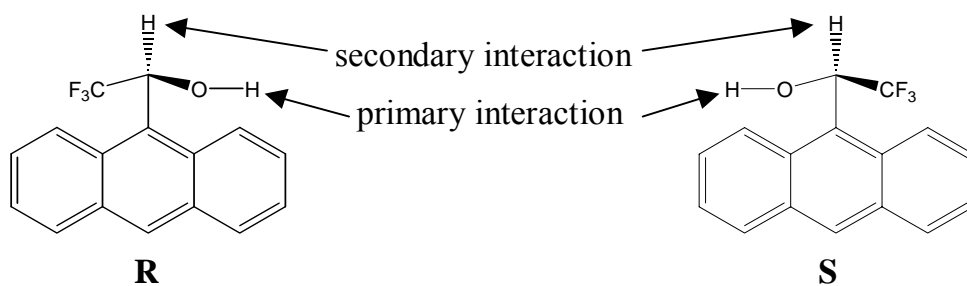


Figure 43 Sites of interactions in analyte enantiomers

sorbent separated non-polar geometric β -carotene isomers in the RP mode, due to the shape selective properties of the *trans* aligned alkyl chains in the copolymer. This sorbent separated 2,2,2-trifluoro-(9-anthryl)ethanol in the NP mode, due to the chiral recognition center in the immobilized (*S*)-(+)-*N*-(3,5-dinitrobenzoyl)- α -phenylglycine selector molecule. These findings can be ascertained in a further analyte selector interaction study

by employing ^1H suspended-state HR/MAS NMR spectroscopy. Therefore, the rationale for the chiral recognition effect in the newly synthesized sorbents will be discussed here.

A minimum of three interaction points are necessary in order for a chiral selector molecule to differentiate between two enantiomers [124]. NMR studies before proved, that interactions of chiral analyte molecules like fluoroalcohols (such as the (*S*)- and (*R*)-enantiomers of 2,2,2-trifluoro-1-(9-anthryl)ethanol) form a two-point mode of interaction with an appropriate selector molecule (such as (*S*)-(+)-*N*-(3,5-dinitrobenzoyl)- α -phenylglycine). Figure 43 and 44 show the corresponding sites of interactions of these molecules [129].

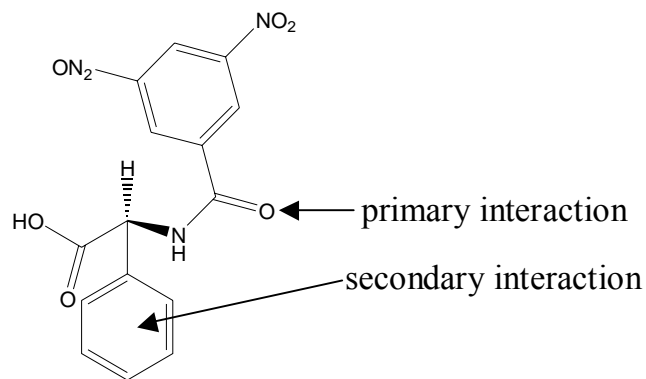


Figure 44 Sites of interactions in the chiral selector molecule

Thereby, the primary interaction is a hydrogen bond interaction between the amide group in the selector molecule and the hydroxyl hydrogen of the fluoroalcohol, the secondary is a carbonyl interaction in between the phenyl group in the selector molecule and the carbonyl hydrogen in the fluoroalcohol. Thus, two diastereomeric solvates are formed, see Figure 45. These diastereomeric solvates differ in stability. This is due to the

fact that the remaining substituents of the fluoroalcohol analyte molecules interact differently with the chiral selector molecule, depending on their diastereomeric configuration ((*R*) or (*S*) form). In case of the (*R*) form, the remaining anthryl group, an

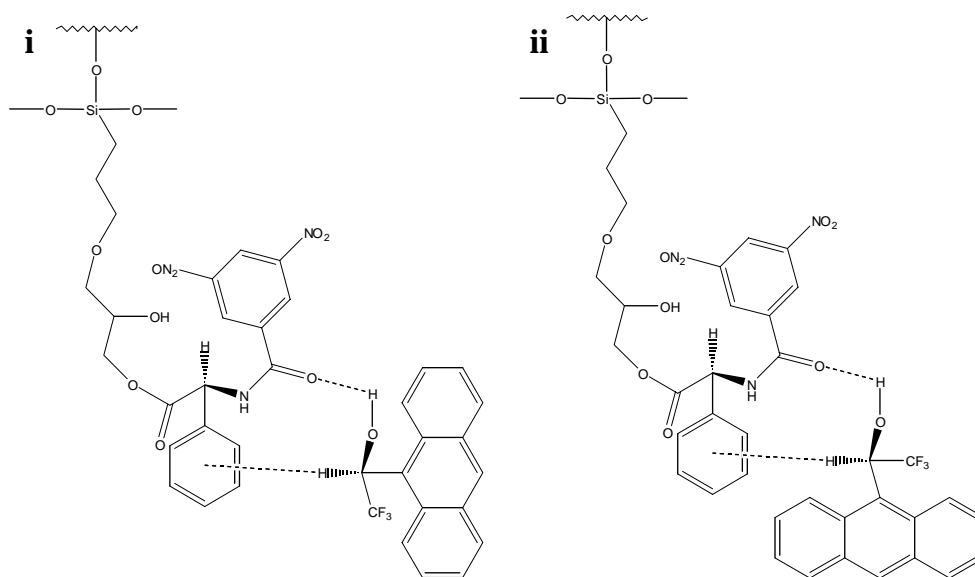


Figure 45 Diastereomeric complexes formed upon the interactions between the immobilized chiral selector (*S*)-(+)-*N*-(3,5-dinitrobenzoyl)- α -phenylglycine (chiral polymer based sorbent **F**) and the chiral (*S*) and (*R*) isomers of 2,2,2-trifluoro-1-(9-anthryl)ethanol. The primary interaction is a hydrogen bond between the basic oxo group in the selector and the hydrogen of the hydroxyl group in the analyte molecules (continuous circle). The secondary interaction is between the carbonyl hydrogen and the basic aromatic ring (dotted circle). The π - π -interactions between the anthryl group and the dinitrobenzoyl group determine the chiral discrimination and are stronger in the case of the (*R*) enantiomer (**ii**) compared to the (*S*) enantiomer (**i**)

electron rich π - base, can interact stronger with the dinitrobenzoyl group, which is a electron deficient π -base, of the chiral selector molecule. This is simply caused by steric alignment of the remaining substituents in the analyte molecules. Therefore, the anthryl group, or the strength of the π - π -donor-acceptor interaction with the dinitrobenzoyl group govern the enantioselectivity. The other remaining substituent, the trifluoro group, mainly strengthens the primary and secondary interactions by conferring acidity upon the hydroxyl and carbinyl groups.

In the case of the enantiomers of astaxanthin, basically the same applies as for the enantiomers of 2,2,2-trifluoro-1-(9-anthryl)ethanol. In this case, however, the π -base is the conjugated isoprenoic frame, which consists of 11 conjugated double bonds. From the results obtained in the chromatographic experiments, also here, the π - π -donor-acceptor interactions between the selector and the analyte are stronger in the case of the (3*R*, 3'*R*) isomer compared to the (3*S*, 3'*S*) astaxanthin enantiomer. Figure 46 shows a schematic visualization of these effects. The fact that the identical meso-forms elute between the two racemic forms shows that the π - π -donor-acceptor interactions are intermediate.

In order to further elucidate the strength of interactions that take place and govern the chiral discrimination process, the novel chiral polymer based sorbent materials can be investigated by using ^1H suspended-state NMR spectroscopy. Experiments such as 2D Nuclear Overhauser Effect Spectroscopy (NOESY) can give spectroscopic proof of interactions and their intensities under conditions similar to those used in HPLC [79, 80]. It has to be mentioned that the chiral recognition process is based on interactions taking place via the described three points of interactions in the NP mode; implying non-polar

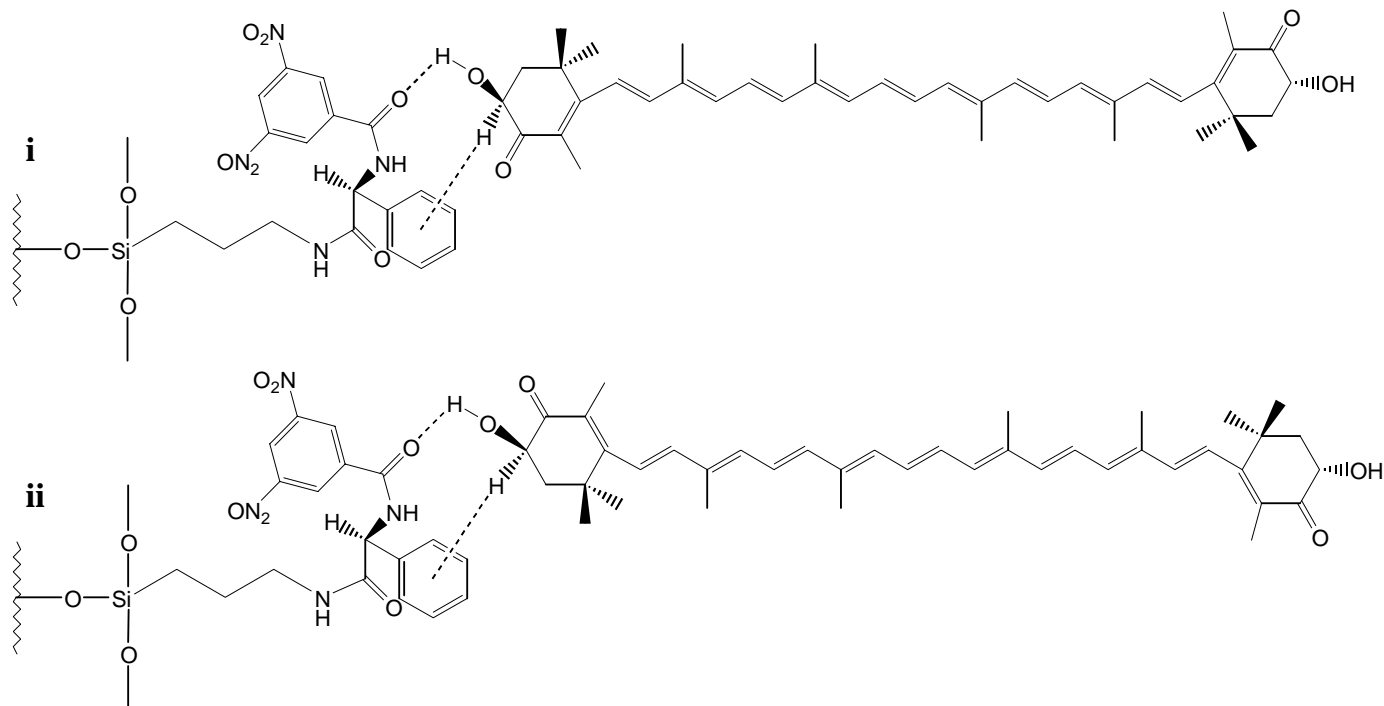


Figure 46 Proposed diastereomeric complexes formed upon the interactions between the immobilized chiral selector (*S*)-(+)-*N*-(3,5-dinitrobenzoyl)- α -phenylglycine (chiral polymer based sorbent **E**) and the (*3S*, *3'S*) and (*3R*, *3'R*) enantiomers of astaxanthin. The primary interaction is a hydrogen bonding between the basic oxo group in the selector and the hydrogen of the hydroxyl group in the analyte molecules (continuous circle). The secondary interaction is between the carbonyl hydrogen and the basic aromatic ring (dotted circle). The π - π -interactions between the anthryl group and the dinitrobenzoyl group determine the chiral discrimination and are stronger in the case of the (*3R*, *3'R*) isomer (**ii**) compared to the (*3S*, *3'S*) isomer (**i**)

solvents like *n*-hexane or *n*-heptane being employed to elute the chiral analyte molecules from the stationary phases. By employing the non-polar solvents the three point chiral

interactions can take place. The polarity of an organic modifier in the RP mode would interfere with the three point chiral discrimination ability of a chiral selector molecule like (*S*)-(+)-*N*-(3,5-dinitrobenzoyl)- α -phenylglycine, e.g. the necessary π - π -donor-acceptor interactions might not take place.

The separation of shape constrained *cis/trans* carotenoid isomers was above all achieved in the RP mode using the chiral polymer based column **E**. By additionally covalently immobilizing the poly(ethylene-*co*-acrylic acid) copolymer with an acid mass fraction of 5 %, the highly shape selective properties of the polymer based sorbents, elaborately described and characterized in chapters 4 and 5, were incorporated in the chiral sorbent materials. This means in principle, that a column material was synthesized that works in both modes: In the NP mode separations of enantiomers can be obtained. In the RP mode separations of shape constrained enantiomers can be obtained.

8 SUMMARY AND OUTLOOK

Several chromatographic sorbents were synthesized by immobilizing different polymers on silica gel. The materials were characterized using ^{13}C and ^{29}Si solid- and suspended-state NMR spectroscopy, ellipsometry, and contact angle measurements.

The influence of different factors on the retention mechanism such as different degrees of immobilization, different mobile phase compositions, different temperatures, different polymer chain lengths and polarities, and different strategies of immobilization were investigated by comparing spectroscopic evidence with chromatographic experiments. Thereby, the dependence of the retention mechanism from the alkyl chain morphology in the stationary phases was approved. Only the stationary phases containing rigid *trans* aligned copolymeric chains were able to fully separate shape constrained solutes which did not differ in polarity.

Ideal separations of shape constrained solutes like β -carotene *cis/trans* isomers or PAHs were achieved with the poly(ethylene-*co*-acrylic acid) copolymer with an acid mass fraction of 5 %, which contained the longest alkyl chain units, immobilized on silica gel using a glycidoxypropyl linkage. For this sorbent, the surface coverage did not degrade the selectivity. Lower degrees of immobilization actually allowed for faster separations, thus by properly adjusting the synthesis conditions, tailored polymer based sorbents for rapid separations can be achieved. Separations with high selectivities can also be achieved with an isocratic mobile phase of either methanol but also acetonitrile. The temperature

range for maximum separation efficiencies of shape constrained solutes was between 288 K and 298 K.

Among the synthesized polymer based materials, the sorbent which showed the highest selectivities towards shape constrained solutes was chosen to be applied in the hyphenation of capillary HPLC to NMR spectroscopy. Therewith, an analyte mixture of tocopherols isomers was separated and identified. Due to the high loadability of polymer based chromatographic sorbents, a concentration of the tocopherol homologues higher than usual (compared to C₃₀ sorbents) could be injected which yielded a better signal-to-noise-ratio in the ¹H NMR spectroscopic detection of the separated compounds. Therefore, the polymer based chromatographic sorbents will assure distinct improved sensitivities in the hyphenation of capillary HPLC to ¹H NMR spectroscopy. Beyond it, the polymer based sorbents did not exhibit overloading effects compared to a C₃₀ based sorbent when acetonitrile was used as mobile phase. Sufficient selectivities were achieved, thus disturbing solvent signals in the ¹H NMR spectra will no longer have to be suppressed. This also means, in principle, that possible applications of the novel polymeric sorbents in preparative chromatography are evident.

Finally, a chiral “Pirkle-type” selector molecule was incorporated in the polymer based sorbents with the highest selectivities towards shape constrained solutes. This was achieved by attaching the chiral selector with the same immobilization chemistry as to immobilize the polymers on the silica surface. This “mixed-mode” sorbent functioned in the reversed-phase mode as shape selective sorbent with comparable superior selectivities as described above. In the normal-phase mode this polymer based chiral sorbent separated

enantiomers such as the (*R*) and (*S*) form of 2,2,2-trifluoro-(9-anthryl)ethanol. In this case, the underlying chiral separation mechanism was governed by π - π -acceptor-donor-interactions. Since these interactions can also take place with the conjugated double bonds of carotenoid molecules, a separation of astaxanthin enantiomers was also achieved employing the polymer based chiral chromatographic sorbents. Thus, a step forward in the analysis of chiral and geometric isomers of carotenoids was achieved.

9 EXPERIMENTAL

9.1 Chemicals

3-Aminopropyltriethoxysilane (98.5 %) was obtained from ABCR (Karlsruhe, Germany). 3-Glycidoxypropyltrimethoxysilane (98 %), poly(ethylene-*co*-acrylic acid) copolymers with acrylic acid mass fractions of 5, 10, and 15 %, and (*S*)-(+)-*N*-(3,5-dinitrobenzoyl)- α -phenylglycine were obtained from Aldrich Chemical Company Inc. (Milwaukee, WI, USA). ProntoSIL-300-3-SI silica (3 μm particle size, 300 \AA pore size) with a surface area of 150 m^2/g was obtained from Bischoff Chromatography (Leonberg, Germany). 1-Hydroxybenzotriazole (99 %), (*S*)- (98 %), and (*R*)- (98 %) 2,2,2-trifluoro-(9-anthryl)ethanol, and *N,N'*-Diisopropylcarbodiimide (99 %) were obtained from Sigma-Aldrich Chemie GmbH (Steinheim, Germany). All-*trans* β -carotene was purchased from Fluka (Buchs, Switzerland) and isomerized using the procedure described by Zechmeister to obtain a mixture of 13-*cis*, all-*trans*, and 9-*cis* β -carotene [75]. Lutein, zeaxanthin, and astaxanthin were a kind gift from BASF Aktiengesellschaft (Ludwigshafen, Germany). SRM 869 column selectivity test mixture for LC was obtained from the NIST standard reference materials program (NIST, Gaithersburg, MD, USA) [77]. The tocopherols were obtained from Calbiochem (San Diego, CA, USA). All solvents used in the HPLC experiments were of HPLC grade (Solusorb, Mallinckrodt Baker Inc., Phillipsburg, PA, USA and LiChrosolve, Merck, Darmstadt, Germany). The solvents used for the suspended-state NMR experiments and the capillary HPLC-NMR experiments were

methanol- d_4 (Uvasol, 99.8 %), and D_2O (Uvasol, 99.8 %) (Merck, Darmstadt, Germany).

The silica wafers were obtained from Wacker Chemitronic (Burghausen, Germany).

9.2 Synthesis of the poly(ethylene-*co*-acrylic acid) chromatographic sorbents

Synthesis of 3-aminopropylsilica respectively 3-glycidoxypropylsilica

The silica was dried under vacuum at 453 K for 4 h in order to remove all adsorbed water from the surface and then cooled to room temperature and stored under N_2 atmosphere.

The silica (4 g) was suspended in dry toluene (20 mL) in a three necked round bottomed flask equipped with a reflux condenser. Then, a three fold excess of 3-aminopropyltriethoxysilane (3.0 mL) respectively 3-glycidoxypropyltrimethoxysilane (2.5 mL) was added with a syringe and refluxed under nitrogen atmosphere for 12 h. The hot slurry was filtered and washed with aliquots of toluene, acetone, and *n*-hexane. The 3-aminopropylsilica and 3-glycidoxypropylsilica were dried at room temperature for 24 h.

Synthesis of chromatographic sorbents A, B, and C

1.6 g Poly(ethylene-*co*-acrylic acid) with a 5 % mass fraction of acrylic acid was dissolved with hydroxybenzotriazole (80 mg) and dry *N,N*-dimethylformamide (50 mL) in dry xylene (50 mL). Then after slowly stirring under nitrogen atmosphere at 273 K for 30 min diisopropylcarbodiimide (0.6 mL) was added, after another 30 min the 3-aminopropylsilica (4.0 g) was suspended in the solution. Within 3 h the temperature was

raised to room temperature. After refluxing for 44 h the hot slurry was filtered and washed with aliquots of hot xylene/*N,N*-dimethylformamide, xylene, acetone, methanol, methanol/water (50/50, v/v), methanol, acetone, and *n*-pentane. The resulting yellow-brownish colored chromatographic sorbent **A** was dried for 24 h. The two other chromatographic sorbents **B** and **C** were synthesized from poly(ethylene-*co*-acrylic acid) with mass fractions of 10 % and 15 % respectively, using the same procedure.

Synthesis of chromatographic sorbent D

1.6 g of poly(ethylene-*co*-acrylic acid) with a 5 % mass fraction of acrylic acid was dissolved in dry xylene (50 mL). After refluxing for 30 min under nitrogen atmosphere the 3-glycidoxypropylsilica (4.0 g) was added and refluxed for 24 h. Then the slurry was filtered hot and washed with aliquots of hot xylene (isomeric mixture of *o*-, *m*-, and *p*-xylene), acetone, methanol, methanol/water (50/50, v/v), methanol, acetone, and *n*-pentane. The resulting white colored chromatographic sorbent **D** was dried for 24 h.

Synthesis of the chiral polymer based chromatographic sorbent E

6 g Aminopropylsilica were added to a solution of 3 g (*S*)-(+)-*N*-(3,5-dinitrobenzoyl)- α -phenylglycine in 80 mL tetrahydrofuran. 2.4 g of 2-ethoxy-1-ethoxycarbonyl-1,2-dihydroquinoline was added and the solution was stirred for 24 h at ambient conditions. Then the slurry was filtered and washed with aliquots of tetrahydrofuran, acetone, and *n*-pentane. The resulting pinkish colored intermediate product was dried for 24 h. Then 1.6 g poly(ethylene-*co*-acrylic acid) with a 5 % mass fraction of acrylic acid was dissolved

with hydroxybenzotriazole (80 mg) and dry *N,N*-dimethylformamide (50 mL) in dry xylene (50 mL). Then after slowly stirring at 293 K for 30 min diisopropylcarbodiimide (0.6 mL) was added, after another 30 min the intermediate product (2.0 g) was suspended in the solution. After refluxing for 44 h the hot slurry was filtered and washed with aliquots of hot xylene (isomeric mixture)/*N,N*-dimethylformamide, xylene (isomeric mixture), acetone, methanol, methanol/water (50/50), methanol, acetone, and *n*-pentane. The resulting pinkish colored chromatographic sorbent **E** was dried for 24 h.

Synthesis of the chiral polymer based sorbent **F**

0.8 g of poly(ethylene-*co*-acrylic acid) with a 5 % mass fraction of acrylic acid and 0.5 g (*S*)-(+)-*N*-(3,5-dinitrobenzoyl)- α -phenylglycine was dissolved in 50 mL dry xylene (isomeric mixture)/THF (v/v). After stirring for 30 min the 3-glycidoxypropylsilica (4.0 g) was added and stirred for 24 h. Then the slurry was filtered and washed with aliquots of hot xylene (isomeric mixture), acetone, methanol, methanol/water (50/50), methanol, acetone, and *n*-pentane. The resulting white colored chromatographic sorbent **F** was dried for 24 h.

9.3 Synthesis of the poly(ethylene-*co*-acrylic acid) silica wafers

The modification of the silica wafers was carried out by cutting single-side polished wafers with a natural SiO₂ layer of about 2 nm into 15 mm² pieces. The silicon pieces were cleaned and activated for 15 min with a freshly prepared piranha solution

($\text{H}_2\text{SO}_4/\text{H}_2\text{O}_2 = 2/1$ (v/v)) in an ultrasonic bath. Afterwards the wafers were rinsed with ultra clean water ($>18 \text{ M}\Omega$ resistivity) and dried with nitrogen. In order to determine the thickness of the natural SiO_2 layer, the cleaned wafers were measured with the null ellipsometer. The freshly cleaned wafers were deposited into a solution of 20 mL toluene and 20 μL 3-aminopropyltriethoxysilane respectively 20 μL 3-glycidoxypropyltrimethoxysilane for 1 h at room temperature. After removing the wafers from the solution, they were rinsed with toluene and the surfaces were characterized with ellipsometric measurements. The copolymers were immobilized corresponding to the reaction procedures for the synthesis of chromatographic sorbents **A**, **B**, **C**, and **D** as described above. The surfaces were characterized by ellipsometry and water contact angle measurements.

9.4 NMR spectroscopy

The solid-state NMR spectra were recorded at 295 K on a Bruker ASX 300 (7.05 Tesla) spectrometer (Bruker BioSpin, Rheinstetten, Germany). The minimum number of scans recorded was 2048 in each experiment. To process the NMR spectra, 1D WINNMR software (Bruker Biospin GmbH, Rheinstetten, Germany) was used. Zero filling up to 2K data points and an exponential multiplication of the FID with a line broadening of 20 Hz for ^{29}Si CP/MAS NMR spectra and 10 Hz for the ^{13}C CP/MAS NMR spectra respectively, were performed before Fourier transformation. For the HPLC-NMR coupling experiments a AMX 600 spectrometer (Bruker Biospin GmbH, Rheinstetten, Germany) was

employed. Suspended-state NMR experiments were carried out at 295 K on the Bruker ASX 300 (7.05 Tesla) spectrometer (Bruker BioSpin, Rheinstetten, Germany).

²⁹Si CP/MAS NMR spectroscopy

The spectra were recorded with the chromatographic sorbents packed into 7 mm double bearing rotors of ZrO₂ at a spinning rate of 3500 Hz. The proton 90° pulse length was 6.5 μs and the cross-polarization contact time 5 ms. The pulse intervals were 1 s. All chemical shifts were referenced externally to TMS.

¹³C MAS NMR spectroscopy

For the ¹³C NMR experiments the chromatographic sorbents were packed into 4 mm double bearing rotors of ZrO₂.

The ¹³C CP/MAS experiments were carried out at a spinning rate of 4000 Hz, the proton 90° pulse length was 3 μs and the spectra were obtained with a cross-polarization contact time of 3 ms. The pulse intervals were 1 s. Glycine was used as a reference and to adjust the Hartmann-Hahn condition.

The ¹³C HPDEC/MAS NMR spectra were obtained with a ¹³C 90° pulse length of 6.5 μs and a delay time of 5 s at a spinning rate of 3000 Hz.

The spin-diffusion MAS NMR measurements were recorded at 295 K. A dipolar filter with ten repetition cycles (*I0*) and a delay time of 8 μs (*d9*) between the ¹H pulses was applied. A 7 mm probe was employed at a spinning rate of 4000 Hz and a sample temperature of 295 K (90° pulse angle 5.9 μs, contact time 2 ms, delay time 1 s). The

simulation of the spin-diffusion was performed with a self-developed computer program (MR-SpinDiff) on a PC (Pentium, 200 MHz).

For the suspended-state NMR experiments two mobile phase compositions, methanol- d_4 and methanol- d_4 /D₂O (50/50, v/v), were added to the chromatographic sorbents with a syringe in 4 mm double bearing rotors of ZrO₂. The ¹³C MAS NMR spectra were obtained with a ¹³C 90 ° pulse length of 6.5 μs and a delay time of 5 s at a spinning rate of 3000 Hz.

Temperature NMR experiments

The spectra were recorded in the group of Dr. Detlef Reichert in cooperation with Ovidiu Pascui (Department of Physics, University of Halle). A Varian VT 7 mm MAS probe (Jackobsen design) on a Varian Inova spectrometer operating at a resonance frequency of 100.54 MHz for ¹³C (Varian Inc., Palo Alto, USA) was used. The temperature was calibrated using Pb(NO₃)₂ as standard [136]. For the line shape experiments ¹³C CP/MAS NMR spectroscopy at a spinning rate of 1200 Hz was used. The 90° pulse length was 5 μs for ¹³C and 4.6 μs for ¹H. The pulse interval time $d1$ was 3 s. For each experiment 512 transients were recorded with a CP contact time of 0.5 ms and an acquisition time of 20 ms. For each DIPSHIFT experiment to measure C-H dipolar couplings 1024 transients were accumulated at a spinning rate of 4711 Hz and otherwise with the same experimental parameters as described above. For the DIPSHIFT experiment, ¹H-¹H homonuclear decoupling was achieved by the frequency switched Lee-Goldburg (FSLG) sequence [89]. The 360 ° ¹H decoupling pulses had a duration of 15-17 μs with an

effective decoupling field strength of 70-80 kHz. Since the dipolar-induced signal decay is periodic with the MAS rotor period, it was only necessary to acquire the signal over one rotor period in the indirect dimension. Therefore the DIPSHIFT spectra were only Fourier transformed in the direct dimension, and the dipolar dephased signal was extracted for each resolved peak. The one rotor period time domain data were fitted to yield the coupling strength of interest. The time evolution under the C-H dipolar couplings in 2D DIPSHIFT experiments was simulated for one rotor period with a self written FORTRAN program. Simulations were performed for varying dipolar coupling strengths. Powder averaging was performed in 2 ° and 3 ° increments for the α and β Euler angles, respectively. Other input parameters included the number of t_1 increments, the dwell time and the spinning rate. For all experiments, the simulated curves were multiplied by an exponential decay to account for T_2 relaxation effects during the time evolution. Best agreement between simulation and experiment was determined by the smallest root-mean-square deviation values.

9.5 Ellipsometry

The ellipsometric measurements of the layer thickness were performed with a null ellipsometer ELX-02-C (Dr. Riss Ellipsometerbau, Ratzeburg, Germany) in the group of Prof. Dr. Günter Gauglitz in cooperation with Stefan Busche (Institute of Physical Chemistry, University of Tübingen). Changes in the state of polarization caused by reflection at the probe interfaces are measured with ellipsometry. All measurements were

performed at least three times and the mean values and standard deviation are given in Figure 10.

9.6 Contact angle measurements

The contact angle measurements were performed with an optical contact angle meter from KSV (Finland). Measurements were repeated at least three times and mean values and standard deviations are given in Table 3.

9.7 HPLC

All chromatographic sorbents were slurry packed into 125 x 4.6 mm stainless steel columns at 40 MPa on a Knauer Pneumatic HPLC pump (Berlin, Germany) using standard methods.

A stock solution of β -carotene was prepared (1 mg/mL) in *n*-hexane and isomerized under UV light for 30 min by adding 10 μ L of a 100 μ g/mL solution of iodine in *n*-hexane. The isomerized stock solution was further diluted to 100 μ g/mL with methanol, stored at 277 K and used for analysis; the peak identification is based on the literature [76]. Lutein and zeaxanthin and also astaxanthin were dissolved in the corresponding mobile phase to yield a concentration of 100 μ g/mL and used for peak identification and analysis. The different carotenoid standards were eluted using different mobile phase compositions of methanol/water as well as acetonitrile. SRM 869 was eluted using a mobile phase

composition of methanol/water (95/5, v/v). The stock solution of the (*S*) and (*R*) 2,2,2-trifluoro-(9-anthryl)ethanol enantiomers with a concentration of 100 µg/mL in the mobile phase was eluted from the chiral sorbents using *n*-heptane/2-propanol 95/5 (v/v). (**3S**, **3'S**), (**3R**, **3'R**), (**3S**, **3'R**) and (**3R**, **3'S**) all-*trans* astaxanthin (*c* = 100 µg/mL) were eluted from the chiral sorbents using a mobile phase composition of *n*-heptane/methylene chloride/2-propanol 70/25/5 (v/v/v). All analyte mixtures were either introduced via a injector equipped with a 100 µL loop and isocratically separated on an Agilent Series 1100 instrument (Agilent, Waldbronn, Germany) or via a Dionex autoinjector ASI-100 (injection volume 10 µL) and separated on a Dionex P580 instrument (Dionex, Sunnyvale, CA, USA) both with an UV-detector. Detection was adjusted to 455 nm for the β-carotene isomers as well as lutein and zeaxanthin, at 480 nm for the astaxanthin isomers, and at 254 nm for SRM 869 as well as for the 2,2,2-trifluoro-(9-anthryl)ethanol enantiomers. The flow rate was 1 mL/min for each elution. In order to confirm the obtained retention factors and selectivities each chromatographic experiment was performed at least twice. The void volume was determined from a void volume marker molecule which was not retarded. The column temperature was controlled within ±0.1 K by a circulating methanol jacket, and was 298 K, if not designated otherwise.

9.8 Capillary HPLC-NMR hyphenation

For packing capillaries, 20 mg of the polymer based chromatographic sorbent was suspended in 300 µL of carbon tetrachloride and put in an ultrasonic bath for 10 min; then

the slurry was transferred in a chamber and forced downward into a 250 μm (inner diameter) x 150 mm fused-silica capillary using a Knauer Pneumatic HPLC pump (Berlin, Germany). Hereby, initially a pressure of 400 bar was used and increased to 650 bar within 5 min. The capillary end fittings consisted of zero dead volume unions ZU1C, steal screens 2SR1, and ferrules FS1.4-5 (Vici AG Valco Int., Schenkong, Switzerland). A capillary HPLC system was utilized consisting of an Eldex MicroPro dual-syringe pump (Eldex Laboratories, Napa, CA) equipped with on-column (100 μm inner diameter) UV detection performed at 285 nm on a Knauer UV-detector K-2500 (Knauer, Berlin, Germany) and a microinjection valve kit (Upchurch Scientific, Oak Harbor, WA) with a 200 nL fused-silica injection loop. The employed tocopherol standards were prepared by dissolving the tocopherols in methanol- d_4 to gain the desired concentration of either 1.6 mg/mL or 5.66 mg/mL (each tocopherol).

The capillary HPLC NMR system was set-up was as follows: The outlet of the UV detector was connected with the 1.5 μL active volume ^1H selective capillary NMR probe (Protasis Corp., Marlboro, MA) inlet using a 3 m fused-silica transfer capillary (50 μm inner diameter) in order to couple the capillary HPLC system to the NMR spectrometer (AMX 600, Bruker Biosin GmbH, Rheinstetten, Germany). For stopped flow measurements, an additional peak parking valve had to be inserted prior to the injection valve.

An isocratic mixture of methanol- d_4 and D_2O (85/15, v/v) was applied for the continuous-flow experiment which was performed using the pulse program lc2pnps. 16 transients with 4 k complex data points and a spectral width of 7246 Hz were accumulated with a

relaxation delay of 1 s. The pulse angle was set to 30°. During the separation, 128 rows with an acquisition time of 72 s per row were recorded. Prior to Fourier transformation, a square bell function was applied to the FID.

10 REFERENCES

- [1] Unger K K (1990) *Chromatogr Sci (Packings and Stationary Phases in Chromatographic Techniques)* Vol 47 Marcel Dekker Inc New York
 - [2] Meyer V (1998) *Praxis der Hochleistungs-Flüssigkeitschromatographie 5. Auflage* Verlag Diesterweg Sauerländer Frankfurt/Main
 - [3] Sander L C, Wise S A (1984) *Anal Chem* 56: 504-510
 - [4] Wise S A, Sander L C (1985) *J High Resolut Chromatogr Commun* 8: 248-255
 - [5] Sander L C, Wise S A (1993) *J Chrom A* 656: 335-351
 - [6] Sander L C, Wise S A (1995) In: *Retention and Selectivity in Liquid Chromatography*, Smith R M (Ed) *J Chrom Libr* 57: 337-369 Elsevier Sciences B V Amsterdam
 - [7] Sander L C, Wise S A (1995) *Anal Chem* 67: 3284-3292
 - [8] Sander L C, Pursch M, Wise S (1999) *Anal Chem* 71: 4821-4830
 - [9] Martire D E, Boehm R E (1983) *J Phys Chem* 87: 1045-1062
 - [10] Yan C, Martire D E (1992) *J Phys Chem* 96: 3489-3504
 - [11] Yan C, Martire D E (1992) *Anal Chem* 64: 1246-1253
 - [12] Alpert A J (1986) *J Chrom* 359: 85-97
 - [13] Krasilnikov I, Borisova V (1988) *J Chrom* 446: 211-219
 - [14] Jilge G, Unger K K, Esser U, Schafer H J, Ratherberger G, Mueller J (1989) *J Chrom* 476: 37-48
 - [15] Kennedy L A, Kopaciewicz W, Regnier F E (1986) *J Chrom* 359: 73-84
 - [16] Kolla P, Kohler J, Schomburg G (1987) *Chromatogr* 23: 465-472
 - [17] Cserhati T J, Forgacs E (1996) *J Chrom* 728: 67-73
 - [18] Millot M, Seville B J (1987) *Chromatogr* 408: 263-273
 - [19] Vanderkam S K, Bocarsly A B, Schwartz (1998) *Chem Mater* 10: 685-687
 - [20] Wegmann J, Albert K, Pursch M, Sander L C (2001) *Anal Chem* 73: 1814-1820
 - [21] Rimmer C, Sander L C, Wise S A (2005) *Anal Bioanal Chem* published online
-

-
- [22] Meyer C, Skogsberg U, Welsch N, Albert K (2005) *Anal Bioanal Chem* published online
- [23] Abel E W, Pollard F H, Uden P C, Nickless G (1966) *J Chromatogr* 22: 23-28
- [24] Stewart H N M, Perry S G (1968) *J Chromatogr* 37: 97
- [25] Neue U D (1997) *HPLC columns, theory, technology, and practice*. Wiley, New York
- [26] Sander L, Lippa K A, Wise S A (2005) *Anal Bioanal Chem* published online
- [27] www.bischoff-chrom.de
- [28] Pursch M, Sander L C, Albert K (1996) *Anal Chem* 68:4107-4113
- [29] Maciel G E, Sindorf D W (1980) *J Am Chem Soc* 102:7606–7607
- [30] Scholten A B, de Haan J W, Claessens H A, van de Ven L J, Cramers C A (1996) *Langmuir* 12:4741-4757
- [31] Earl W L, Vandenhart D L (1979) *Macromolecules* 12: 762-767
- [32] Gao W, Dickinson L, Grozinger C, Morin F G, Reven L (1996) *Langmuir* 12: 6429-6435
- [33] Gao W, Reven L (1995) *Langmuir* 11: 1860-1863
- [34] Gao W, Dickinson L, Grozinger C, Morin F G, Reven L (1997) *Langmuir* 13: 115-118
- [35] Srinivisan G, Pursch M, Sander L, Müller K (2004) *Langmuir* 20: 1746-1752
- [36] Sindorf D W, Maciel G E (1983) *J Am Chem Soc* 105: 1845-1851
- [37] Bayer E, Albert K, Reiners J, Nieder M, Müller M (1983) *J Chromatogr* 264: 197-213
- [38] Albert K, Pfeleiderer B, Bayer E (1987) *Chemically Modified Surfaces in Science and Industry* OPA Amsterdam 287-303
- [39] Fatunmbi H O, Bruch M D, Wirth M J (1993) *Anal Chem* 65: 2048-2054
- [40] Buszewski B, Jezierska M, Welniak M, Berek D (1998) *J High Resolut Chromatogr* 21: 267-281
- [41] Hanson M, Unger K K, Schmid J, Albert K, Bayer E (1993) *Anal Chem* 65: 2249-2253
- [42] Pursch M, Brindle R, Ellwanger A, Sander L C, Bell C M, Händel H, Albert K (1997) *Solid State Nucl Magn Res* 9: 2-4
- [43] Pursch M, Sander L C, Albert K (1999) *Anal Chem* 71: 733-741
-

-
- [44] Pursch M, Sander L C, Egelhaaf H J, Raitza M, Wise S A, Oelkrug D, Albert K (1999) *J Am Chem Soc* 121: 3201-3213
- [45] Albert K (2003) *J Sep Sci* 26: 215-224
- [46] Albert K, Lacker T, Raitza M, Pursch M, Egelhaaf H J, Oelkrug D (1998) *Angew Chem Int Ed* 37: 777-780
- [47] Clauss J, Schmidt-Rohr K, Adam A; Boeffel C, Spiess H W (1992) *Macromol* 25: 5208-5214
- [48] Schmidt-Rohr K, Spiess H W (1994) *Multidimensional Solid State NMR and Polymers Academic Press San Diego* 402-439
- [49] Mellinger F, Wilhelm M, Landfester K, Spiess H W, Haunschild A, Packusch J (1998) *Acta Polym.* 49: 108-115
- [50] Tieke B (1997) *Makromolekulare Chemie VCH Weinheim*
- [51] Elias H G (1996) *Polymere. Von Monomeren und Makromolekülen zu Werkstoffen Hüthig & Wepf Verlag Zug*
- [52] Raitza M, Wegmann J, Bachmann S, Albert K (2000) *Angew Chem Int Ed* 39: 3486-3489
- [53] Wegmann J (2001) *Doctoral Thesis, Tuebingen*
- [54] Goldman M, Shen L (1961) *Phys Rev* 144: 321-328
- [55] Clauss J, Schmidt-Rohr K, Spiess H W (1993) *Acta Polym* 44: 1-17
- [56] Kimura T, Neki K, Tamuar N, Horii F, Nakagawa M, Odani H (1992) *Polymer* 33: 493-497
- [57] Ishida M, Yoshinaga K, Horii F (1996) *Macromol* 29: 8824-8829
- [58] Eckman R R, Henrichs P M, Peacock A J (1997) *Macromol* 30: 2474-2481
- [59] Hu W G, Schmidt-Rohr K (2000) *Polymer* 41: 2979-2987
- [60] Azzam R M A, Bashara N M (1977) *Ellipsometry and Polarized Light North Holland Amsterdam*
- [61] Raitza M, Herold M, Ellwanger A, Gauglitz G, Albert K (2000) *Macromol Chem Phys* 201: 825-829
- [62] Spaeth K, Kraus G, Gauglitz G (1997) *Fres J Anal Chem* 357: 292-296
-

-
- [63] Boccara A C, Pickering C, Rivory J (eds.) (1993) *Spectroscopic Ellipsometry* Elsevier, Amsterdam
- [64] Kessel C R, Granick S (1991) *Langmuir* 7: 532-538
- [65] Calistri-Yeh M, Kramer E J, Sharma R, Zhao W, Rafailovich M H, Sokolov J, Brock J D (1996) *Langmuir* 12: 2747-2755
- [66] Karger B L, Gant J R, Hartkopf A, Weiner P H (1976) *J Chrom* 128:65-78
- [67] Horvath C S, Melander W R, Molnar I (1976) *J Chrom* 125: 129-156
- [68] Horvath C S, Melander W R (1977) *J Chrom Sci* 15: 393 –404
- [69] US Environmental Protection Agency (1979) *Fed Regist* 44: 233
- [70] Jinno K (1997) *Chromatographic separations based on molecular recognition*. Wiley, New York
- [71] Moore T A, Gust D, Moore A L (1998) *Carotenoids, Chemistry and Biology* (Editors: Krinsky N I, Matthews-Roth M M and Taylor R F) Plenum Press, New York and London 223
- [72] Sander L C, Sharpless K E, Craft N E, Wise S A (1994) *Anal Chem* 66: 1667-1674
- [73] Bell C M, Sander L C, Fetzer J C, Wise S A (1996) *J Chrom A* 753: 37-45
- [74] Sander L C, Pursch M, Märker B, Wise S A (1999) *Anal Chem* 71: 3477-3483
- [75] Zechmeister L, Tuzson P (1939) *Chem Ber* 72: 1340-1346
- [76] Strohschein S, Pursch M, Albert K (1999) *J Pharm Biomed Anal* 21: 669-677
- [77] Sander L C, Wise S A (1990) SRM 869 Column Selectivity Test Mixture for Liquid Chromatography (Polycyclic Aromatic Hydrocarbons). Certificate of Analysis. NIST Gaithersburg MD
- [78] Skogsberg U, Händel H, Sanchez D, Albert K (2004) *J Sep Sci* 26: 1119-1124
- [79] Hellriegel C, Skogsberg U, Albert K, Lämmerhoffer M, Maier N E, Lindner W (2004) *J Am Chem Soc* 126: 3809-3816
- [80] Skogsberg U, Händel H, Sanchez D, Albert K (2004) *J Chromatogr A* 1023: 215-223
- [81] Strohschein S, Pursch M, Lubda D, Albert K (1998) *Anal Chem* 70: 13-18
-

-
- [82] Carr P W, Doherty R M, Kamlet M J, Taft R W, Melander W, Horvath C (1986) *Anal Chem* 58: 2674-2680
- [83] Haidacher D, Vailaya A, Horvath C (1996) *Proc Natl Acad Sci USA* 93: 2290-2295
- [84] Vailaya A, Horvath C (1996) *J Phys Chem* 100: 2447-2455
- [85] Vailaya A, Horvath C (1998) *J Phys Chem* 102: 701-718
- [86] Shashikala S, Wegmann J, Albert K, Müller K (2002) *J Phys Chem B* 106: 878-888
- [87] Pursch M, Strohschein S, Händel H, Albert K (1996) *Anal Chem* 68: 386-393
- [88] Bachmann S, Hellriegel C, Wegmann J, Händel H, Albert K (2000) *Solid State Nucl Magn Res* 17: 39-51
- [89] Kolbert AC, de Groot HJM, Levitt MH, Munowitz MG, Roberts JE, Harbison GS, Herzfeld J, Griffin RG (1990) In: *Multinuclear magnetic resonance in liquids and solids - chemical applications*, Granger P, Harris RK (eds) Kluwer Academic Publishers, Dordrecht 339-354.
- [90] Hong M, Gross JD, Griffin RG (1997) *J Phys Chem* 101: 5869-5874
- [91] Huster D, Xiao L, Hong M. *Biochemistry* 2001, 40: 7662-7674
- [92] Lipari G, Szabo A (1982) *J Am Chem Soc* 104: 4559-4570
- [93] Böhm V (1999) *Chromatogr* 50: 282- 286
- [94] Bell C M, Sander L C, Wise S A (1997) *J Chrom A* 757: 29-39
- [95] Wheeler J F, Beck T L, Klatt S J, Cole L A, Dorsey J G (1993) *J Chrom* 656: 317-333
- [96] Tchaplal A, Heron S, Lesellier E, Colin H (1993) *J Chrom* 656: 81-112
- [97] Sander L, Wise S (1996) SRM 1647 Column Selectivity test Mixture for Liquid Chromatography (Polycyclic Hydrocarbons). Certificate of Analysis. NIST Gaithersburg MD
- [98] Chmielowiec J, Sawatzky H (1979) *J Chrom Sci* 17: 245-252
- [99] Sander L C, Wise S (1989) *Anal Chem* 61: 1749-1754
- [100] Yang S S, Gilpin R K (1987) *J Chrom* 394: 295-303
- [101] Lork K D, Unger K K, Brueckner H, Hearn M T W (1989) *J Chrom* 476: 135-145
- [102] Cole L A, Dorsey J G, Dill K A (1992) *Anal Chem* 64: 1324-1327
-

-
- [103] Cole L A, Dorsey J G (1992) *Anal Chem* 64: 1317-1323
- [104] Snyder L R (1979) *J Chrom* 179: 167-172
- [105] Dill K A (1987) *J Phys Chem* 1: 1980-1988
- [106] Sentell K B, Dorsey J G (1989) *Anal Chem* 61: 930-934
- [107] Krucker M, Lienau A, Putzbach K, Grynbaum M D, Schuler P, Albert K (2004) *Anal Chem* 76: 2623-2628
- [108] Albert K, Ed (2002) *On-line LC NMR and Related Techniques* John Wiley & Sons Ltd, Chichester UK
- [109] Spraul M, Freund A S, Nast R E, Withers R S, Mass W E, Corcoran O (2003) *Anal Chem* 75: 1536-1541
- [110] Olson D L, Lacey M E, Sweedler J V (1998) *Anal Chem* 70: 257-264
- [111] Behnke B, Schlotterbeck G, Tallarek U, Strohschein S, Tseng L H, Keller T, Albert K, Bayer E (1996) *Anal Chem* 68: 1110-1115
- [112] Wu N, Peck T L, Webb A G, Magin R L, Sweedler J (1994) *Anal Chem* 66: 3849-3857
- [113] Olson D L, Peck T L, Webb A G, Magin R L, Sweedler J V (1995) *Science* 270: 1967-1970
- [114] Schlotterbeck G, Tseng L H, Händel H, Braumann U, Albert K (1997) *Anal Chem* 69: 1421-1425
- [115] Lienau A, Glaser G, Tang G, Dolnikowski G G, Grusak M A, Albert K (2003) *J Nutr Biochem* 16: 663-670
- [116] Abidi S L (2000) *J Chrom A* 881: 197-216
- [117] Strohschein S, Pursch M, Lubda D, Albert K (1998) *Anal Chem* 70: 13-18
- [118] Dachtler M, Glaser T, Händel H, Lacker T, Tseng L H, Albert K, in *Level II* pp 747-760 of *Encyclopedia of Separation Science* Eds: Wilson I D, Adlard E R, Cooke M, Poole C F (2000) Academic Press, London, UK
- [119] Pryor W A, Bowman B A, Russel R M, Eds (2001) *Present Knowledge in Nutrition International* Life Sciences Institute Press, Washington, DC, USA
- [120] Marchioli R (1999) *Pharmacol Res* 40: 227-238
-

-
- [121] Stöggli M, Huck C W, Scherz H, Popp M, Bonn G K (2001) *Chromatographia* 454: 179-185
- [122] Hoult D I, Richards R E (1976) *J Magn Res* 24: 71-85
- [123] Pirkle W H, House D W (1979) *J Org Chem* 44: 1957-1960
- [124] Pirkle W H, House D W, Finn J M (1980) *J Chrom* 192: 143-158
- [125] Pirkle W H, Welch C J, Hyun M H (1992) *J Chrom* 607: 126-130
- [126] Pirkle W H, Welch C J (1992) *J Chrom* 589: 45-51
- [127] Pirkle W H, Welch C J (1992) *J Liq Chrom* 15: 1947-1955
- [128] Welch C J (1994) *J Chrom* 666: 3-26
- [129] Pirkle W H, Welch C J (1994) *J Chrom* 683: 347-353
- [130] Abu-Lafi S, Turujman S A (1997) *Enantiomer* 2: 17-25
- [131] Abu-Lafi S, Turujman S A (1999) *J Chrom A* 855: 157-170
- [132] Turujman S A (1993) *J Chrom A* 631: 197-199
- [133] Grewe C, Menge S, Griehl C (2004) *ISC Paris*
- [134] Osterlie M, Bjerkgeng B, Liaaen-Jensen S (1999) *J Nutr* 192: 391-398
- [135] Breithaupt D E, Weller P, Wolters M, Hahn A (2004) *Brit J Nutr* 91: 707-713
- [136] Bielecki A, Burum D P (1995) *J Magn Reson A* 116: 215-220
-

Meine akademischen Lehrer waren:

K. Albert, E. Bayer, H. Bertagnolli, F. Brandstetter, D. Burkey, D. Chatfield, D. Christen, H. Eckstein, H. Egelhaaf, G. Gauglitz, W. Göpel, D. Grotjahn, G. Häfelinger, M. Hanack, D. Hoffmann, V. Hoffmann, W. Jäger, G. Jung, W. Koch, N. Kuhn, E. Lindner, M.E. Maier, H.A. Mayer, H.-J. Meyer, K. Müller, U. Nagel, H. Oberhammer, C. Ochsenfeld, D. Oelkrug, H. Pommer, G. Reinhardt, O. Rössler, W. Rosenstiel, V. Schurig, E. Schweda, F.F. Seelig, B. Speiser, G. Staudt, J. Strähle, W. Tong, P. Walsh, U. Weimar, L. Wesemann, K. H. Wiesmüller, K.-P. Zeller, T. Ziegler

Lebenslauf:

Persönliche Daten:

Name: Christoph Meyer
Geburtsdatum/-Ort: 23.02.1976, Schorndorf bei Stuttgart
Anschrift: Quenstedtstraße 20, 72076 Tübingen
Familienstand: ledig
Staatsangehörigkeit: deutsch
Konfession: evangelisch

Schulbildung:

1982-1986 Grundschule Winterbach im Remstal
1986-1995 Burggymnasium Schorndorf
27.06.1995 Allgemeine Hochschulreife (Note: 2,2)

Wehrdienst:

07/95-04/96 Grundwehrdienst, 4. Panzergrenadierbataillon, Stetten am kalten Markt

Hochschulausbildung:

10/96-08/98 Grundstudium der Chemie an der Eberhard-Karls-Universität Tübingen
03.08.98 Diplomvorprüfung Chemie (Note 2,5)
09/98-07/99 Studium der Chemie an der San Diego State University, San Diego, CA, USA
10/99-06/02 Hauptstudium der Chemie an der Eberhard-Karls-Universität Tübingen
07/02-11/02 Diplomarbeit am Institut für Organische Chemie an der Universität Tübingen unter Anleitung von Prof. Dr. K. Albert über das Thema: „Synthese, Festkörper-NMR-Spektroskopie und Anwendung von polymermodifizierten Kieselgelen“
27.11.02 Chemie Diplom (Note 2,2)
seit 12/02 Mitglied des Graduiertenkollegs der Deutschen Forschungsgemeinschaft „Chemie in Interphasen“

- 12/02-07/05 Anfertigung einer Dissertationsarbeit unter der Anleitung von Prof. Dr. K. Albert am Institut für Organische Chemie der Universität Tübingen mit dem Thema: „Polymer based chromatographic sorbents: Synthesis, characterization, and application“
- 07/99-09/99 Forschungsaufenthalt an der San Diego State University bei Prof. Douglas Grotjahn, San Diego, CA, USA.
- 06/04-08/04 Forschungsaufenthalt am National Institute of Standards and Technology (NIST) bei Drs. Lane Sander und Stephen Wise, Gaithersburg, MD, USA.

Tübingen 04.06.2005